Università degli Studi di Urbino "Carlo Bo"

Department of Biomolecular Sciences

Ph.D. PROGRAMME IN: BIOMOLECULAR AND HEALTH SCIENCES

XXXV CYCLE

miRNAs AS POTENTIAL REGULATORS OF MYELIN BASIC PROTEIN RECOVERY DURING DEVELOPMENT IN A MURINE MODEL OF PHENYLKETONURIA

ACADEMIC DISCIPLINE: BIO/10

Coordinator: Prof. **MARCO BRUNO LUIGI ROCCHI**

Supervisor: Chiar.ma Prof.ssa **LUIGIA ROSSI**

Ph.D. student: Dott. **ALESSANDRO BREGALDA**

ACADEMIC YEAR 2021/2022

ABSTRACT

Untreated phenylketonuria (PKU) patients and PKU animal models show hypomyelination in the central nervous system and white matter damages. These cerebral alterations are accompanied by myelin basic protein (MBP) impairment, which could be the reason of the clinical traits mentioned above, as MBP is crucial for the correct assembling of the myelin sheath. In this study, we analyzed MBP protein and mRNA expression on brains of WT and phenylketonuric (ENU2) mice during post-natal development (14-60-180-270-360-540 post-natal days, PND). The results showed a progressive MBP protein expression recovery during post-natal development, together with an unaltered MBP mRNA expression. Furthermore, for the same time intervals, a significant decrease of the phenylalanine concentration in the bloodstream of PKU mice was detected, as well as in the PKU mice brains from 14 to 60 PND. To try to explain this scenario, we hypothesized a hindrance during MBP translation in the early development, leading us to perform a microRNA microarray analysis on 60 PND mice. Microarray output and the following *in silico* analyses underlined the potential role of microRNAs in the PKU cerebral outcomes. In addition, in order to link predictive analysis with concrete data, we performed a proteomic assay on ENU2 brains of 60 and 360 PND. Taken together, we assessed miR-218-1-3p, miR-1231-3p and miR-217-5p as the most promising microRNAs, since that an alteration on their predicted and downregulated targets (MAG, CNTNAP2 and ANLN, respectively) could indirectly lead to a low MBP protein expression. Moreover, their expression shows an opposite trend to that observed for MBP protein during development, except for miR-217-5p. Furthermore, target proteins revealed a complete normalization in aged ENU2 mice. In conclusion, these results provide a new perspective on the PKU pathophysiology understanding and treatment, emphasizing the possible role of differentially expressed microRNAs in PKU brains, especially during early development.

CONTENT INDEX

ABBREVIATIONS

PKU: Phenylketonuria
HPA: Hyperphenylalaninemia
MBP: Myelin Basic Protein
PAH: Phenylalanine Hydroxylase
BH4: Tetrahydrobiopterin
PAL: Phenylalanine Ammonia Lyase
CNS: Central Nervous System
PNS: Peripheral Nervous System
OLs: Oligodendrocytes
L-Phe: L-Phenylalanine
L-Tyr: L-Tyrosine
L-Trp: L-Tryptophan
LNAAs: Large Neutral Amino Acids
miRNA: microRNA
ANLN: Anillin
MAG: Myelin-Associated Glycoprotein
CNTNAP2: Contactin Associated Protein 2
PLP1: Myelin Proteolipid Protein 1
MOG: Myelin Oligodendrocyte Glycoprotein
MOBP: Myelin Associated Oligodendrocyte Basic Protein
CNP: 2’3’-cyclic-nucleotide 3’-phosphodiesterase
SYT2: Synaptotagmin 2
WB: Western Blot
RT-qPCR: Real Time Quantitative Polymerase Chain Reaction
ORT: Object Recognition Test
OFT: Open Field Test
IF: Immunofluorescence

1. INTRODUCTION

1.1 PHENYLKETONURIA (PKU) GENERAL ASPECTS

Phenylketonuria (PKU; OMIM 261600) is a rare metabolic disease with autosomal recessive inheritance that had a fundamental place in the history of the study of metabolic diseases. In fact, it has been classified as the most common inborn error of amino acid metabolism and as the first disease to be associated with a form of mental retardation. Furthermore, PKU appears to be the first genetic condition to be successfully treated, thus guaranteeing a fulfilling life for phenylketonuric subjects (Camp *et al.*, 2014). This disease is characterized by a defect in the phenylalanine hydroxylase (PAH, phenylalanine 4-monooxygenase, EC 1.14.16.1) functionality, which is caused by mutations on the PAH genomic sequence. This enzyme is actively expressed in the liver and is involved in the catabolism of phenylalanine (L-Phe), an essential amino acid that is obtained from the diet and from the degradation of endogenous proteins. Usually, this enzyme metabolizes about 75% of L-Phe from the diet and protein turnover under physiological conditions (Scriver, 2007), ensuring the conversion of L-Phe to tyrosine (L-Tyr). The reaction is also supported by the tetrahydrobiopterin cofactor (BH4), a molecule of O_2 and a Fe^{2+} ion (**Figure 1**, (Wyse *et al.*, 2021)). The conversion of L-Phe to L-Tyr is typically well regulated to provide an adequate level for a correct protein synthesis, thus keeping L-Phe levels low enough to not be toxic to the body (Regier and Greene, 1993; Flydal and Martinez, 2013).

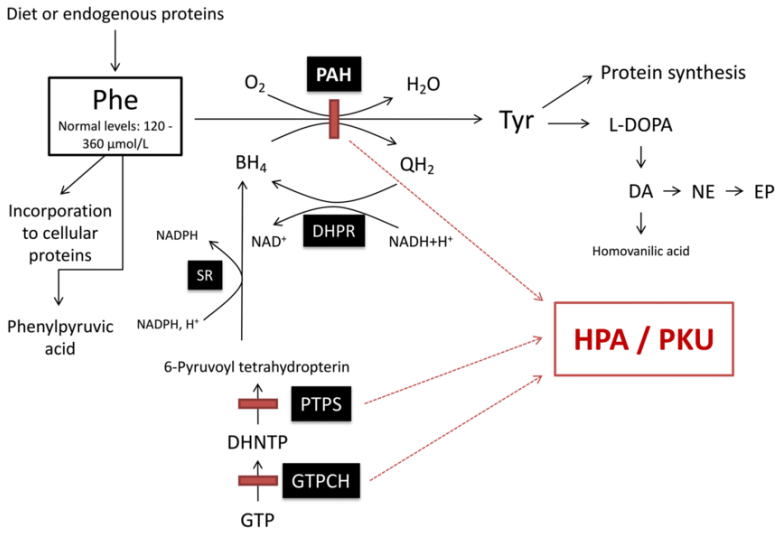

Figure 1: **Metabolism of L-Phe. PKU and hyperphenylalaninemia (HPA) are caused by a deficiency on the phenylalanine hydroxylase (PAH) activity**. Both the diseases can also occur due to a defect in the regeneration of the cofactor tetrahydrobiopterin (BH4) by the enzyme dihydropteridine reductase (DHPR), and by a defect on its synthesis carried out by multiple enzymes such as GTP-cyclohydrolase I (GTPCH), pyruvoyl-tetrahydropterin synthase (PTPS) or sepiapterin reductase (SR). Tyrosine (L-Tyr), product of the oxidation reaction, is the precursor of L-DOPA from which dopamine is derived, which is in turn a precursor of noradrenaline and adrenaline. Picture taken from *Wyse et al., 2021*.

Dysfunctions caused by the altered PAH sequence lead to high L-Phe concentration in the bloodstream and in the brain (a condition called hyperphenylalaninemia, HPA), resulting in neurotoxic effects (Klippel *et al.*, 2021).

HPA can be caused by either mutations at the PAH locus, which results in more or less severe forms of PKU, or mutations in the genes encoding the enzymes involved in the biosynthesis or regeneration of the cofactor BH4, resulting in non-PKU HPA (Donlon *et al.*, 2019). A defect in the synthesis of the cofactor can result from multiple causes, such as a deficiency in GTP-cyclohydrolase (GTPCH), a deficiency in 6-pyruvate-tetrahydropterin synthase (PTPS) or a deficiency in the enzyme sepiapterin reductase (SR). A deficit of the enzyme dihydropteridine reductase, on the other hand, can lead to a defect in the regeneration of the cofactor BH4 (**Figure 2**).

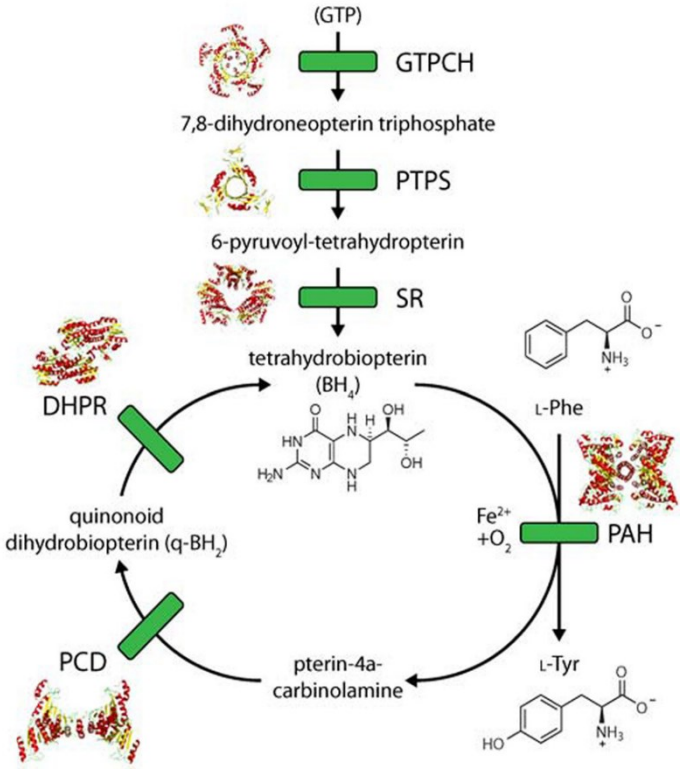

Figure 2: **The biosynthetic and regeneration pathways of BH4 and the reaction catalyzed by PAH**. Picture taken from *Underhaug et al., 2012.*

All these factors lead to the accumulation of L-Phe in tissues and biological fluids, resulting in the formation of metabolites such as phenylpyruvate, phenyllactate and phenylacetate (Regier and Greene, 1993; Kaufman, 1999; Mitchell, Trakadis and Scriver, 2011). The L-Phe that no longer takes part in the reaction mediated by PAH, in fact, is transformed into phenylpyruvic acid (PPA) through a transamination reaction catalyzed by the enzyme phenylalanine transaminase. Since this reaction is activated by the presence of the substrate, it becomes more relevant when

blood L-Phe levels are very high (Scriver and Rosenberg, 1973). L-Phe can also be decarboxylated to phenylethylamine, through the action of phenylalanine decarboxylase (Rampini *et al.*, 1974).

1.1.1 PAH GENE AND PKU MUTATIONS

HPA and PKU are two pathological conditions whose clinical manifestations are due to the accumulation of L-Phe in tissues and body fluids consequently to a defect in the metabolism of the amino acid itself. At the basis of the disease there are several genetic deficits, the most important of which is the mutation of the PAH gene (NCBI Entrez Gene: 5053 Ensembl: ENSG00000171759), which leads to a reduction or absence of the activity of the PAH enzyme. The human PAH gene is located on the long arm of chromosome 12 (12q22-12q23.2), contains 13 exons and 12 introns and extends for 90 kb in length (**Figure 3**) (Scriver, 2007). The enzyme is expressed in the liver and, marginally, in the kidney and the gall bladder (Wang *et al.*, 1992; Tessari *et al.*, 1999) as a monomer of 452 amino acids (MW: 51.8 kDa) with regulatory, catalytic, and tetramerization domains. The complete PAH sequence harbors 1435 loci in 130683379 base pairs of non-overlapping sequence with minus strand orientation, accommodating ≈ 4.5% of the human genome. In the initial part of the gene the exons are separated by long introns, while in the second part the distances between one exon to the other are shorter, with a greater percentage of modifications in these exons, especially the 3, 6, 7 and 11 (Blau, Shen and Carducci, 2014). In fact, exon 6 contains the greatest number of variants (14.1%), followed by exon 7 (12.2%) and exon 3 (9.9%). Most variants (59.2%) are in the central catalytic domain, 17.5% in the N-terminal regulatory domain, and 5.4% in the C-terminal oligomerization domain of the PAH monomer (Hillert *et al.*, 2020).

To date, more than 1000 mutations in the PAH gene have been reported. Most variants for PAH are point modifications of a single nucleotide leading to the replacement of one amino acid with another (missense mutations, 63%), followed by the less common frameshift mutations (addition or subtraction of a nucleotide, 13%), splice variants (11%), putative silent (7%), stop/nonsense (5%) and small insertions (1%) (**Figure 3**). Large deletions account for 3% of PKU-causing mutations (Kozak *et al.*, 2006).

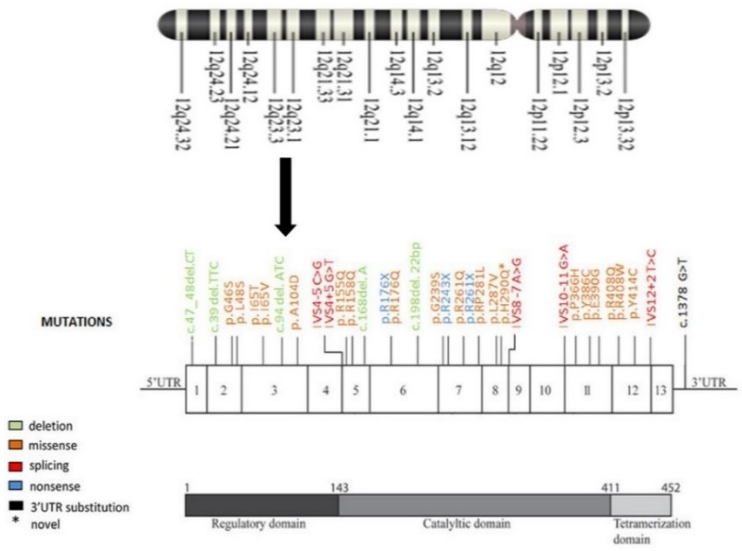

Figure 3: Human PAH gene location on chr.12 and the most relevant detected mutations.

The most common mutations (c.1222 C>T-p.Arg408Trp and c.1066-11 G>A-p.Gln355_Tyr356insGlyLeuGln) are responsible for abolishing PAH activity (Gjetting *et al.*, 2001). Other variants of the gene are silent mutations with little or no effect on PAH activity (Wettstein *et al.*, 2015), while the alterations which destroy enzyme functionality, named "null" mutations (Mitchell, Trakadis and Scriver, 2011; Zhou *et al.*, 2012), interfere with the correct folding of the protein, the tetramerization process or destroying the catalytic domain, thus accelerating its degradation and compromising the enzyme catalytic activity; however, these mutations do not completely destroy the PAH enzymatic activity.

1.1.2 PKU EPIDEMIOLOGY

PKU is one of the most widespread metabolic diseases in the world, although its prevalence varies greatly depending on the geographic area (**Figure 4**). Europe is the continent with the highest prevalence rate, with an estimation of 1:10000 live births (Loeber, 2007). In some areas of Europe, the prevalence is even higher, such as in Spain, where there is a high prevalence of the mild form of hyperphenylalaninemia (Desviat *et al.*, 1999). Finland has the lowest prevalence in all of Europe, amounting to 1 case in 1000000 (Guldberg *et al.*, 1995). In Turkey, values equal to 1:2600 births are reached, while in Northern Ireland the prevalence is 1:4000 newborns, perhaps due to the high consanguinity among the population (Zschocke *et al.*, 1997). In the USA, the prevalence is 1:15000 (National Institutes of Health Consensus Development Panel, 2001), while in Latin America it ranges from 1:50000 to 1:25000 births (Borrajo, 2007). In Asia, the values tend to be lower than in Europe or the United States; for example, in Japan the incidence

is 1 case in 100000, in Thailand is less than 1: 200000 (Pangkanon *et al.*, 2009), while in China the values range from 1:15000 to 1:100000 (Zhan, Qin and Zhao, 2009). On the other hand, PKU prevalence in Africa is estimated to be very low (Phenylketonuria (PKU): screening and management. NIH Consensus Statement, 2000).

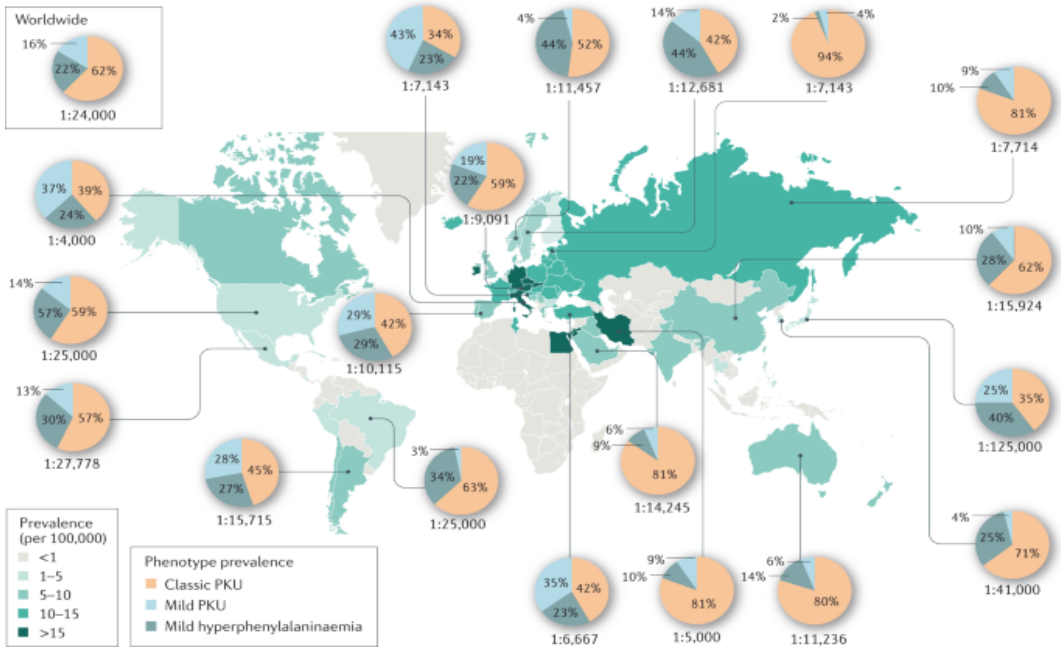

Figure 4: Phenylketonuria incidence by country.

1.1.3 PKU CLASSIFICATION

The various forms of PKU can be classified on the severity of hyperphenylalaninemia (HPA), thus evaluating the ranges of blood L-Phe concentrations and considering that the normal range for plasma L-Phe levels is between 120-360 µmol/l (de Baulny *et al.*, 2007; Mitchell, Trakadis and Scriver, 2011). The various levels of PKU can be classified as follows:

- Mild HPA, for pretreatment L-Phe blood concentrations between 120 and 600 µmol/l
- Mild PKU, for plasma levels of L-Phe between 600 and 900 µmol/l
- Moderate PKU, for blood levels of L-Phe between 900 and 1200 µmol/l
- Classic PKU, for blood L-Phe concentrations greater than 1200 µmol/l

L-Phe concentrations are measured at birth and the amino acid does not always have the time to reach the maximum peak at the time of evaluation (Blau, van Spronsen and Levy, 2010), therefore applying this type of classification is not always so simple. For this reason, another

classification based on tolerance to dietary L-Phe can be applied, which in turn leads to an identification of four different genotypes:

- Classic PKU: L-Phe tolerance <20 mg/kg/day, corresponding to 250-300 mg L-Phe/day
- Moderate PKU: L-Phe tolerance of 20-25 mg/kg/day (350-400 mg/day)
- Mild PKU: L-Phe tolerance of 25-50 mg/kg/day (400-600 mg/day)
- Mild HPA: patients not requiring dietary restriction

This evaluation is settled by the amount of daily L-Phe intake that a patient can tolerate without reaching maximum L-Phe level. L-Phe tolerance is usually determined at the age of 5 years (van Spronsen *et al.*, 2017; van Wegberg *et al.*, 2017) but recent research showed that also at 2 years a reliable determination is possible, since that the tolerance at 2, 3 and 5 years correlates with that observed at 10 years age (van Spronsen *et al.*, 2009). On the contrary, L-Phe tolerance must be reevaluate in adulthood in relation to body weight in order to satisfy as much as possible the criterion of 9.1 mg L-Phe/kg/day with 95% confidence limits of 4.6–13.6 mg L-Phe/kg/day in adults without PKU (MacLeod *et al.*, 2009). For patients ≥12 years old with untreated L-Phe levels <600 µmol/l, follow-up at a lower frequency is recommended, together with lifetime compliance to the diet (Brenton *et al.*, 1996).

1.1.4 PKU DIAGNOSIS

The PKU screening test was firstly introduced in the 1960s by Guthrie (Guthrie and Susi, 1963) and has been applied massively to newborns as it was a quick and inexpensive test. This newborn screening method (NBS) is based on *Bacillus subtilis* activity, which requires L-Phe for its growth, and includes a blood drop collection from the heel of the newborn, which is placed on a filter paper disc (or spot) and left to dry. The sample is then analyzed with the bacterial inhibition assay with the addition of a substance, β-2-thienyalanine, which limits bacterial growth. If the bacteria continue to grow, high levels of L-Phe are present; consequently it is necessary that the newborn undergoes further analysis (Guthrie and Susi, 1963). Nowadays, this technique has been replaced by more modern procedures that are characterized by an improved efficiency, sensitivity, precision, and rapidity. For example, it is possible to conduct a neonatal screening test analyzing the L-Phe and L-Tyr concentrations in the blood spot through mass spectrometry (MS/MS) (Chace *et al.*, 1993). By doing so, knowing the L-Tyr levels, it is possible to calculate the L-Phe:L-Tyr ratio already 24 hours after birth and, in order for the screening test to be considered

positive, the following cut-offs (or threshold values) have been identified: L-Phe of 130 μM and L-Phe:L-Tyr > 3 (McHugh *et al.*, 2011). The positivity to the test leads to the execution of a second evaluation, which includes tests for the identification of deficiencies in the synthesis and regeneration of BH4, including the pterin test conducted on urine or blood samples (Blau *et al.*, 2011) or the test for measuring dihydropterin reductase in erythrocytes on blood spots (**Figure 5**). This aspect is particularly important because it allows to discriminate between patients with deficits in BH4 synthesis or with alteration on PAH functionality. In fact, 2% of all HPA are due to disorders on BH4 metabolism, with differential frequency depending on the country (i.e. higher frequency has been reported in Turkey and Saudi Arabia) (Blau *et al.*, 2011).

Another possibility to diagnose PKU is the molecular screening over PAH gene locus, which could provide indications about mutations and associated polymorphic haplotypes, revealing the nature of the alterations and providing insights about a potential residual enzymatic activity (Blau *et al.*, 2011). However, it is not possible to precisely test the activity of the enzyme L-Phe hydroxylase because it should be observed at the renal or hepatic level and not at the level of urine and blood (Thöny and Blau, 2006; Blau *et al.*, 2011). In addition, other diagnostic tests for PKU are available, including the analysis of plasma amino acids with tandem mass-spectrometry (TMS), which represents a standard method for confirming the high levels of L-Phe in infants already undergoing NBS (Chace *et al.*, 1998), the fluorimetric assay (Gerasimova, Steklova and Tuuminen, 1989) and the reverse phase liquid chromatography (Pecce *et al.*, 2013).

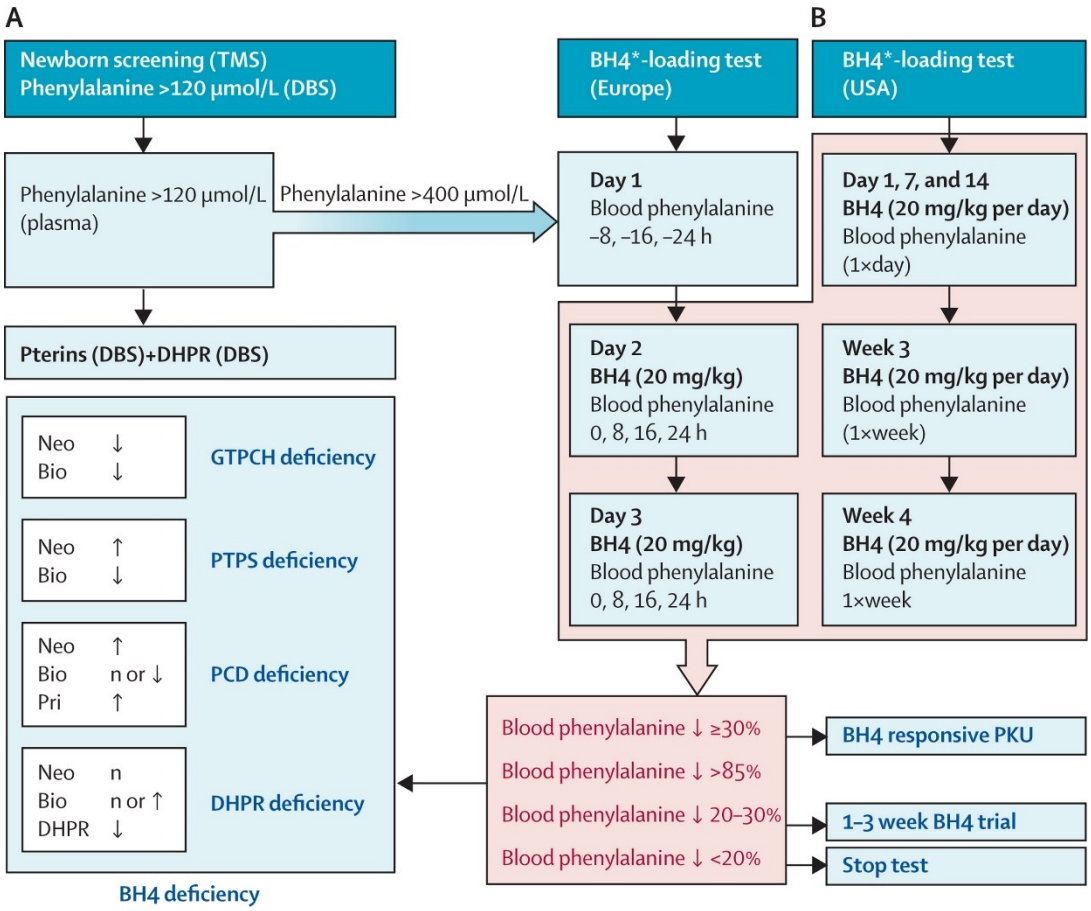

Figure 5: (**A**) Flowchart of the differential diagnosis of hyperphenylalaninaemia with relevance to phenylalanine hydroxylase and tetrahydrobiopterin deficiencies. (**B**) Tetrahydrobiopterin-loading test in Europe and the USA. TMS=tandem mass-spectrometry. Phe=phenylalanine. BH4=tetrahydrobiopterin. PKU=phenylketonuria. DHPR=dihydropteridine reductase. Neo=neopterin. Bio=biopterin. Pri=primapterin. DBS=dried blood spots. GTPCH=GTP-cyclohydrase I. PTPS=6-pyruvoyl-tetrahydropterin synthase. PCD=pterin-4a-carbinolamine dehydratase. Picture taken from *Blau et al., 2010.*

1.1.5 THERAPEUTIC STRATEGIES

Subjects with PKU have high levels of L-Phe in the bloodstream and therefore the main therapeutic strategy to lower these levels is a dietary plan based on a L-Phe restricted diet. This plan must be applied from the first days of life (in the first week or within the first 10 days) to have immediate improvements in blood levels and avoid the onset of clinical manifestations. This therapeutic strategy is necessary when a newborn has a blood concentration of L-Phe > 600 µmol/l (Weglage *et al.*, 1996) and it is recommended throughout life. Thus, in order to reach L-Phe normal levels, the applicable dietary treatment consists of a restriction of the intake of the amino acid. However, since that L-Phe is an essential amino acid, it cannot be completely eliminated from the diet and as such it must necessarily be taken with food to allow protein synthesis in both childhood and adulthood (Macleod and Ney, 2010). In addition to L-Phe restriction, three other aspects are important: low protein food intake, dietary restriction of natural proteins and amino acid supplementation without L-Phe (van Wegberg *et al.*, 2017).

Although the dietary treatment shows various benefits for the alleviation and the onset of the classical PKU symptoms, it also has negative aspects related to the palatability of foods and the restrictive diet that must be planned and strictly followed. For these reasons, subjects tend to abandon it and, due to its difficult management, encounter difficulties in social adaptation (Levy and Waisbren, 1994) and in the emotional and family sphere. In recent years, numerous studies have been conducted to identify other therapeutic strategies aside from the L-Phe restricted diet, and among these we have:

Use of glycomacropeptide (GMP)

GMP is a protein derived from whey, which is rich in essential amino acids but does not contain phenylalanine, tyrosine, or tryptophan (Laclair *et al.*, 2009). It is an adequate supplement to the dietary restriction of L-Phe (Blau *et al.*, 2011).

Treatment with LNAAs (large neutral amino acids - tyrosine, valine, leucine, isoleucine, tryptophan, threonine, methionine, and histidine)

Supplementation of LNAAs alone or in combination with a diet low in L-Phe has been shown to be effective in improving health of PKU patients who were unable to follow a low L-Phe diet (Ashe *et al.*, 2019). In fact, it has been proven that the treatment with LNAA is able to improve neurological functions, reducing the concentrations of L-Phe in the brain and increasing L-Tyr levels in sub-optimally controlled adult PKU patients (Burlina *et al.*, 2019). This treatment is aimed to overcome the impaired transport of LNAAs from blood to brain through BBB (blood-brain barrier) in presence of high L-Phe concentrations (**Figure 6**). In fact, LNAAs compete for transport by the LNAA type I (LAT1) transporter (Hargreaves and Pardridge, 1988; Pardridge, 1998), for which L-Phe has the highest binding affinity (Hargreaves and Pardridge, 1988; Pardridge, 1998). This competition between LNAAs for blood-to-brain uptake can also occurs at other transporters, such as SLCA19 and SLCA15 (O'Mara, Oakley and Bröer, 2006), and the low LNAA presence in the brain is believed to reduce the cerebral protein synthesis (CPS) (Hoeksma *et al.*, 2009).

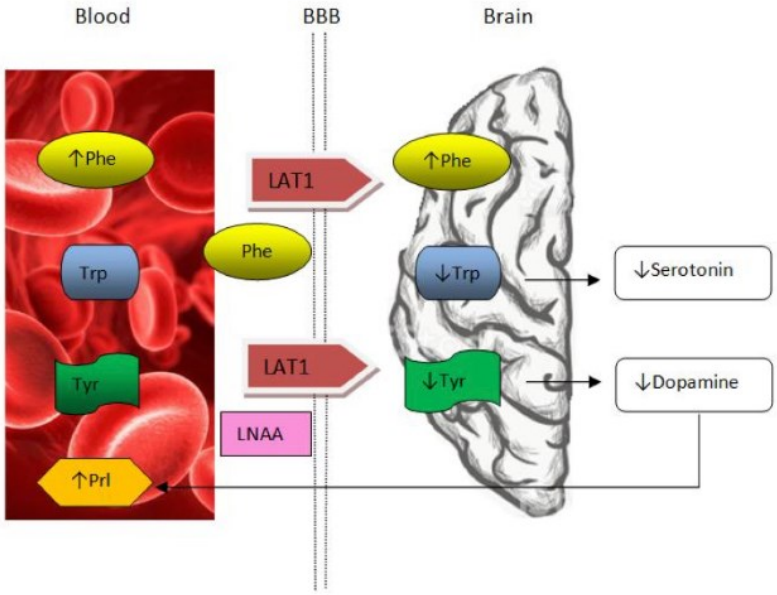

Figure 6: **Schematic illustration of L-Phe toxicity in the brain**. Phe: phenylalanine; Trp: tryptophan; Tyr: tyrosine; Prl: prolactin; LNAA: large neutral amino acids; LAT1: L-type amino acid carrier; BBB: blood-brain barrier. Picture taken from *Nardecchia et al., 2018*.

Treatment with exogenous BH4

Tetrahydrobiopterin, which normally acts as a cofactor of PAH, plays the role of a pharmacological chaperone by promoting the correct folding and stability of the PAH enzyme (Pey *et al.*, 2007). However, the stabilization capacity of the protein in presence of PAH deficits is only in a subgroup of subjects who have residual enzymatic activity or in those who have problems in the synthesis and regeneration of the cofactor (Thöny and Blau, 2006). The formulation approved by the Food and Drug Administration (FDA) and European Medicines Agency (EMA) is sapropterin ((6R)-2-amino-6-[(1R,2S)-1,2-dihydroxypropyl]-5,6,7,8-tetrahydro-4(3H)-pteridinone) dihydrochloride (Kuvan®, BioMarin Pharmaceutical Inc, Novato, CA) developed by BioMarin Pharmaceutical Inc. The responsivity to BH4 increases alongside the severity of the phenotype decrease and the treatment with this cofactor is well tolerated, allowing the increase of L-Phe tolerance and improving the quality of patients' life (Vockley *et al.*, 2014).

Gene therapy

Given that PKU occurs following a hereditary genetic deficit, the possibility of studying an *ad hoc* gene therapy was evaluated to allow the restoration of the complete functionality of the PAH enzyme (Blau, van Spronsen and Levy, 2010). The main target for this gene therapy is represented by the liver, since PAH is a hepatic enzyme, into which vectors obtained from the recombinant adeno-associated virus (rAAV) are introduced. rAAVs are used as they are non-

pathogenic and low immunogenic viruses; in addition, they can mediate long-term episomal transgenic expression in cells both undergoing cell division and that do not (Mingozzi and High, 2013); moreover, they can specifically deliver genome editing systems such CRISPR/Cas9 into the targeted tissues. Although promising, the usage of the CRISPR/Cas9 system, which is aimed to correct the PAH gene defects, is still controversial and it remains, so far, restricted to the preclinical level (Koppes *et al.*, 2020; Richards *et al.*, 2020). In fact, studies carried out on PKU mouse model ($PAH^{ENU2(-/-)}$ mouse) using CRISPR/Cas9 machinery together with rAAV vectors which target hepatic cells, revealed a partial restoration of liver PAH activity, substantial reduction of blood L-Phe, and prevention of maternal PKU effects during breeding (Villiger *et al.*, 2018; Richards *et al.*, 2020). However, the use of these technologies in the clinical setting is still far away due to the possible off-target mutations that can be integrated into the subject's genome.

Hepatic cell transplantation

Therapy represented by therapeutic liver repopulation (TLR), which consists in the transplantation of liver cells in the liver of subjects affected by PKU, allow the replacement of diseased cells with fully functional hepatocytes. This type of treatment is possible in the liver both because PAH is a liver enzyme and because it is an organ with great regenerative capacity. Even though the efficacy of whole liver transplant and hepatocyte transplantation as therapies for PKU is limited by the lifelong need for immunosuppression, successful liver transplants have been achieved throughout years (Jenkins *et al.*, 1993; Raghu *et al.*, 2022).

Enzyme Replacement Therapy

Enzyme Replacement Therapy (ERT) allows to overcome the lack or deficiency of an enzyme and represents a valid alternative to dietary therapy in patients with PKU. The direct usage of an exogenous PAH is not recommended in this therapy because it is an unstable enzyme and it would require the presence of the cofactor to perform its function (Sarkissian and Gámez, 2005; Wang *et al.*, 2005). Therefore, ERT for PKU has been performed with another enzyme which is equally capable of metabolizing L-Phe but works through a different pathway compared to PAH. This enzyme is phenylalanine ammonia lyase (PAL; EC 4.3.1.5), a plant-based enzyme derived from the cyanobacteria *Anabaena variabilis* (AvPAL) that converts L-Phe to trans-cinnamic acid and ammonia (**Figure 7**).

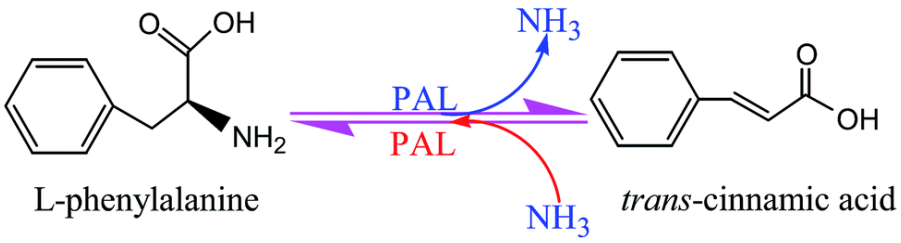

Figure 7: Phenylalanine ammonia-lyase (PAL) mechanism of action.

The products obtained from this reaction are then easily excreted from the body through the urine (Sarkissian *et al.*, 1999). Usually, this enzyme is administered linked to a synthetic molecule such as polyethylene glycol (PEG, a flexible, uncharged and highly hydrophilic polymer with low immunogenicity), which promotes less renal excretion and makes the enzyme more resistant to the action of proteases (Sarkissian *et al.*, 2008). The negative drawback for an extensive usage of PAL is that being the enzyme of heterologous origin, it can cause immune reactions within the host organism, thus compromising the pharmacological duration of the activity of the recombinant protein and potentially provoking serious adverse effects. These aspects pushed the research to find a way to make AvPAL more likely to be used for human PKU treatment. Currently, the best results have been obtained with C503S/C565S double mutant rAvPAL – modified with PEG – since it displays elevated specific activity and protease resistance, good thermal stability and lower Km value respect to the others (Wang *et al.*, 2008). The AvPAL enzyme (**Figure 8**) is a homotetrameric protein composed of 567 amino acids, with each monomer being of 64 kDa. The enzyme consists in alpha-helices and it is subdivided into three domains: central catalytic domain, N-terminal and C-terminal domains.

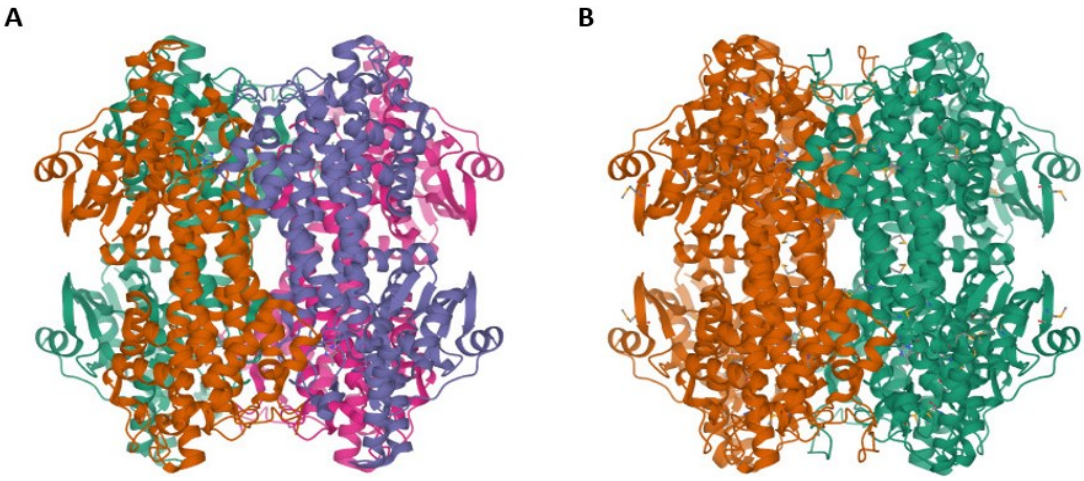

Figure 8: (**A**) Crystal structure of phenylalanine ammonia-lyase from *Anabaena variabilis*, ref. **2NYN**. (**B**) Crystal structure of double mutant C503S/C565S phenylalanine ammonia-lyase from *Anabaena variabilis*, ref. **3CZO**. Pictures taken from RCSB PBD protein repository databank.

Its catalytic activity requires the electrophilic prosthetic group 4-methylideneimidazole-5-one (MIO) and does not require any external additional cofactor (Moffitt *et al.*, 2007; Wang *et al.*, 2008). Over the years, the recombinant enzyme rAvPAL (C503S, C565S) has been produced and developed as a drug called Palynziq^{TM} by BioMarin Pharmaceutical Inc. This drug was approved by the FDA in 2018 and in 2019 by the EMA (https://www.fda.gov/; http://investors-.biomarin.com/) and is, so far, the only available therapy for PKU. The drug is administered through multiple subcutaneous injections that can reduce blood L-Phe levels. Despite the undoubted beneficial effects, it is not devoid of adverse effects; in fact, the drug can lead to vomiting, dizziness, infections, arthralgia and anaphylactic reactions (Longo *et al.*, 2019).

Erythrocytes as a transport system for AvPAL

To avoid the risk of anaphylactic reactions and adverse reactions in sick subjects, in recent years it has been appropriate to seek alternative therapies, including the encapsulation of the recombinant enzyme in erythrocytes (RBCs) (Rossi *et al.*, 2014, 2020, 2021; Pascucci *et al.*, 2018). In fact, erythrocytes represent an excellent transport system for proteins, drugs, recombinant enzymes and contrast agents for diagnostics thanks to their unique biological characteristics, such as:

- elevated biocompatibility, especially if autologous RBCs are used;
- good biodegradability;
- long in vivo life-span, which influences the encapsulated drug or agent availability;
- great flexibility and deformation capacity, thanks to their biconcave shape;
- capability to work like an osmometer, shrinking or swelling according to the salt content of the external medium, thus permitting the loading of many non-diffusible large compounds (such as proteins and peptides) inside the cell, maintaining its morphological, biochemical and immunological properties;
- protective ability against the premature degradation or inactivation by the host immune system promoting a longer persistence of the drug in the body;

To perform their function, the erythrocytes are subjected to an encapsulation procedure (loading), which can be carried out in various ways including hypotonic hemolysis, which is the most widely used method (Robert *et al.*, 2022) (**Figure 9**).

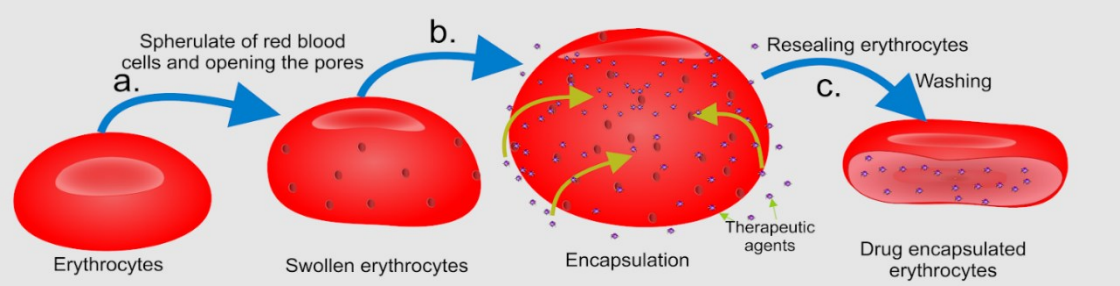

Figure 9: **Schematic illustration of hypotonic hemolysis drugs loading method**. Picture taken from *Jeewantha and Slivkin, The Terpene-Indole Alkaloids Loaded Erythrocytes As A Drug Carrier: Design And Assessment, 2018.*

Several treatments with loaded-RBCs have been developed throughout the years by the two biopharmaceutical companies ERYTECH pharma (http://erytech.com/) and EryDel S.p.A (http://www.erydel.com/). EryDel S.p.A is the proprietary of a non-invasive electromechanical device named Red Cell loader® (RCL). The RCL is a fully automated apparatus with a dedicated software, conceived to function with disposable and CE marked kit, designed to reproducibly load human autologous red blood cells with different drugs (such as dexamethasone), in safe, sterile and apyrogenic conditions (Magnani *et al.*, 1998; Mambrini *et al.*, 2017). Among the diseases which could be treated with loaded-RBCs we find chronic obstructive pulmonary disease (Rossi *et al.*, 2001), cystic fibrosis (Rossi *et al.*, 2004), Crohn's disease (Castro *et al.*, 2007) (ID NCT01277289), ulcerative colitis (Bossa *et al.*, 2013) and ataxia-telangiectasia (ID NCT01255358). Concerning PKU treatment with loaded erythrocytes, several studies have been conducted at the preclinical levels in $PAH^{ENU2(-/-)}$ mice using the double mutant rAvPAL (C503S, C565S) produced by BioMarin Pharmaceutical Inc. as exogenous enzyme capable of metabolizing the L-Phe in circulation (Rossi *et al.*, 2014; Pascucci *et al.*, 2018). The provided results showed a significant lower levels of L-Phe in the bloodstream of treated ENU2 mice, as well as synaptic and cognitive recovery (Pascucci *et al.*, 2018), thus highlighting the potential benefits of the PKU treatment using erythrocytes as carriers of AvPAL.

1.1.6 SYMPTOMATOLOGY AND CLINICAL MANIFESTATIONS

Clinical manifestations related to PKU have various degrees of severity depending on whether they are treated early, treated late and untreated. Infants with PKU present themselves as normal-looking children who in 90% of cases have fair skin, blond hair, and blue eyes (Okano *et al.*, 1991). These characteristics cannot be an exclusion criterion for those subjects affected by PKU with darker skin, hair and eyes, since they still present hypopigmentation (Okano *et al.*, 1991). Those with untreated PKU also show skin lesions, a higher frequency in the onset of congenital heart disease and gait impairment (Paine, 1957). Regarding neurological dysfunctions

(which represent the predominant clinical manifestation) and psychiatric disorders, the degree and time of exposure to high plasma L-Phe concentrations play an important role (Bilder *et al.*, 2013). In fact, the excess of L-Phe in the brain negatively impacts brain and cognitive functions, interfering with the transport of amino acids across the blood brain barrier and consequently reducing the resulting neurotransmitters (Surtees and Blau, 2000). Untreated individuals or those born from untreated PKU mothers suffer from intellectual disabilities, microcephaly, seizures, behavioral problems, developmental disorders and also psychiatric symptoms (van Wegberg *et al.*, 2017). From a neuropsychiatric point of view, depression, anxiety, psychosis, hyperactivity disorder and attention deficit disorder (ADHD) also fall into the symptoms. The pathogenetic mechanism underlying depression in these subjects is given by the high levels of L-Phe, that cause a low concentration of monoaminergic neurotransmitters in the brain, inducing a low monoaminergic transmission (ten Hoedt *et al.*, 2011). The presence of anxiety-related disorders, on the other hand, is associated with low levels of serotonin in the brain (Ressler and Nemeroff, 2000) as a result of high levels of L-Phe (Manti *et al.*, 2016).

1.1.7 PKU ALTERED BIOCHEMICAL AND CEREBRAL PATHWAYS

The high levels of L-Phe in phenylketonuric patients lead to metabolic alterations at the brain level such as oxidative stress, mitochondrial dysfunction, impaired synthesis of proteins and neurotransmitters (Schuck *et al.*, 2015) (**Figure 10**).

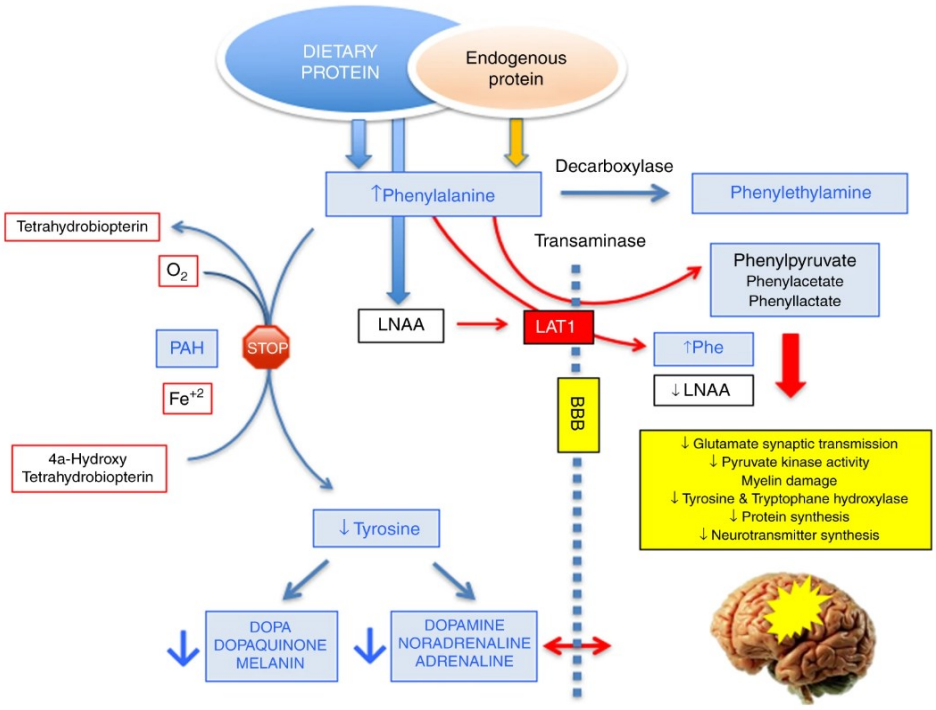

Figure 10: PKU flowchart and altered biochemical pathways that lead to neurological defects. Patients with phenylketonuria (PKU) lack PAH, and as consequence L-Phe plasma levels increase achieving toxic levels in the brain. L-Phe in excess is converted in Phenylpyruvate, Phenylacetate, and Phenyllactate, that are highly toxic for the brain. L-Phe competes with the other large neutral aminoacids (LNAA) for the same L-type carrier (LAT-1) to cross the blood–brain barrier (BBB). In addition, circulating L-Tyr decreases and subsequently the synthesis of metabolites such as dopamine, noradrenaline, and adrenaline diminishes. Picture adapted from *Rausell et al., 2019*.

Oxidative stress

Regarding oxidative stress, damage to DNA, proteins and lipids have been reported in peripheral blood of patients with PKU *in vivo* and *in vitro* in a dose-dependent manner (Sitta, Manfredini, *et al.*, 2009). In the plasma and erythrocytes of phenylketonuric patients, oxidative protein and lipid damage has been described, measured by carbonyl formation, oxidation of sulfhydryl, content of reactive substances of thiobarbituric acid (TBA-RS) and malondialdehyde (MDA) (Sirtori *et al.*, 2005; Sanayama *et al.*, 2011). At cerebral level, DNA oxidative damage has been reported in PKU patients, implying that ROS (Reactive Oxygen Species) production is increased in this disorder. In addition, ERK1/2, crucial enzymes in the MAPK signaling pathway and in the myelination process (Newbern *et al.*, 2011; Jeffries *et al.*, 2016), showed an altered expression and an impaired phosphorylation activity in a PKU rat model (Martinez-Cruz *et al.*, 2002; Li *et al.*, 2010). Low levels of total antioxidants in plasma, such as L-carnitine, β-carotene, coenzyme Q10 and an alteration in the activity of the enzyme catalase (CAT, EC 1.11.1.6), superoxide dismutase (SOD1, EC 1.15.1.1) and glutathione peroxidase (GPX1, EC 1.11.1.9), indicate impaired antioxidant defense, thus causing oxidative stress (Sirtori *et al.*, 2005; Sitta, Barschak, *et al.*, 2009). Several studies carried out on a PKU mouse model, confirm the alteration of these enzymes and report changes in the metabolism of glutathione (GSH) in the various brain tissues.

In this scenario, therefore, the high concentration of L-Phe leads to an increase in the oxidation of sulfhydryl, an increase in the levels of TBA-RS and MDA and the oxidation of 2'-7'-dichlorofluorescin; all this causes lipid and protein damage, as well as an increase in the production of the corresponding reactive oxygen species (Fernandes *et al.*, 2010; Moraes *et al.*, 2013). In addition to L-Phe, *in vitro* studies have also shown that the metabolites that derive from L-Phe including phenylpyruvate (PPA), phenyllactate (PLA) and phenylacetate (PAA), can affect the action of the antioxidant enzymes. While PLA and PAA increase the activity of the SOD1 enzyme, PPA decreases glucose-6-phosphate dehydrogenase (EC 1.1.1.49), indicating a possible indirect mechanism by which L-Phe leads to oxidative stress (Dorland *et al.*, 1993; Ribas *et al.*, 2011; Bortoluzzi, Dutra Filho and Wannmacher, 2021).

Neurotransmitters deficiency

The main hypothesis is that the high levels of the amino acid and its metabolites act as neurotoxic substances for the brain (Ressler and Nemeroff, 2000; Joseph and Dyer, 2003). Several studies report that high levels of L-Phe in humans and in the mouse model of PKU lead to a decrease in serotonin, dopamine, and norepinephrine levels, making patients more susceptible to neurological symptoms (Ressler and Nemeroff, 2000; Surtees and Blau, 2000). In fact, since L-Tyr is a precursor of the most of the abovementioned neurotransmitters, the L-Tyr decreasing observed during PKU leads to the subsequent diminishing of the synthesis of L-Tyr metabolites such as dopamine, noradrenaline, and adrenaline (Sawin, Murali and Ney, 2014). Moreover, L-Phe, at high concentrations, appears to be a competitive inhibitor of tyrosine hydroxylase (EC 1.14.16.2) and tryptophan hydroxylase (EC 1.14.16.4), enzymes important for the synthesis of neurotransmitters such as dopamine and serotonin (Choi and Pardridge, 1986; Harding *et al.*, 2014). The metabolites of L-Phe also inhibit an enzyme involved in the metabolism of neurotransmitters, such as 5-hydroxytryptophan decarboxylase/dopa decarboxylase (Justice and Hsia, 1965). The high levels of L-Phe in the brain, therefore, cause neurological damage due to the amino acid's ability to cross the blood brain barrier via the neutral amino acid transporter 1 (LAT1). As LAT1 is a transporter that allows tyrosine and tryptophan to enter brain cells (Pietz *et al.*, 1999), high concentrations of L-Phe hinder their entry and thus L-Phe accumulates in the brain, interfering both with the synthesis of neurotransmitters and with the possibility of synthesizing proteins where tryptophan and tyrosine are significantly present (Hoeksma *et al.*, 2009).

Brain protein synthesis

As mentioned before, protein synthesis and metabolism are altered in PKU patients and animal model, especially at the brain level; in fact, it was reported a negative correlation between cerebral protein synthesis rate and supra-physiological plasma concentrations of L-Phe (200-500 μM) (Pardridge, 1998). Moreover, it was documented that an increase in the circulating L-Phe concentration was inversely proportional to the cerebral protein synthesis rate, presumably via impaired LNAA transport across blood-brain barrier (de Groot *et al.*, 2013) and decreased L-Tyr incorporation into protein in central nervous system in PKU patients (de Groot *et al.*, 2015). Nonetheless, although playing an important role, decreased LNAA availability is reported to be not pivotal to the low protein synthesis rate observed in the PKU murine model (Smith and Kang, 2000). The differential cerebral protein expression profile between brain protein expression of PKU heterozygous healthy mice and $PAH^{ENU2(-/-)}$ mice has also been observed by Imperlini *et al*. (2014); what resulted, using the electrophoretic technique, was the identification of 21 differentially expressed proteins: 4 of these were over-expressed (GLU2/3, NR1), while 17 were under-expressed (e.g. CKB, DPYSL2, ENO, PGAM1, PKM and SYN2) (Imperlini *et al.*, 2014).

Lipid metabolism

Protein metabolism is not the only one to undergo changes caused by the high level of L-Phe; in fact, even the lipid metabolism undergoes important changes. Nagasaka *et al.* (2014), demonstrated that PKU patients had altered levels of lipoproteins, including total cholesterol, HDL, LDL, and apolipoprotein A-I/A-II and B (Nagasaka *et al.*, 2014). Low cholesterol levels can be caused by impaired synthesis of the cholesterol itself due to a low expression of hydroxymethylglutaryl-CoA reductase (HMGR), a key enzyme in the genesis of cholesterol (Shefer *et al.*, 2000). L-Phe, PPA and PAA have been shown to inhibit, *in vitro*, both the activity of mevalonate 5-pyrophosphate decarboxylase (EC 4.1.1.33) and the activity of HMGR in chicken liver at similar concentrations found in PKU patients (Castillo *et al.*, 1991). Furthermore, the levels of docosahexaenoic acid (DHA) and arachidonic acid (AA) are also decreased and this deficit seems to play a key role in those diseases in which neurological damage is present (Cockburn *et al.*, 1996).

Bioenergetics defects and calcium homeostasis

Energy metabolism impairment has been reported in PKU animal models and patients. In fact, significant decrease of succinate dehydrogenase (EC 1.3.5.1) and mitochondrial respiratory chain complexes I-III functionality were detected in the cerebral cortex of rats with experimentally induced HPA (Rech *et al.*, 2002), as well as creatine kinase (CK; EC 2.7.3.2) activity (a key enzyme

for maintenance of ATP homeostasis (Wallimann, Tokarska-Schlattner and Schlattner, 2011)). Moreover, decreased serum ubiquinone-10 (Coenzyme Q) concentrations are significantly inhibited in phenylketonuric patients (Costabeber *et al.*, 2003).

Altered calcium homeostasis is also one of the hypotheses made in order to explain the neuropathological outcomes observed in PKU. In fact, calcium homeostasis is crucial for brain function and its dysregulation in PKU was suggested by several works which report dysfunction of Ca^{2+}/calmodulin-dependent protein kinase IIα (Liang *et al.*, 2011), along with altered Ca^{2+} uptake and efflux (Yu *et al.*, 2007) in PKU mice and in high L-Phe treated cortical neurons, respectively.

Hypomyelination

As reported previously, the most important outcomes observed in PKU patients and animal model (i.e. $PAH^{ENU2(-/-)}$ mouse) are white matter pathologies, which include hypomyelination, cortical neurons alterations and injuries to the corpus callosum and striatum; taken together, these white matter damages contribute to the neurodegeneration and intellectual deficits observed during HPA (González *et al.*, 2018; Klippel *et al.*, 2021).

The impaired myelination at the CNS levels, which is reported in PKU subjects, is often associated with psychiatric conditions, such as bipolar disorders, psychosis and schizophrenia (Lewandowski *et al.*, 2015; Mighdoll *et al.*, 2015). Myelination in the CNS is the process by which the myelin sheaths, which are produced by oligodendrocytes (OLs), surround and isolate the axons, supporting the saltatory action potentials (Nickel and Gu, 2018). Axon integrity depends on the support of the myelin body and myelin plays an important role in axonal metabolic support (Saab and Nave, 2017). Several works in the literature state that, in PKU murine model and in treated and untreated PKU patients, the main neuropathological aspects found in the brain, in addition to those described, are hypomyelination and gliosis (Malamud, 1966; Dyer *et al.*, 1996; Schoemans *et al.*, 2010; González *et al.*, 2018). In rodents, the proliferation and maturation of oligodendrocytes occurs during postnatal life and myelination is virtually complete at 30 days of age (Norton and Poduslo, 1973). In the same period, the brain of phenylketonuric mice is exposed to a notable increase in the concentration of L-Phe in the blood and the oligodendrocytes seem to be specifically influenced by the high levels, undergoing to a significant reduction in myelinated axons (Schoemans *et al.*, 2010; Pascucci *et al.*, 2018). Nonetheless, oligodendrocyte development and myelin sheath quantity (the latter measured *in vitro* with indirect methods), seems not to be affected by high levels of L-Phe or its derivatives (Schoemans *et al.*, 2010). Studies carried out on the BTBR mouse model have also found a

reduction in an important protein associated with myelin, namely the basic myelin protein (MBP), which is essential for the assembly (wrapping) of the myelin sheath. Preclinical studies showed that MBP is downregulated in the presence of high levels of L-Phe in the bloodstream, resulting in defective myelination (Dyer *et al.*, 1996; Pascucci *et al.*, 2018), which may be prevented (Rossi *et al.*, 2014; Pascucci *et al.*, 2018) or reversed (Burri *et al.*, 1990) by lowering blood L-Phe levels (**Figure 11**).

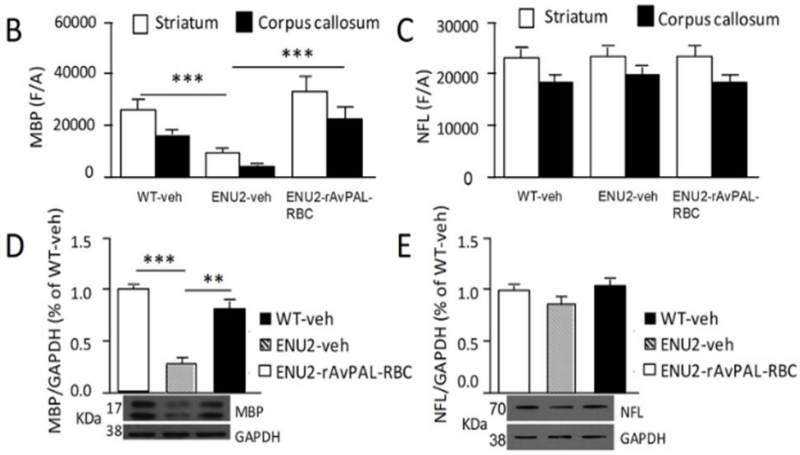

Figure 11: Representative immunoblots and densitometric graphs of MBP (**D**) and NFL (**E**) showing the expression level of the two proteins in WT-veh, ENU2-veh and ENU2-rAvPAL-RBC mice. Picture taken from *Pascucci et al., 2018.*

Regarding hypomyelination, it should be emphasized the potential role of the altered lipid metabolism observed in PKU patients (Nagasaka *et al.*, 2014), already discussed. In fact, changes in the synthesis and/or availability of cholesterol and other lipoproteins can lead to hypomyelination, since that cholesterol is the only integral myelin component that is essential and rate-limiting for the development of myelin in the central and peripheral nervous system (Saher *et al.*, 2005). Taken together, all these aspects try to explain the CNS damages observed in untreated PKU patients and mice; however, the exact pathophysiology underlying the brain damage caused by the excess of L-Phe is not yet clear (Schuck *et al.*, 2015; Klippel *et al.*, 2021).

1.1.8 CHROMATIN REMODELING IN PKU BRAIN AND miRNA HYPOTHESIS

Epigenetic regulation is one of the most important components within the eukaryotic genomes and is essential in the development of mammals. Epigenetics is the study of all the heritable modifications that lead to variations in gene expression without altering the DNA sequence. The epigenetic modifications regulate the access of transcription factors to their sites binding on the DNA, directly controlling the functional activation of genes (Hamilton, 2011). Among the main epigenetic mechanisms, the DNA methylation and changes in histones are of particular interest,

as they can lead to a change in the phenotype without a concomitant alteration of the genotype (Zhang, Lu and Chang, 2020). The transcription of the genome is a finely regulated process, in which proteins known as transcription factors play a crucial role. The latter bind to specific DNA sequences (for example the promoters), activating or repressing the expression of single genes and consequently their translation into proteins (Mazzio and Soliman, 2012). In this scenario, DNA is characterized by a complex structure, and it is organized in subunits called nucleosomes. In short, the nucleosomes contain 150 pairs of nucleotide bases wrapped around a central basic protein complex composed of histones, and the set of DNA and histones together constitutes the chromatin (Sundaramoorthy and Owen-Hughes, 2020; Stepanov *et al.*, 2022). The greater or lesser level of compactness of the DNA in the nucleosomes, controls the levels of gene transcription. Chromatin is divided in two categories, which depend on many epigenetic mechanisms:

1. Euchromatin: open shape
2. Heterochromatin: closed and condensed shape

The most important epigenetic mechanisms are methylation, phosphorylation, and acetylation of DNA and/or histones. Acetylation and phosphorylation take place on the N-terminal tails of histone proteins, which loosen, leaving the DNA free for transcription (Sundaramoorthy and Owen-Hughes, 2020). Methylation, on the other hand, which consists in the addition of a methyl group $-CH_3$ on the cytosine residues of the DNA and on the N-terminal tails, transforms euchromatin into heterochromatin and causes the repression/decrease of gene expression in the affected genes (**Figure 12**).

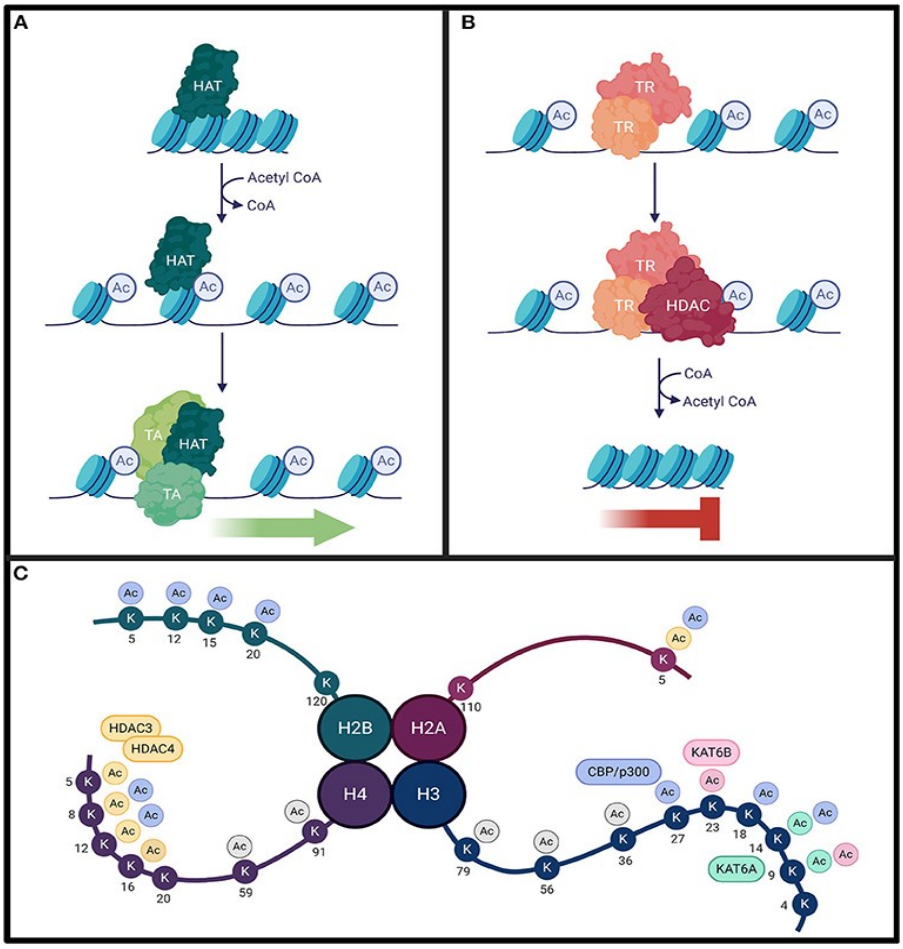

Figure 12: **(A) Histone acetyltransferases (HAT) acetylate histone lysine residues using acetyl CoA cofactor**. This provokes the weakening of the electrostatic interactions between positively-charged histones and negatively-charged DNA to loosen chromatin structure. The final outcome is DNA exposure, allowing for the recruitment of transcriptional activators (TA). (**B**) On the other hand, transcriptional repressor (TR) complexes can interact with histone deacetylases (HDAC) to remove these modifications. This strengthens the electrostatic interactions between the DNA and the histones, resulting in compact chromatin, inhibiting transcription. (**C**) Lysine acetylation can occur on all four histone subunits. Each HAT/HDAC has preferred target sites. While KAT6A and KAT6B acetylate residues with high specificity, CREB-binding protein (CBP, part of the histone acetyltransferases group) and HDAC4/HDAC3 complexes have a broader range of targets. Picture taken from *Fallah et al., 2021*.

In this way, the coupling of the RNA polymerase does not occur, and the transcription process is inhibited. It is therefore possible to include DNA methylation among the mediators of gene function (both normal and pathological) and several pathologies present this type of chromatin remodeling (Mazzio and Soliman, 2012; Zhang, Lu and Chang, 2020), including PKU. In fact, aberrant DNA methylation has been observed in postmortem brains of PKU patients and an extensive epigenome repatterning has been detected in the CNS of $PAH^{ENU2(-/-)}$ mice (Dobrowolski *et al.*, 2014, 2015, 2016). These epigenetic modifications may lead to an abnormal expression of important proteins involved in many neurological processes, such as axon guidance, synaptic transmission, and dendritic spines development (Dobrowolski *et al.*, 2015, 2016), contributing to explain abnormal synaptogenesis and dendritic development found in PKU patients and in ENU2 mice (Bauman and Kemper, 1982; Huttenlocher, 2000; Andolina *et al.*,

2011). Interestingly, L-Phe restricted diet in ENU2 mice displayed an attenuated pattern of aberrant DNA methylation, highlighting the fact that high L-Phe toxic exposure can modify the brain epigenome, leading in turn to hypermethylated or hypomethylated gene coding regions (Dobrowolski *et al.*, 2016). Among the latter, differential DNA methylation has been observed in genomic loci enriched in microRNAs (miRNAs), which are able to inhibit the translation or to degrade target mRNAs via base pairing to complementary sites in the target mRNA 3'-UTR (Bartel, 2004) (see following paragraph). Therefore, miRNAs upregulation in PKU mice and patients may have secondary effects upon the expression of targeted proteins.

1.1.8.1 miRNAs BIOGENESIS AND MECHANISM OF ACTION

As mentioned in the previous paragraph, microRNAs (miRNA) are a class of non-coding RNAs with an average length of 22 nucleotides that play important roles in regulating gene expression. miRNAs are involved in practically every cellular process and are mandatory for animal development, cell differentiation and homeostasis (Bartel, 2004). The miRNA primary repository database miRbase (www.mirbase.org) currently counts 38589 entries and more than 60% of human protein-coding genes could potentially harbor predicted miRNA target sites (Kozomara, Birgaoanu and Griffiths-Jones, 2019). Deregulation of miRNA function and up/downregulation of miRNAs expression are associated with numerous diseases such as neurodegenerative disorders and cancer (Bartel, 2004; Kehl *et al.*, 2017). The latter has been extensively studied over the years, considering miRNAs as both oncogenes (the so-called oncomirs) or tumor suppressors. Moreover, some miRNAs are deemed to be affordable prognostic markers or potential targets for novel cancer therapies, as well as a potential new class of drugs against multiple diseases (Macfarlane and Murphy, 2010). The majority of miRNAs are transcribed in the nucleus from DNA sequences into primary miRNAs (pri-miRNAs) by RNA polymerase II (Pol II); during this phase, pri-miRNAs present the characteristic hairpin structure. Pri-miRNAs are then processed into precursor miRNAs (pre-miRNAs) thanks to the cleavage mediated by the microprocessor complex, which consists in a RNA binding protein DiGeorge Syndrome Critical Region 8 (DGCR8) and a ribonuclease III enzyme, Drosha (Han *et al.*, 2004; Macfarlane and Murphy, 2010; Gebert and MacRae, 2019). The presence of this complex discriminates between the canonical miRNA biogenesis pathway (with complex) and the non-canonical miRNA biogenesis pathways (without complex). Following the canonical pathway, pre-miRNAs are then exported to the cytoplasm by an exportin 5 (XPO5)/RanGTP complex and subsequently processed by the RNase III endonuclease Dicer1 to produce the mature miRNA duplex

(Bohnsack, Czaplinski and Gorlich, 2004). The name of the mature miRNA form depends on the direction of the miRNA. In fact, the -5p strand arises from the 5' end of the pre-miRNA hairpin, while the -3p strand emerges from the 3' end (O'Brien *et al.*, 2018). Lately, either the -5p or -3p strands of the miRNA duplex is loaded into the Argonaute (AGO1-4) family of endonucleases in order to form a miRNA-induced silencing complex (miRISC) (Gebert and MacRae, 2019; Jin, Zhan and Zhou, 2021). Most of the mature miRNAs mediate gene regulation by binding to a specific sequence at the 3' UTR of their target mRNAs; this process usually interfere with the eIF4F complex, provoking translational repression and mRNA deadenylation and decapping (**Figure 13**).

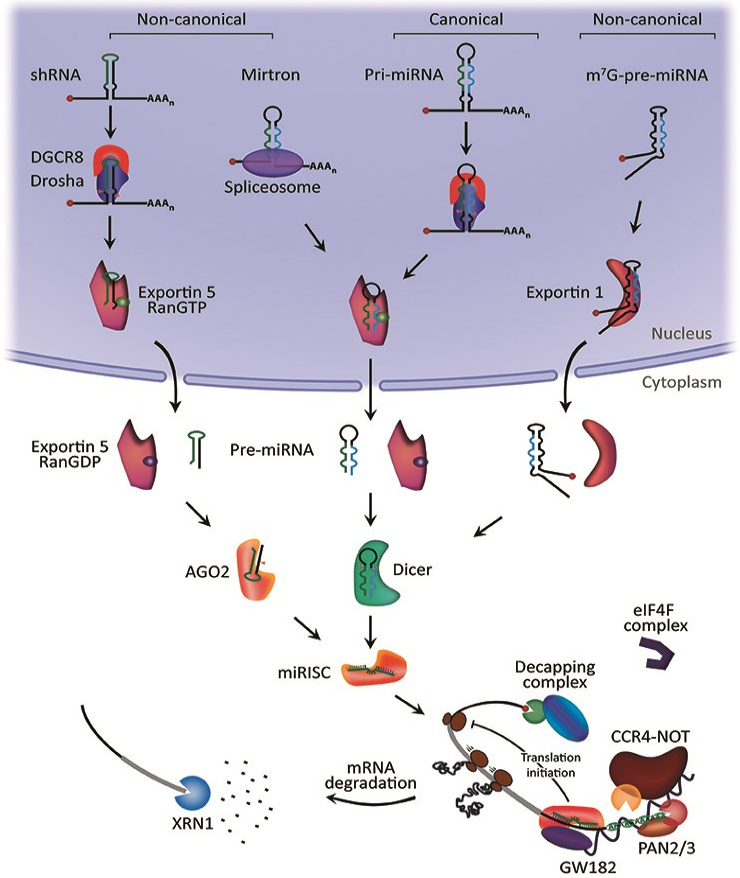

Figure 13: **microRNA biogenesis and mechanism of action**. Canonical miRNA pathway begins with the generation of the pri-miRNA transcript. The microprocessor complex, constituted of Drosha and DiGeorge Syndrome Critical Region 8 (DGCR8), cleaves the pri-miRNA to create the precursor-miRNA (pre-miRNA). The pre-miRNA is exported to the cytoplasm by the Exportin5/RanGTP complex and processed to produce the mature miRNA duplex. Finally, either the 5p or 3p strands of the mature miRNA duplex is loaded into the Argonaute (AGO) family of proteins to form a miRNA-induced silencing complex (miRISC). In the non-canonical pathways, small hairpin RNA (shRNA) is initially cleaved by the microprocessor complex and exported to the cytoplasm via Exportin5/RanGTP. They are further processed via AGO2-dependent, but Dicer-independent, cleavage. Picture taken from *O'Brien et al., 2018.*

miRISC complex target specificity is achieved thanks to the interaction with complementary sequences on target mRNA, which are called miRNA response elements (MREs). The whole miRNA:MRE recognition process is led by a small sequence of the miRNA called seed region or

seed sequence, which is a conserved heptametrical sequence mostly located at positions 2-7 from the miRNA 5´-end (Kehl *et al.*, 2017; O'Brien *et al.*, 2018). Even though base pairing of the entire miRNA and its target mRNA does not match perfectly, the seed sequence needs to be totally complementary. The extent of the MRE complementarity is fundamental in determining the target mRNA's fate (Agarwal *et al.*, 2015; Kehl *et al.*, 2017); in fact, a near full complementarity between miRISC and target mRNA leads to mRNA cleavage due to the action of the endonuclease AGO2, while the presence of mismatches in the miRNA:MRE interaction complex results in imperfect RNA hybrids with bulges and in the subsequent translational inhibition and target mRNA decay mediated by miRISC (Kehl *et al.*, 2017).

Noteworthy, miRNA binding sites have also been detected in other mRNA regions, such as the 5' UTR and the CDS (coding sequence) (Lee *et al.*, 2009). As the canonical binding on the 3' UTR, miRNA binding in these non-canonical regions results in silencing effects on gene expression. Moreover, binding sites have been discovered also in promoter regions, resulting in transcriptional activation of the interested genes (Vasudevan, 2012). However, these interactions require more studies in order to understand their functional activity.

1.1.8.2 miRNA TARGETS PREDICTION

The experimental validation of miRNA:mRNA target interactions relies primarily on computational prediction targets that involve the usage of bioinformatic prediction tools (Peterson *et al.*, 2014). These tools enclose a range of different computational approaches, ranging from the modeling of physical interactions to the incorporation of machine learning, and usually focus their attention on 4 main features:

- seed sequence match – as reported before, the seed sequence is a short sequence of 2-8 nucleotides located at the 5' end of the miRNA. For most tools, a perfect match between miRNA seed sequence and mRNA 3' UTR has no gaps in the alignment and involves a Watson-Crick (WC) match, which is characterized by the well-known pairs between adenosine (A) with uracil (U) and guanine (G) with cytosine (C). There are multiple types of seed match that can be considered and evaluated depending on the algorithm and, so, on the chosen prediction tool (Lewis *et al.*, 2003):

    1. 6mer: A perfect WC match between the miRNA seed sequence and mRNA for six nucleotides.
    2. 7mer-m8: A perfect WC match from nucleotides 2–8 of the miRNA seed.

3. 7mer-A1: A perfect WC match from nucleotides 2–7 of the miRNA seed in addition to an A across from the miRNA nucleotide 1.
4. 8mer: A perfect WC match from nucleotides 2–8 of the miRNA seed in addition to an A across from the miRNA nucleotide 1.

- free energy - free energy (or Gibbs free energy) is recognized as a reliable feature for assessing the stability of a biological system. If the binding of a miRNA to a candidate target mRNA through WC is predicted to be stable, it is considered more likely to be a precise evaluation of a true target of the miRNA. Nonetheless, given the difficulty in measuring free energy directly, usually the change in free energy during a reaction is considered (ΔG). In fact, thermodynamic stability (ΔG) of the miRNA-mRNA duplex is given by the free energy gained by binding of miRNA to the target site, and reactions with a negative ΔG have less energy available to react with other system, thus resulting in an increased stability (Yue, Liu and Huang, 2009).

- conservation – conservation is referred to as the maintenance of a sequence across species. Analysis on the conservation of a miRNA sequence is a useful tool to predict potential miRNA:mRNA interactions because, in case of conservation between species, an already experimentally validated miRNA for one species (i.e., Homo sapiens) could provide insights about target prediction and functionality of a miRNA from another species (i.e., Mus musculus). Generally, there is higher conservation in the miRNA seed sequence than in the non-seed region (Lewis *et al.*, 2003; Fujiwara and Yada, 2013).

- site accessibility - site accessibility is a measure of the capability of a miRNA to locate and hybridize with an mRNA target. In fact, after the transcription process, mRNA can assume secondary structures (i.e. bulges or stem loops) which can interfere with a miRNA's ability to bind to a target site (Mahen *et al.*, 2010). This feature is used in the bioinformatic prediction tools to assess the predicted amount of energy required to make a site accessible to a miRNA, thus evaluating the probability that an mRNA is the target of a miRNA (Long *et al.*, 2007).

The most important web-based free miRNA:mRNA prediction tools are TargetScan, miRDB, PICA, RNAhybrid, DIANA-microT-CDS and miRanda (Paraskevopoulou *et al.*, 2013; Agarwal *et al.*, 2015; Chen and Wang, 2020).

1.1.8.3 miRNAs ON NEURODEVELOPMENTAL DISEASES

Over the last decade, microRNA regulation on oligodendrocytes development and myelination has received growing interest. In fact, due to the capability of miRNAs to control and mediate multiple biomolecular and cellular processes (i.e. cell differentiation, inflammation and apoptosis), they have emerged as crucial molecules that could regulate a variety of pathogenic mechanisms in demyelinating disease such as multiple sclerosis (MS) leukodystrophies and perinatal hypoxia (Bartel, 2004; Galloway and Moore, 2016). Approximately 70% of known miRNAs are expressed in the brain (Cao *et al.*, 2006), highlighting the potential involvement of these molecules in the mammalian CNS, and conditional deletion of Dicer1 gene in mice are associated to embryonal lethality (Bernstein *et al.*, 2003). Moreover, the absence of Dicer1 complex in the transgenic mice results in reduced expression of several myelin protein (MAG, MOG, PLP1, and CNP) and a different miRNA profiling, with downregulation of miR-32, -144 and -219 and upregulation of miR-7a, -7b, 181a-1 and -592 (Dugas *et al.*, 2010; Zhao *et al.*, 2010). Other studies have recognized specific miRNAs as crucial for normal CNS development, in particular for the transition from progenitor cell to myelinating oligodendrocytes. These findings were observed especially for miR-219 and miR-338, which are two of the most highly downregulated miRNAs in MS (Lau *et al.*, 2008; Dugas *et al.*, 2010; Zhao *et al.*, 2010); in fact, these miRNAs are critical in oligodendrocyte differentiation and thus their downregulation could suggest a failure of OPCs (oligodendrocyte precursor cells) into mature OLs in chronic MS. On the other hand, perinatal hypoxia-ischemia (HI) has been associated with an increase of miR-138, -338 and -21 in a murine model of HI (Birch *et al.*, 2014).

Another miRNA which is implicated in CNS development is miR-23a, which has been identified as a regulator of lamin B1, an inhibitor of myelin genes expression; in fact, miR-23a upregulation promotes CNP and MBP in glial cultures and an increase of miR-23a has been observed in active MS lesions, indicating that this miRNA is crucial for the correct axon myelination (Lin and Fu, 2009; Lin *et al.*, 2013). Other miRNAs critical for the OLs maturation are miR-9, which represses PMP22 protein (peripheral myelin protein 22) (Lau *et al.*, 2008), and miR-124, which is highly expressed in mature neurons and mediates the differentiation of precursor cells to neurons. This miRNA is also increased during hippocampal demyelination in both mice undergoing cuprizone-induced demyelination and human MS lesions (Dutta *et al.*, 2013). miR-146a, on the other hand, promotes the differentiation of MBP expressing OLs from OPCs (Liu *et al.*, 2017) and the miR-181 family has been implicated in CNS ischemia and inflammation (Hutchison *et al.*, 2013; Moon, Xu and Giffard, 2013).

Taken together, these findings suggest the potential role of multiple miRNAs on CNS development and regulation. Nonetheless, most of the obtained results must be assessed in the context on the pathological brain and *in vivo* and *in vitro* models of remyelination will be necessary to confirm and validate the exact mechanism by which these molecules act on the cerebral level.

1.2 OLIGODENDROCYTES AND MYELIN ORGANIZATION

1.2.1 GLIAL CELLS

The nervous system is made up of neurons and glial cells that perform multiple functions such as (1) nourishing and supporting neurons, (2) nerve tissue isolation, and (3) protection from foreign bodies in the event of injury. There are four main classes of glial cells in the central nervous system (CNS): astrocytes, oligodendrocytes, ependymal cells and microglia, each with different functions. In the peripheral nervous system (PNS), in place of oligodendrocytes there are Schwann cells, which are responsible for the myelination of axons and their regeneration (Jäkel and Dimou, 2017).

1.2.2 OLIGODENDROCYTES PRECURSOR CELLS AND OLIGODENDROCYTES

Oligodendrocytes (OLs) are highly specialized central nervous system (CNS) cells; they are equipped with thin, scarcely branched extensions and a knotty surface, which isolate the neuronal axons to provide them with trophic, metabolic and functional support. OLs are necessary for the correct transmission of neuronal action potential and, during brain development, they are the last cells to be generated (El Waly *et al.*, 2014). Their main function is to form the myelin sheath, arising from tubular neuroepithelial cells after being generated from oligodendrocyte progenitor cells (OPCs) usually located in the subventricular zone (Hayashi and Suzuki, 2019; Kuhn *et al.*, 2019). Before reaching complete maturation, the oligodendrocytes go through several stages of development, with a final differentiation into mature cells which are responsible for the production of myelin (Kuhn *et al.*, 2019). The process is finely and well-regulated, and can be divided into (1) proliferation and migration of OPCs from the subventricular area to the white matter of the CNS and (2) formation of precursors of OLs, differentiation of OLs and final formation of myelinated OLs (Elbaz and Popko, 2019). This differentiation is well regulated by many intrinsic and extrinsic factors, which determine the extent and time of their differentiation during the development of the CNS (Sock and Wegner,

2019). However, it is imperative that a small population of OPCs remain immature or quiescent during development, in order to have a potential source of OLs in case of future demyelination (Dawson *et al.*, 2003) (**Figure 14**).

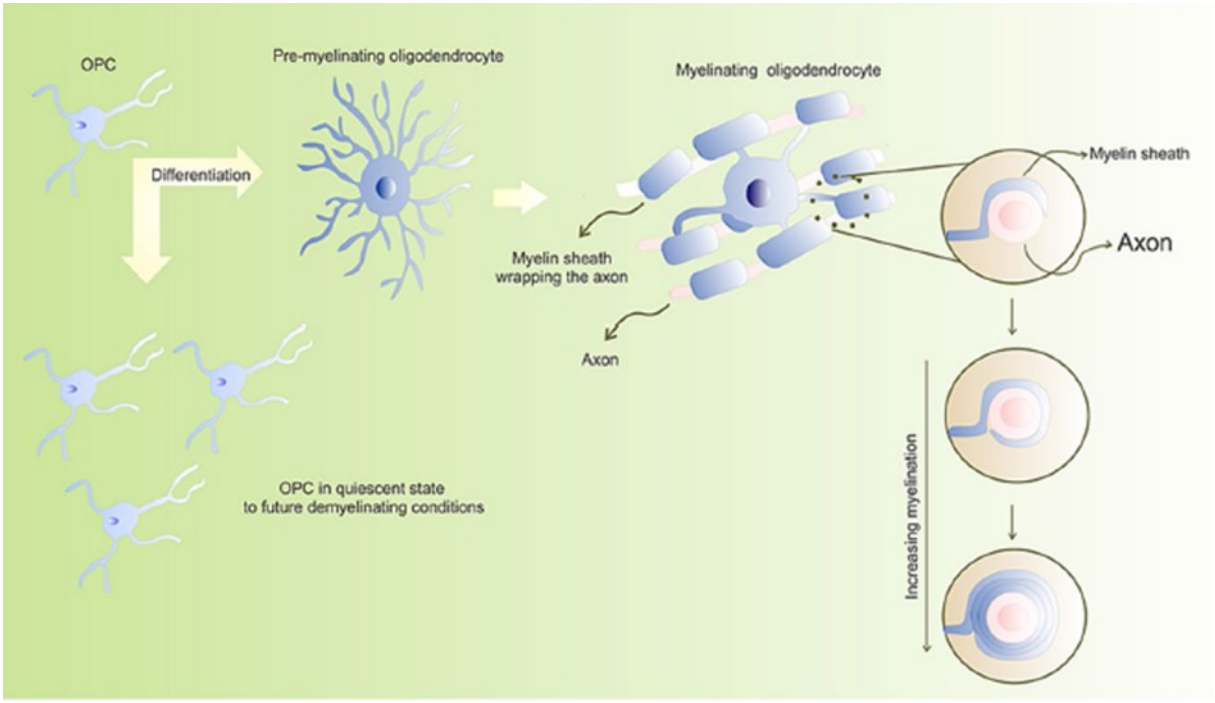

Figure 14: **Scheme of the differentiation of oligodendrocyte progenitor cells (OPCs) into mature and myelinated oligodendrocytes (OLs)**. While many of the OPCs differentiate into pre-myelinated OLs and then into myelinated OLs, a small fraction of these immature cells remains in the quiescent state, providing a source of OLs in potential demyelination conditions, such as PKU. The myelinated oligodendrocytes produce myelin sheaths, which progressively envelop the axons forming insulating layers, thus supporting the propagation of the neuronal action potential along these structures. Picture taken from *Ferreira et al., 2021.*

To ensure that the number of oligodendrocytes (OLs) corresponds to the number of axons to be myelinated, an excess of cells is produced and subsequently eliminated by the process of apoptosis (Trapp *et al.*, 1997). A mechanism that determines the final number of oligodendrocytes is the regulation of a quantity of growth and survival factors, such as platelet-derived growth factor (PDGF-AA), fibroblast growth factor (FGF-2), insulin growth factor (IGF-1), neurotrophin (NT-3) and the ciliary neurotrophic factor (CNTF) (Miller, 2002). This mechanism was confirmed in mice that exhibited over-expression of the PDGF-AA factor, which caused a dramatic increase in the number of OPCs in the embryonic spinal cord, followed in turn by the production of oligodendrocytes at the ectopic level (Calver *et al.*, 1998). Several studies underline the importance of PDGF-AA in inducing mitosis in OPCs, thus supporting their survival and regulating their differentiation rate (Calver *et al.*, 1998). In addition to these factors, during the initial differentiation of OPCs, there are other extrinsic signals that act on the multipotent neural progenitor cell, triggering a cascade of signals that converge on specific transcriptional regulators of the OLs line. Ventrally, one of the predominant extrinsic signals is the sonic

hedgehog protein (SHH), which triggers the expression of oligodendrocyte transcription factor 2 (OLIG2), thus inducing the first embryonic wave of OPCs in the CNS (Winkler and Franco, 2019). Therefore, the exposure of the dorsal neuroepithelium to the SHH protein triggers oligodendrogenesis, while the absence of this protein limits the presence of OLs throughout the central nervous system (Tekki-Kessaris *et al.*, 2001). In summary, OLs are cells capable of myelinating the entire CNS and above all play an important role in maintaining axonal integrity and neuronal survival (**Figure 15**).

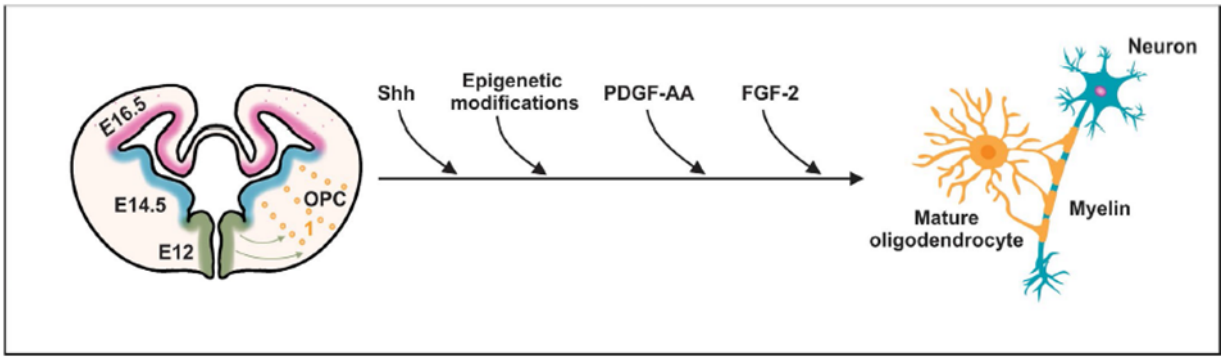

Figure 15: **Process of formation of mature oligodendrocytes**. The first embryonic wave of OPCs begins on day 12 (E12; green). The second wave emerges on the 14.5th day (blue) and the last one on the 16th day (pink). Shh protein, epigenetic modifications, platelet growth factor (PDGF-AA) and fibroblast growth factor (FGF-2) enhance oligodendrocyte maturation and myelin sheath formation. Picture taken from *Ferreira et al., 2021*.

1.2.3 MYELIN STRUCTURAL ORGANIZATION

The myelin sheath is a multilamellar assembly of lipid-rich membranes and proteins that surrounds nerve axons, and it is pivotal for the normal functioning of the nervous system. Its main function is to isolate the axons with a lipid coating in order to guarantee a high electrical resistance and low conductance. The presence of the myelin sheath allows a correct conduction of nerve impulses, amplifying the transmission speed through the so-called "saltatory conduction". In myelinated fibers, in fact, the myelin does not cover the axons in a uniform way, but covers them at intervals, forming characteristic constrictions that topologically resembles the rolling up of a sleeping bag. The interruptions of the myelin sheath, between one segment and the other, are defined as Nodes of Ranvier (**Figure 16**), areas in which voltage-gated sodium channels are concentrated. Thanks to the saltatory conduction, the transmission speed along the axon goes from 0.5-10 m/s in the unmyelinated axons up to 150 m/s for the myelinated ones (Bolino, 2021).

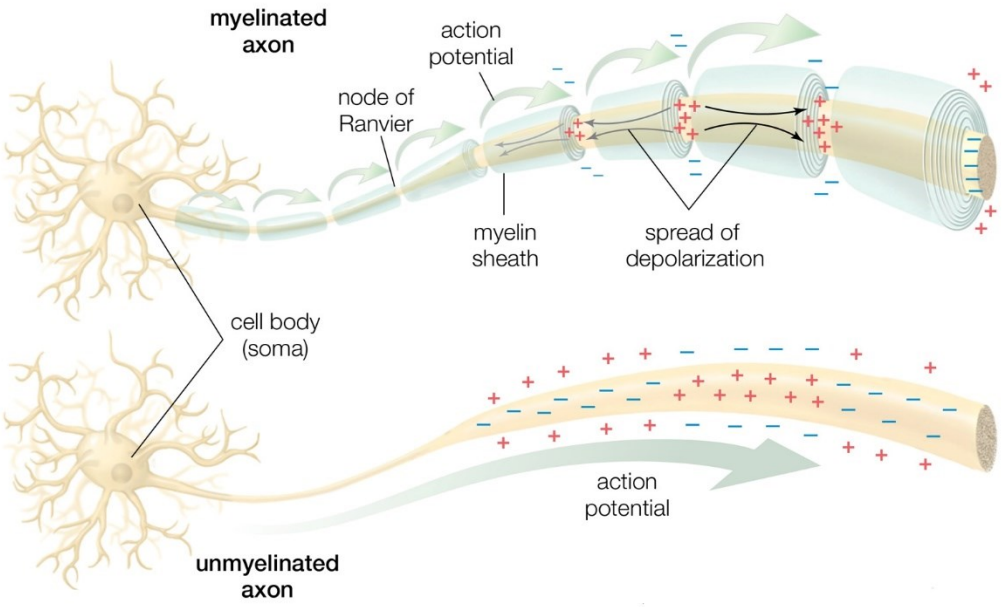

Figure 16: **Propagation of the nerve impulse through Ranvier's nodes**. Picture adapted from *Encyclopaedia Britannica*.

The myelin ultrastructure has been evaluated through years mainly with the electron microscope (EM); myelin features a multi-layered compact membrane (up to 300 coils) formed by an interplay between the so-called major dense line (MDL) and the intraperiod line (IPL). The major dense line represents the tightly condensed cytoplasmic surfaces, while the intraperiod line is an area at which the external surfaces of adjacent myelin membranes are brought together and compacted at a distance of 2–3 nm (Baumann and Pham-Dinh, 2001; Aggarwal, Yurlova and Simons, 2011; Salzer and Zalc, 2016). The space between the extracellular surfaces of adjacent membranes and the presence of cytoplasm on the inner side of the membranes is ~ 12-14 nm. If the myelin is not compact, then a thin layer remains between the two leaflets and the distances between two IPLs are greater than 12 nm, while if the myelin is compact, as reported before, the membranes clump together and the intraperiod distance decreases to 2 nm. At their edges, the myelinated lamellae are strictly connected by tight junctions (TJs) between the membranes of the external flap thanks to the action of the protein claudin-11 (CLDN11) (Morita *et al.*, 1999; Denninger *et al.*, 2015). These interlamellar filaments radially cross the myelin, forming the so-called "radial components" which are fundamental for myelin permeability and paracellular diffusion (Denninger *et al.*, 2015).

Most of these findings on myelin ultrastructure are based on EM studies performed on glutaraldehyde-fixed and dehydrated tissues; however, these treatments were often associated with narrowing and collapse of intracellular spaces. Over the years, technical advances have been reached, with the high-pressure freezing (without fixation) for EM visualization that

provides a better preservation of tissue architecture, including the visualization of cytoplasmic spaces within myelin (Möbius *et al.*, 2010) (**Figure 17**).

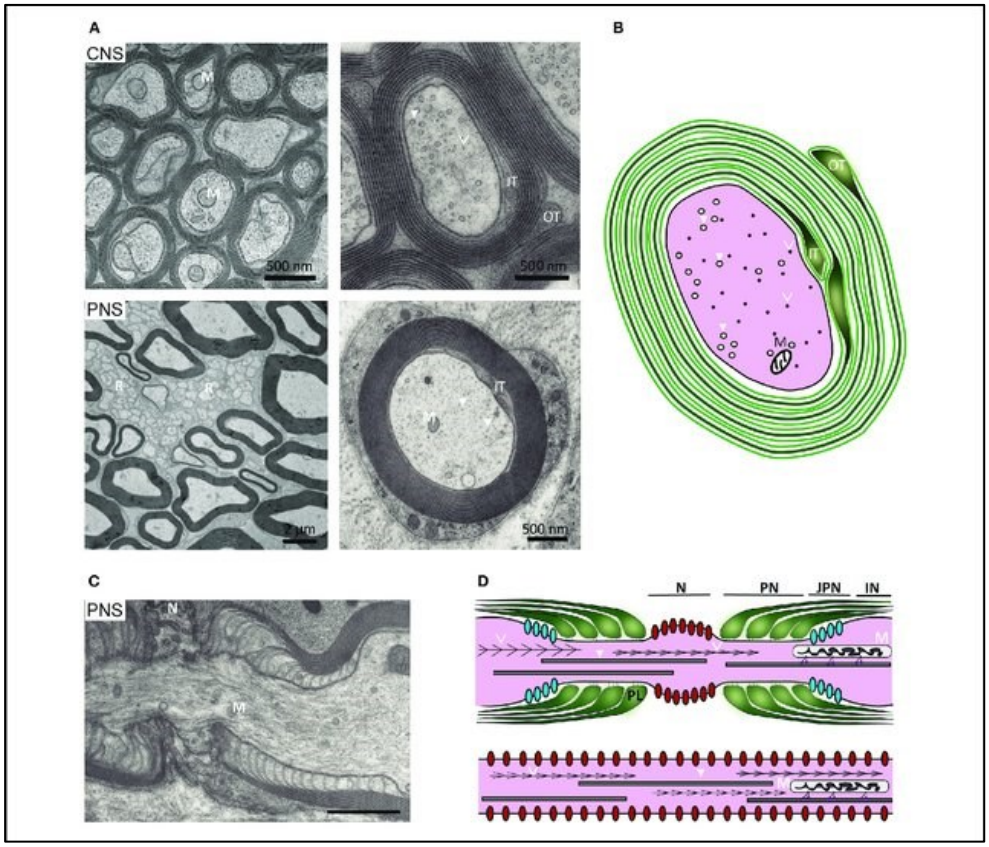

Figure 17: **Ultrastructure of myelinated axons in the CNS and PNS**. (**A, upper**) In the CNS, myelinated axons are densely packed within white matter and the myelin sheaths of neighboring fibers often directly touch. (**A, lower**) In the PNS, the Schwann cell plasma membrane is covered with a basal lamina and the myelinated fibers are separated by connective tissue. (**B**) Schematic representation of a myelinated CNS fiber. (**C**) Electron micrograph of a PNS node of Ranvier and (**D, upper**) schematic representation of the elements of a node: paranodal loops of the myelin sheath (green), Nav1.6 channels (red), Kv1 channels (blue), neurofilaments (arrowheads), microtubules (open arrowheads), mitochondria (M), which are transported along microtubules. N, node; PN, paranode; JPN, juxta paranode; IN, internode. (**D, lower**) Schematic representation of non-myelinated axon with uniform distribution of Nav1.6 channels along the axolemma. Picture and caption taken from *Stassart et al., 2018*.

These are non-compacted regions that include the outer and inner periassonal "tongues" (or "lips") of the myelin membranes, the "paranodal loops" and the "Schmidt-Lanterman incisions" (the latter in the PNS). Cytoplasmic channels, reminiscent of Schmidt-Lanterman incisions, can also be found in the myelin sheaths of the CNS, but largely disappear when myelination is complete (Snaidero *et al.*, 2014). Another method of visualizing these cytoplasmic channels within myelin, called "myelin channels", is to inject diffusible dyes into oligodendrocytes or transgenically expressing fluorescent proteins.

Using the fluorescent dye Lucifer Yellow, a large network of interconnected cytoplasmic pockets (1.9 pockets per 10 µm sheath length) was observed in a previously isolated spinal cord slices (Velumian, Samoilova and Fehlings, 2011). In the adult nervous system, they can provide a functional connection between the oligodendroglial soma and the periassonal space, allowing

the distribution of glial metabolites to the axonal compartment. Considering that oligodendrocytes are also interconnected with astrocytes by means of junctions called gap junctions, glial cells can form a functional "syncytium" within the tracts of white matter (Abrams and Scherer, 2012; Bedner, Steinhäuser and Theis, 2012; Nualart-Marti, Solsona and Fields, 2013). The myelin sheath is also firmly anchored to the axon at each end of an internode, where the myelin membrane never has a compact structure, but ends in the paranodal loops. These loops form septate-like cell-adhesion junctions with the axonal surface and are attached to the axon in the paranodal region by a trimolecular complex formed by the axonal Caspr1-Contactin1 complex and the oligodendroglial neurofascin-155 (NF155) (Dutta and Fields, 2021).

1.2.4 MYELIN COMPOSITION

The myelin sheath is composed of a high percentage of lipids (about 70% -85%) and a low percentage of proteins (about 15-30%). In myelin, the high lipid/protein ratio contributes to the tight packing and organization of the myelin sheaths through non-covalent lipid-protein interactions (Min *et al.*, 2009) (**Figure 18**).

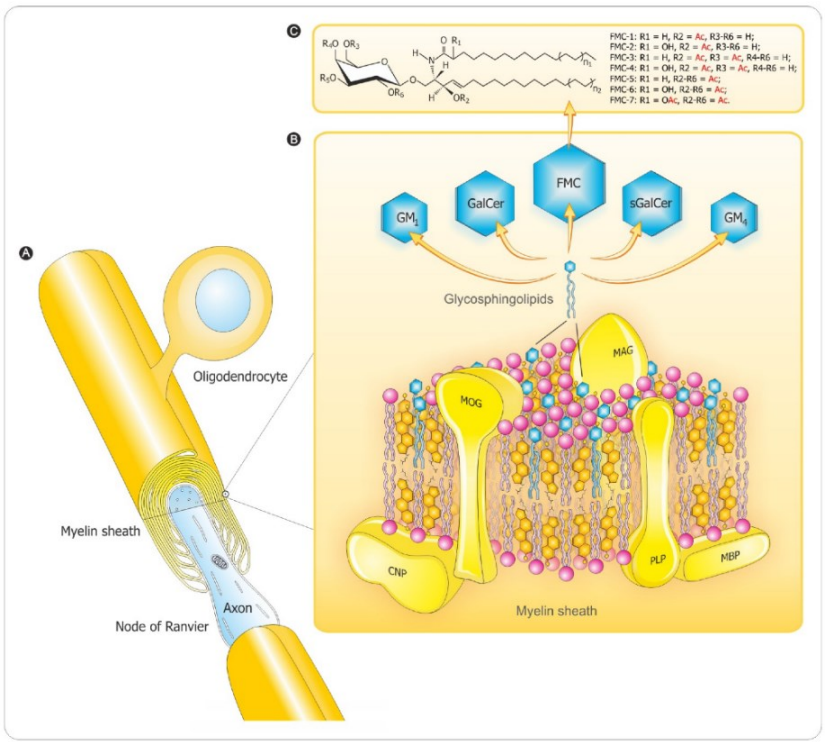

Figure 18: **Schematic representation summarizing features of CNS myelin**: (**A**) architecture; (**B**) 3D-molecular composition and conformation-based assembly and (**C**) the unique sphingosine 3-O-acetylated-GalCer GL series. CNP, 2'3'-cyclic-nucleotide 3'-phosphodiesterase; MAG, myelin-associated glycoprotein; MBP, myelin basic protein; MOG, myelin oligodendrocyte glycoprotein; PLP1, proteolipid protein. Picture taken from *Podbielska et al., 2013*.

Lipid composition: the abundant presence of specific classes of lipids is necessary for the long-term maintenance of myelin (Schmitt, Castelvetri and Simons, 2015). The three main classes of membrane lipids are cholesterol, phospholipids (plasmalogen, lecithin, sphingomyelin) and glycolipids (i.e., galactosylceramide). The lipid composition of the myelin sheath is given by a ratio of 40:40:20 (cholesterol, phospholipids and glycolipids, respectively), unlike other biological membranes which are characterized by a ratio of 25:65:10 (O'Brien, 1965). Myelin is not a simple homogeneous layer of proteins and lipids, but also contains discrete and dynamic lipid domains in the outer leaflet of the plasma membrane that are called lipid rafts. These are characterized by a specific concentration of lipids such as cholesterol and galactosylceramide, together with a low level of phosphatidylcholine, which in turn play a fundamental role in the formation and stabilization of myelin. Cholesterol is one of the most present lipids and in myelin it is inserted into the lipid bilayer to increase its viscosity and to give it stability (Saher *et al.*, 2005; Saher and Stumpf, 2015). Myelin cannot be synthesized without cholesterol, and the availability of cholesterol itself is both a critical prerequisite and a factor limiting the growth of the myelin membrane during CNS maturation (Saher *et al.*, 2005). In fact, synthesis of myelin and oligodendrocytic differentiation are severely disturbed if the oligodendrocytes are not able to synthesize cholesterol, despite their ability to acquire it from neighboring cholesterol-producing cells like the astrocytes (Ferris *et al.*, 2017). Due to the presence of the blood brain barrier (BBB) in the CNS, cholesterol found in myelin comes from *de novo* synthesis in nearby oligodendrocytes or astrocytes (Camargo *et al.*, 2017) and usually its synthesis is higher during myelination. The cholesterol molecules assemble tightly in the lipid rafts and combine with the integral myelin proteins in the Golgi complex in order to reach the myelin sheath through vesicles or via non-vesicular transport (Helle *et al.*, 2013). Another abundant lipid in myelin is the galactosylceramide and its sulfated form, which is called sulfatide. These two glycosphingolipids are abundant in both oligodendrocytes and Schwann cells and, in particular, galactosylceramide is more abundant in the myelin compact form, while sulfatide is more localized in the non-compact myelin (Maier, Hoekstra and Baron, 2008). Together, they account for 20% of the total myelinated lipids in oligodendrocytes. The galactosylceramide present in the myelin bilayer consists of a galactose in the head group, a sphingosine and a terminal group of long-chain fatty acids, which serve to increase the stability of the myelin membrane (Schmitt, Castelvetri and Simons, 2015). Together with highly hydrophobic myelin proteins, these molecules generate important intermolecular hydrophobic forces that contribute to the "zip-fastener" of the myelin membrane. In this way, attractive forces are created, bringing the membranes into close contact, together with repulsive forces against extracellular and cytosolic

fluids (Aggarwal, Yurlova and Simons, 2011). Although galactosylceramides are important for myelin formation, they are not essential and their absence can be partially compensated for by the production of other glycolipids such as glucosylceramide (Saadat *et al.*, 2010). Another category of lipids that is added to cholesterol and galactosylceramides is that of plasmalogens, a subclass of phospholipids mostly found in cell membranes. The ethanolamine plasmalogens are the predominant phospholipids found in myelin and are composed of a choline or ethanolamine head group, a glycerophosphoric acid skeleton and a fatty acid tail (West *et al.*, 2020). Their contribution seems to be to strengthen the bonds with adjacent lipids, thus giving rise to a more compact and stable myelin, although recent studies affirm that the presence of plasmalogens could be crucial to protect myelin from age-related oxidative stress (West *et al.*, 2020). The biosynthesis of plasmalogen begins in the peroxisome and is completed in the endoplasmic reticulum; thereafter, the plasmalogens are transported asymmetrically to the inner leaf of the myelin membrane. Finally, in addition to plasmalogen, phosphatidylcholine is also present, with lecithin and sphingomyelin as the most important molecules. Lecithin is mainly abundant in the PNS and it is useful for the initiation, compaction and maintenance of the plasma membrane (Furse and de Kroon, 2015). Sphingomyelin, on the other hand, is synthesized in many cells in the endoplasmic reticulum and in the Golgi complex; regarding oligodendrocytes, about 50% is synthesized in the plasma membrane in a subcellular zone that is specific for the formation of the phospholipid (Hannun, 1994). Therefore, since myelin requires an abundant presence of fatty acids for its assembly and maintenance, myelinated cells are particularly vulnerable to disorders which involve fatty acids and lipids.

Protein composition: the major protein component of myelin is composed of glycoproteins, followed by basic proteins (**Figure 19**).

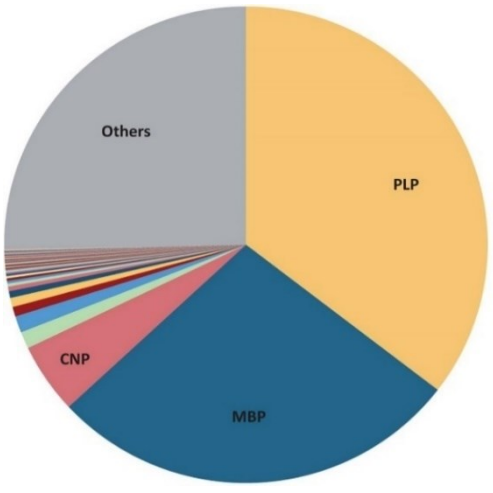

Protein	% (+/- RSD)		Protein	% (+/- RSD)	
PLP1	37,91	0,91	CD9	0,06	0,03
MBP	29,60	0,95	EPB41L2	0,06	0,01
CNP	5,11	0,21	CD82	0,06	0,01
MOG	1,22	0,03	GSN	0,05	0,01
CLDN11	1,20	0,13	CNTN2	0,05	0,00
MOBP	0,70	0,13	CADM4	0,05	0,00
MAG	0,67	0,05	ENPP6	0,05	0,01
SIRT2	0,49	0,03	EPB41L3	0,04	0,00
CD81	0,33	0,073	LGI3	0,04	0,00
TUBB4	0,23	0,051	CFL1	0,04	0,01
BCAS1	0,20	0,02	GPM6B	0,04	0,01
NFASC	0,18	0,01	PADI2	0,04	0,00
CNTN1	0,16	0,02	HEPACAM	0,04	0,01
CA2	0,16	0,03	SEPT2	0,03	0,00
RTN4	0,11	0,02	JAM3	0,03	0,00
SEPT8	0,11	0,02	CD47	0,03	0,01
TSPAN2	0,10	0,02	TPPP3	0,03	0,00
ASPA	0,10	0,07	GPR37	0,03	0,00
SEPT7	0,10	0,01	OPALIN	0,03	0,01
TPPP	0,08	0,01	OMG	0,02	0,01
PLLP	0,08	0,01	GJC3	0,02	0,00
NDRG1	0,08	0,01	CRYAB	0,02	0,00
ANLN	0,07	0,01	Others	27,1	
SEPT4	0,06	0,01			

Figure 19: **Relative abundance of CNS myelin proteins from the brains of healthy c56Bl/6N-mice**. Table taken from *Jahn et al., 2020.*

Among the most important glycoproteins we find:

P0 (myelin protein zero): represents 50-70% of the total myelin proteins in the PNS (Greenfield *et al.*, 1973). It is a 28 kDa integral membrane protein expressed by myelinating Schwann cells (Hai *et al.*, 2002), but also by non-myelinating presynaptic Schwann cells, probably with the function of mediating adhesion between the axon and the Schwann cell (Georgiou and Charlton, 1999). It is highly conserved between species and is encoded by the myelin protein zero (MPZ) gene located on chromosome 1q23.3. P0 occurs in the membrane as a tetramer and interacts with the tetramers of the adjacent membranes to allow the compaction of the myelin. The extracellular domain has similarities with cell adhesion molecules related to immunoglobulins, which could contribute to the formation of the intraperiod of myelin through hydrophobic and electrostatic interactions. The cytoplasmic carboxy terminal domain, together with myelin basic protein (MBP), is probably involved in the formation of the dense myelin line by electrostatic interactions with membrane lipids (Kitamura, Suzuki and Uyemura, 1976).

PMP22 (peripheral myelin protein 22): is a small 22 kDa glycoprotein, with four transmembrane hydrophobic domains. This protein can be found in the PNS compact myelin and it consists of a single N-glycosylation domain. It is also present in small quantities in the plasma membrane of myelinated and unmyelinated Schwann cells, and this suggests its role in the maintenance and assembly of myelin (Snipes *et al.*, 1992).

MAG (myelin associated glycoprotein): is a type I transmembrane glycoprotein and is localized in the periassonal membrane of the Schwann cell and oligodendrocytes; it is also localized in the paranodes and in the Schmidt-Lanterman notches. MAG participates in axonal recognition, adhesion, signaling during the differentiation of glial cells, regulation of axonal growth and in the maintenance of integrity between axon and myelin. The protein contains five immunoglobulin (Ig)-like domains and it belongs to the sialic acid-binding subgroup of the Ig superfamily. Its molecular weight is 100 kDa and binds specific gangliosides present on the axonal membrane. There are 2 isoforms, S-MAG and L-MAG (Quarles, 2007; McKerracher and Rosen, 2015).

MOG (myelin oligodendrocyte glycoprotein): is a 28 kDa transmembrane glycoprotein belonging to the immunoglobulin family and is specific to the central nervous system. It is located on the outermost surface of the myelin sheath and interacts with the components of the extracellular matrix. It seems to be involved in the transduction of extracellular signals in consideration of its localization (Solly *et al.*, 1996).

Among the basic proteins we find:

MBP (myelin basic protein): see dedicated paragraph.

P2 (peripheral myelin protein 2): is a 14.8 KDa cytosolic protein, located on the cytoplasmic side of compact myelin membranes. P2 is a basic protein confined to peripheral nerve myelin and together with myelin basic protein constitute a major fraction of peripheral nervous system myelin protein. The protein is essential for the uptake and transport of fatty acids towards the intracellular organelles, and it is also involved in the targeting of fatty acids to specific metabolic pathways, as well in the maintenance of their pool. The function of binding fatty acids allows the formation and maintenance of the lipid composition of the myelin sheath (Uusitalo *et al.*, 2021).

Other important proteins present in myelin are:

PLP1/DM20 (myelin proteolipid protein): is a 30 kDa integral membrane protein and represents the main protein constituent of myelin in the CNS (Cloake *et al.*, 2018). PLP1 is believed to play primarily a structural role and to be responsible for the formation of the intraperiod line. However, numerous other functions have been proposed for this protein, such as the regulation of the development of oligodendrocytes, the involvement in the initial phases of the interaction between oligodendrocytes and axon, the role in the process of wrapping along the axon by the myelin sheath and axonal and neuronal survival (LeVine, Wong and Macklin, 1990). In PNS, the location and function of this protein is not yet fully understood. DM20, on the other hand, is a protein that derives from the alternative splicing of PLP1 mRNA. The protein sequence of DM20 differs from that of PLP1 by a deletion of 35 amino acids. Although PLP1 and DM20 play important functions in myelin, they are not essential for sheath formation (Dhaunchak and Nave, 2007).

CNP (2',3'-cyclic-nucleotide 3'-phosphodiesterase): is a 47.5 kDa enzyme capable of catalyze the formation of 2'-nucleotide products from 2',3'-cyclic substrates (Schwer *et al.*, 2008). This enzyme is a critical component of the molecular machinery that mediates the early stages of myelination; in fact, it is implicated both in the maintenance of axonal integrity and as an essential factor in generating and maintaining cytoplasm within the myelin compartment (Snaidero *et al.*, 2017). CNP is an oligodendrocyte-specific protein and is localized in the cytoplasm of the glial cells that create the myelin sheath and in the paranodal loops. CNP has been proposed to counteract the membrane zippering mediated by MBP, organizing the actin

cytoskeleton within the cytoplasmic regions of the myelin sheath and thereby keeping the adjacent cytoplasmic leaflets separated. In this way, CNP prevents an excessive membrane compaction mediated by MBP (Snaidero *et al.*, 2017).

Fundamental for the formation of myelin are also the connexins (Söhl, Maxeiner and Willecke, 2005), present in the paranodes and in the Schmidt-Lanterman incisures of the myelin sheath. The connexins constitute the gap junctions that allow the passage of specific substances (ions or low molecular weight molecules) between the cells, having channels that open themselves in response to certain chemical signals (changes in pH or concentration of calcium ions), thus allowing communication between cells (Beyer and Berthoud, 2018). Most neurons express gap junctions, which are regulated during nerve development and differentiation and allow for electrical synaptic transmission. In electrical synapses, unlike chemical synapses, the depolarization wave passes directly from the presynaptic to the postsynaptic neuron without the intervention of chemical mediators. In these synapses, the synaptic surfaces of the two membranes are at intervals fused together, forming tight junctions. These surfaces can also be connected by gap junctions that allow the transmission of the electrical impulse through the passage of ions (Alcamí and Pereda, 2019; Vaughn and Haas, 2022). Among the numerous existing connexins, connexin 26, 32, 36 and 43 are most expressed in the nervous system (Martini and Carenini, 1998). In the formation of myelin, the most present connexin is connexin 32 (called also GJA1) (Martini and Carenini, 1998; Kajiwara *et al.*, 2018).

1.3 MYELIN BASIC PROTEIN

Myelin basic protein (MBP) is the second most abundant protein in the CNS, right after PLP1. It is the only structural protein found so far to be essential for the formation of myelin and is also called "the executive molecule of myelin" (Moscarello, 1997). Classical MBP is encoded by oligodendrocytes from a large gene complex called Golli (Genes of Oligodendrocyte Lineage), present on chromosome 18, from which also families of proteins called Golli-MBP originate. The gene has 11 exons in mice and 10 in humans, including the 7 exons that give rise to classical MBP (Givogri *et al.*, 2001); moreover, it also contains three different transcriptional initiation sites that allow for the expression of two distinct protein subfamilies, which are temporally and locally regulated (Campagnoni *et al.*, 1993; Boggs, 2006; Smith *et al.*, 2013). In fact, while the presence of classical MBP proteins is mainly limited to myelinated cells, Golli-MBP proteins have also been found in neural and non-neural cells (Fulton, Paez and Campagnoni, 2010). In the developing nervous system, an abundant synthesis of the myelin basic protein is required in

oligodendrocytes for the formation of compact myelin sheaths around the axons (Smith *et al.*, 2013).

1.3.1 MBP STRUCTURE AND FUNCTIONS

The isoforms of MBP that originate from the different splicing of a single mRNA transcript are different in mice and humans. In the mouse we find the isoforms 21.5, 20.2, 18.5, 17.24, 17.22 and 14 kDa, while in humans we find the 21.5, 20.2, 18.5 and 17.2 kDa (Harauz and Boggs, 2013; Smith *et al.*, 2013) (**Figure 20**).

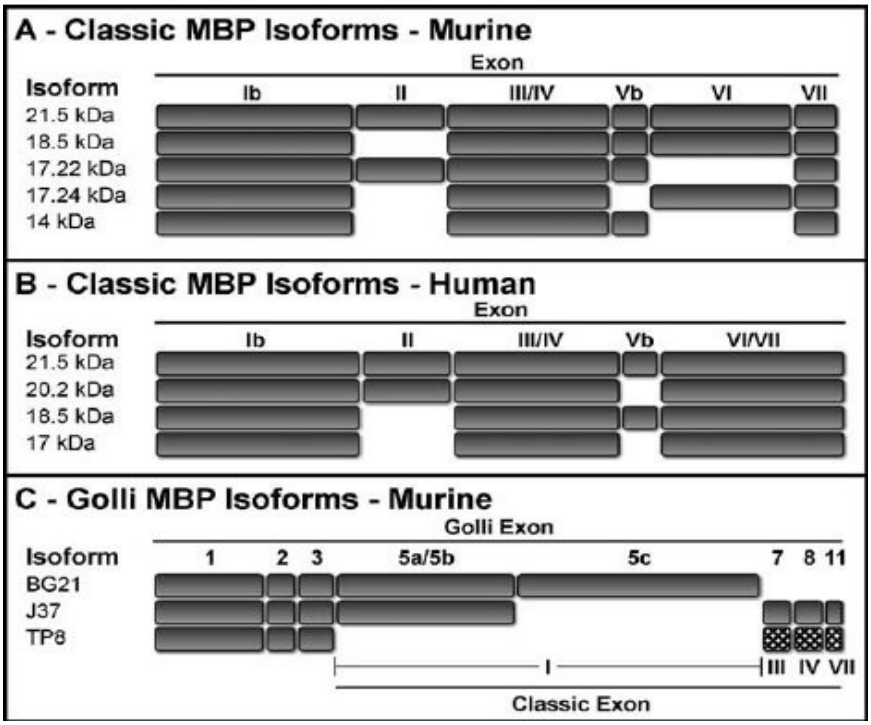

Figure 20: **Organization of the MBP isoforms**. (**A**) The classic murine MBPs (14, 17.22, 17.24, 18.5, 21.5 kDa). (**B**) Alternate splice variants of classic human MBP. (**C**) Golli MBPs isoforms (BG21, J37, TP8). Picture taken from *Asipu and Blair, 1997; Givogri et al., 2000.*

The most present isoform of MBP in humans is the 18.5 kDa one, while in mice is the one which weighs 14 kDa. All the isoforms contain protein domains that are encoded by exons I, III, IV and VII, while only the isoforms 21.5, 20.5 and 17.22 kDa contain the domain encoded by exon II. Isoforms 21.5, 20.2, 18.5, 17.24 and 17.2 kDa also contain exon VI, while isoforms 17.22 and 14 kDa do not contain it. The expression of these isoforms is regulated during development and their different localization in cells and myelin suggests that they have different functions. Isoforms containing the domain encoded by exon II are expressed at high levels at the onset of myelination and in immature OLs in culture, while the forms without this domain are predominantly expressed at a later stage during myelination, in mature OLs and in adult myelin (Smith *et al.*, 2013). Although the 18.5 kDa isoform is the primary form in adult human myelin,

the forms containing exon II are those expressed during fetal development and during remyelination (Boggs, 2006).

Role of MBP

MBP is an intrinsically disordered peripheral membrane protein (IDP) with a net positive charge of +19 (at pH 7), which contains some exceptions to the normal amino acid content in IDPs. For example, MBP has more arginine and less glutamic acid than most IDPs, and this is necessary for MBP to be both sufficiently basic and positively charged, with the purpose to properly interact with the membrane (Boggs, 2006). The interaction of the protein with most of its binding partners (especially with lipids), results in conformational changes and in the creation of ordered secondary structures at the binding site (Vassall, Bamm and Harauz, 2015). In particular, 3 amphipathic α-helices are present in the protein bound to the myelin membrane and they are specifically located in the N-terminal and in the C-terminal (Harauz and Boggs, 2013). The binding of MBP to the cytoplasmic membrane is driven by electrostatic and hydrophobic interactions; among the most important interactions, the one that occurs between the negatively charged membrane lipids and the positively charged MBP is certainly worth mentioning (Boggs *et al.*, 1986) (**Figure 21**).

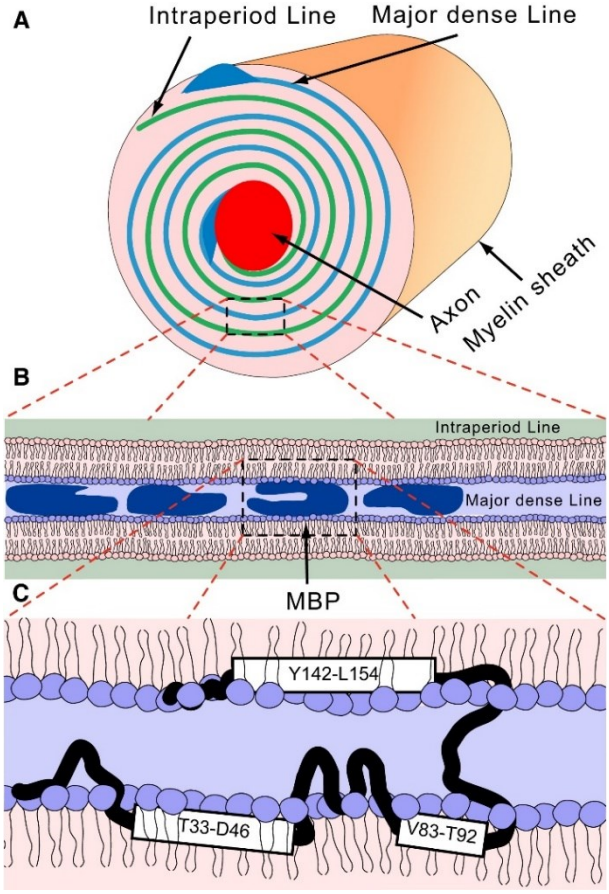

Figure 21: (**A**) **Structure of the myelin sheath**. (**B**) The myelin sheath consists of stacked lipid bilayers. (**C**) There are three potential amphipathic helices in MBP, which may peripherally interact with lipids and represent putative lipid binding domains. Picture taken from *Ahmed et al., 2012*.

The strong interaction of MBP with the oligodendrocytic membrane leads to the dense multilamellar structure of the myelin sheaths, which undergo to a loss of their stable structure when the electrostatic interaction fails, for example due to a change in lipid or protein composition (Ozgen *et al.*, 2016). When the MBP binds to the two opposite cytoplasmic leaflets of the negatively charged myelin membrane, the positive charge of the MBP is neutralized and self-assembly is induced in a polymeric network. This process resembles a phase transition, as it converts soluble, freely dispersed MBP molecules into a liquid-like condensed state. In this way, the cytoplasmic surfaces of the myelin bilayer join together and the multilamellar membranes become extremely compact (Boggs, 2006; Ozgen *et al.*, 2016). MBP is also involved in the regulation of the protein/lipid ratio of myelin membranes. In fact, acting as a molecular sieve, MBP oligomerizes in a cohesive protein lattice that pushes myelinated proteins such as MAG or CNP out of the myelinated sheets, in order to form an insulating membrane rich in lipids and with just two main proteins: PLP1 and MBP (Matthieu, Waehneldt and Eschmann, 1986; Aggarwal *et al.*, 2011; Aggarwal, Yurlova and Simons, 2011). Furthermore, in addition to the function of mediator for the adhesion of the cytosolic faces of myelin, MBP also interacts with the cytoskeleton in OLs through binding with actin and it participates in the transmission of extracellular signals to the cytoskeleton and/or at the communicating junctions (Aggarwal *et al.*, 2011, 2013). In summary, MBP is fundamental in the CNS myelination process; in fact, its impaired functionality can result in shivering symptoms, severe hypomyelination, seizures and early death (Campagnoni and Macklin, 1988; Boggs, 2006).

1.3.2 MBP TRANSLATIONAL REGULATION

MBP mRNA is transported through a vesicular transport system that moves through the cytoplasm to the oligodendrocytes (Müller *et al.*, 2013). This transport depends on two regions within the 3'-UTR, namely the 21 nucleotide RNA trafficking sequence (RTS), required for transport from the cell body to the oligodendrocyte processes, and a second longer tract, namely the 'RNA localization element' (RLR), which is required for final transport to the myelin membrane (Ainger *et al.*, 1997). MBP translation occurs locally in the myelin compartment, thanks to the MBP mRNA transportation from nucleus to cellular membrane inside RNA transport granules that move along microtubules (Herbert *et al.*, 2017) (**Figure 22**).

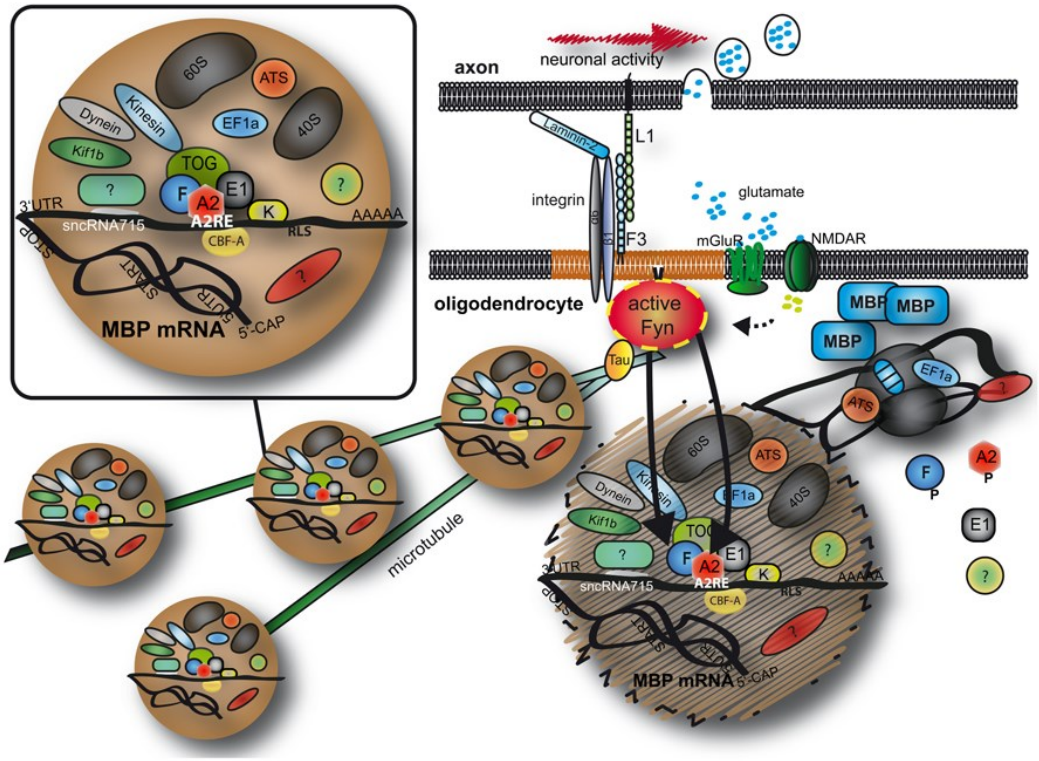

Figure 22: **Transport and localized translation of MBP**. MBP mRNA is transported on microtubules toward the oligodendroglial plasma membrane in RNA granules containing RNA binding proteins, motor proteins and parts of the protein synthesis machinery. At the plasma membrane, Fyn kinase is a crucial signaling molecule and converts axonal signals into localized translation of MBP. Picture and caption obtained from *Müller et al., 2013*.

Cytoplasmic transportation of MBP mRNA is crucial for the correct protein translation and it is regulated by several RNA binding proteins such as hnRNP A2, hnRNP K, hnRNP E1, hnRNP F and hnNRP CBF-A (Laursen, Chan and Ffrench-Constant, 2011; Müller *et al.*, 2013; Torvund-Jensen *et al.*, 2014), which recognize and bind the MBP mRNA through the RTS sequence; altogether, they form the RNA transport granule wherein MBP mRNA is transported through the cytoplasm to the cellular membrane in conjunction with kinesin motor proteins (such as Kif1b) and dynein/dynactin anterograde transport. Studies carried out on zebrafish reveal that an altered expression of Kif1b can lead to ectopic localization of MBP as well as misplaced myelin like membranes (Lyons *et al.*, 2009), while pharmacological dynein inhibition and mutation in the acr10 gene (which encodes the Arp11 subunit of dynactin) result in a misguided distribution of MBP mRNA in oligodendrocytes, which may cause myelination defects (Herbert *et al.*, 2017). Knockdown of both hnRNP K and hnRNP A2 as well can result in impaired MBP transport or protein synthesis inhibition (Laursen, Chan and Ffrench-Constant, 2011; Torvund-Jensen *et al.*, 2014). MBP translation is also regulated by a small non-coding RNA called sncRNA715, which inhibits the synthesis of endogenous MBP in murine primary oligodendrocytes through a specific binding in the 3'-UTR site of MBP mRNA (Bauer *et al.*, 2012; Müller *et al.*, 2015). Moreover, MBP translational deficit has been observed after conditional deletion of ERK2 from cells of the

oligodendrocyte lineage; this protein, called also MAPK1, is a kinase crucial for the transduction of several extracellular signals and it was found to control the timing of remyelination after demyelinating injury by directly regulating the effective MBP translation (Fyffe-Maricich *et al.*, 2011; Michel *et al.*, 2015). In addition, the protein itself interacts with plenty of proteins such as PLP1, MAG, ANLN, CAM, ACTB, L1CAM, CLTC, CNP and CNTNs, thus demonstrating its key role in the neural network (Smirnova *et al.*, 2021). Taken together, all these cis- and trans-acting factors contribute to regulate MBP translation, both developmentally and locally. In fact, as reported before, MBP mRNA can be already detected in immature oligodendrocytes which do not yet synthesize MBP protein, therefore MBP translation could be repressed in immature oligodendrocytes until a minimum degree of differentiation is achieved (Givogri *et al.*, 2001; Smith *et al.*, 2013). Furthermore, in mature myelinating oligodendrocytes, MBP translation can be repressed during cytoplasmic transport from nucleus to membrane in order to avoid misleading localization of the protein, which in turn may lead to an improper myelin sheets compaction and a faulty wrapping around axons (Allinquant *et al.*, 1991).

An exhaustive explanation on how the translational process takes place at the cellular membrane remains tricky. Some experiments hypothesized that MBP translation could be regulated by local axon-glial signaling events, such as the interconnection between the glial membrane with the extracellular matrix molecule laminin and the transmembrane protein L1CAM (Yan *et al.*, 2021). This interaction activates the non-receptor Src-family kinase Fyn, which in turn phosphorylates several components of the MBP mRNA granule and finally allows the release of MBP mRNA from its inhibitors and its subsequent localized translation. Fyn kinase is indeed crucial during the MBP translation process, given that MBP levels are reduced in Fyn-knockout mice (Lu *et al.*, 2005; White *et al.*, 2008).

2. AIM OF THE STUDY

Considering the previously discussed detrimental effects of high L-Phe levels on PKU mice and patients CNS myelination, the aim of this work was to evaluate the levels of MBP in a mouse model of phenylketonuria $PAH^{ENU2(-/-)}$, building up a potential model that could explain its translational regulation. Starting from the assumptions made by Pascucci *et al.* (2018), which demonstrated a lower level of MBP in $PAH^{ENU2(-/-)}$ mice of 60 PND, this thesis was developed in order to understand the mechanisms underlying this protein decrease.

In detail, we evaluated MBP along development analyzing 6 different time points (14-60-180-270-360-540 post-natal days, PND); MBP protein quantification was carried out through Western Blots (WBs) and immunofluorescence (IF), while MBP mRNA expression levels were carried out using the RT-qPCR technique. Subsequently, to better understand the mechanisms that underlie MBP translation in PKU, miRNA profiling was built for young ENU2 at 60 PND and potential miRNAs' targets network was constructed. In addition, we performed a proteomic assay for WT and ENU2 at 60 and 360 PND. Common proteins between miRNAs' predicted targets and ENU2 downregulated proteins that could have an effect over MBP translation and myelination were further evaluated through WB, while the expression of promising miRNAs was assessed along development through RT-qPCR. Moreover, L-Phe expression levels were measured for all the time points considered with MS/MS technique, while LNAAs (large neutral amino acids) brain concentration was estimated using HPLC system only in the first stage of development (14-60 PND).

Taken together, this work is aimed to figure out which are the main causes that could lead to hypomyelination and MBP downregulation in ENU2 mice brains. This preclinical longitudinal analysis over a prolonged period is brand-new, and it is designed to learn more about the potential role of miRNAs on PKU cerebral proteins synthesis, with special attention to MBP translational regulation.

3. MATERIALS AND METHODS

3.1 ANIMALS

BTBR mice have been raised in the animal shelter of the Biochemistry and Biotechnology section of the Department of Biomolecular Sciences of the University of Urbino Carlo Bo. $PAH^{ENU2(-/-)}$ (ENU2) and $PAH^{ENU2(+/+)}$ (wild type; WT) male mice used in this study were obtained from mating between heterozygous animals belonging to the BTBR strain (**Figure 23**). Genetic characterization was performed starting from little tail tissue. The genetic ENU2 modification is chemically induced after treatment of BTBR WT mice with N-ethylnitrosurea. The treatment causes an A>T835C missense mutation at nucleotide position 835 in exon 7, resulting in a phenylalanine-to-serine amino acid substitution in position 263 of the protein chain (F263S) (McDonald and Charlton, 1997). The animals were housed in standard cages, from 3 to 6 mice per cage, with a light-dark cycle of 12 hours and under controlled conditions of temperature (22 ± 1°C), humidity (60%) and air change (every 12 hours). All mice were fed with a Teklad global 18% protein rodent diet (Teklad, Harlan Laboratories Inc., Madison, WI) and water *ad libitum*.

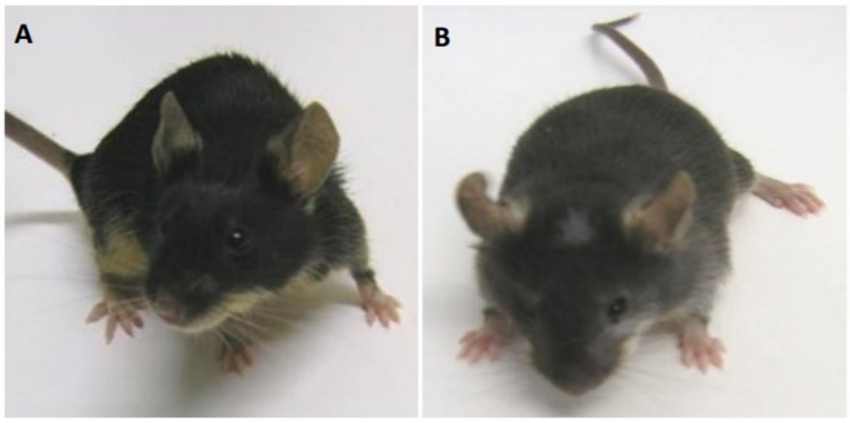

Figure 23: **BTBR mice**. (**A**) Mouse WT (+/+). (**B**) Mouse KO PKU (-/-). It is clear from the image that the PKU mouse has a lighter and sparser fur than the healthy mouse. This color difference derives precisely from the genetic defect in the phenylalanine hydroxylase (PAH) enzyme, which does not metabolize phenylalanine into tyrosine, a precursor of melanin.

All the experiments were conducted in accordance with the European legislation (2010/63/EU), with the Italian national legislation (DL26/2014) which governs the use of animals for research and with the guidelines of the National Institute of Health on the use and the care of laboratory animals (Authorization n° 486/2017-PR).

3.2 BTBR GENOTYPING (DNA EXTRACTION)

DNA extraction was performed in BTBR mice of at least 4 weeks old. Tails were collected and put in lysis buffer (NaCl 0.2 M, Tris-HCl 0.1 M pH 8.5, EDTA 5.5 mM pH 8.0, SDS 1% + Proteinase K (Merck Millipore)) ON at 54°C. The following day, digested tails were pottered and put in an 84°C bath for 1h in order to deactivate Proteinase K. Then a phenol:chloroform DNA extraction method was performed. Tails were centrifuged for 10 min at 10000 *x g* and 80 µl of supernatant were collected in new eppendorfs for each sample. Then 80 µl of phenol:chloroform were added and the mixture was vortexed for 2 mins. After a 10 min centrifuge (10000 *x g*), supernatants (from the aqueous phase) were collected in new eppendorfs and 64 µl of isopropanol were added to each sample. Then the mixture was flipped 6 times and centrifuged 10 min at 10000 *x g*. Supernatants were discarded and 32 µl of 70% ethanol were added to the pelleted DNA. Event proceeded with a new 10 min centrifuge (10000 *x g*) and with the following removal of the ethanol. DNA pellets were then left to dry for 15-20 min and later resuspended in 75 µl of sterile water. DNA concentration was quantified using Nanodrop™ Lite Spectrophotometer, keeping the A260/A230 and A260/A280 ratios >1.8 as default value for the evaluation of DNA purity.

3.3 PCR

DNA from each sample was amplified through the polymerase chain reaction using the following master mix: Buffer 2X (Diatheva Real Time kit), $MgCl_2$, DMSO, Betaine 5 mM (Merck Millipore), Taq Polymerase (Diatheva Real Time kit), Primer Forward (5'–ACTTGTACTGGTTTCCGCCT–3', Merck Millipore) and Primer Reverse (5'-AGGTGTGTACATGGGCTTAG–3', Merck Millipore). Primers were designed in order to amplify a specific sequence in the exon 7 of the PAH gene, focusing on the mutation carried by $PAH^{ENU2(-/-)}$ mice. Thermocycler program was set as reported in **Table 1**:

Cicle Name	Temperature (°C)	Time	Cicle Number
Activation	+95	1 min	1
Denaturation Annealing Extension	+95 +64/+61/+58/+55 +72	15 sec 15 sec 1.30 min	2 cycles (for the first 2 annealing temperatures); 20 cycles for the annealing temperatures of +58°C; 10 cycles for the annealing temperatures of +55°C
Final extension and ligation	+72	10 min	1
Final phase	+4	∞	

Table 1: **Thermocycle parameters**. The denaturation, annealing and extension sequence was repeated for 4 times, varying the annealing temperature from +64 °C for the first step to +55 °C for the last step in order to increase the specificity of the reaction.

Then, amplified DNA samples were left ON in a 55°C bath with a digestion buffer composed by 20 µl of PCR sample, 1 µl H2O, 2.5 µl CutSmart Buffer 10X (NEB) and 1.5 µl BsmAI (NEB). The restriction enzyme used recognizes the 5'-GTCTC(1/-5)-3' sequence within PAH gene, highlighting the difference between WT and ENU2 genotypes, since $PAH^{ENU2(-/-)}$ mutation creates a new BsmAI restriction site in exon 7. The following day samples were prepared (16 ul of digested DNA and 4 µl of loading dye 6X) and loaded in a 4-15% Mini-PROTEAN® TGX™ Precast Gels (Bio-Rad) with marker M23 (Puc19 dna/Mspl (Hpall), 23, Thermo Fisher Scientific). Gels were previously put in a Mini-PROTEAN Tetra Cell system and covered thoroughly by TBE 1X. Restriction fragments were separated by electrophoresis at 80-100 V for 1.30 h. At the end of the run, gels were submerged in an EtBr solution and bands were visualized (and therefore acquired) at the Bio-Rad Gel DOC 1000 UV transilluminator. From the obtained images, it is possible to see the run of the individual samples and, based on the reference marker M23, 3 possible genotypes are identified. In particular, for the healthy homozygous mouse, two fragments at 82 and 50 bp are displayed, the heterozygote generates 4 fragments at 82, 50, 48 and 34 bp, while the mutated homozygotes generate 3 fragments at 50, 48 and 34 bp, as reported in **Figure 24**.

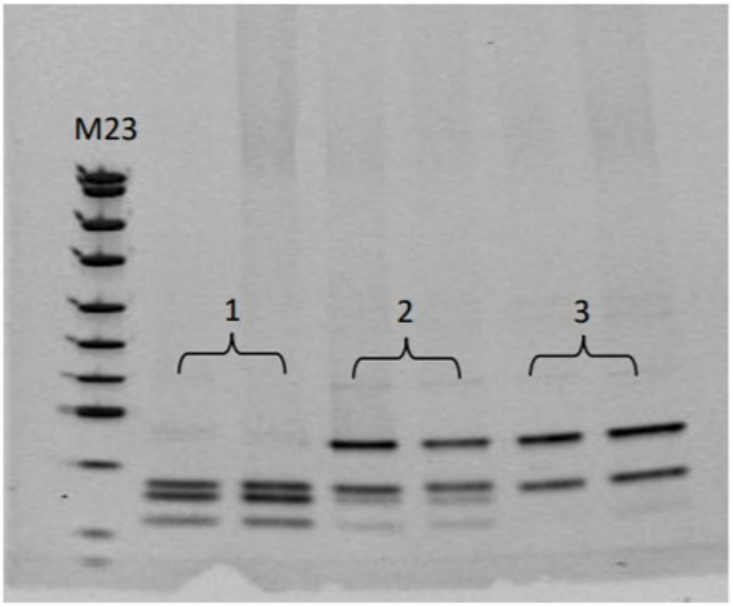

Figure 24: **Electrophoretic running gel**. In addition to the marker (M23), the two homozygous conditions (+/+; -/-) and the heterozygous condition (+/-) for PAH^{ENU2} mice are distinguished from the image. (**1**) the 3 bands corresponding to 50, 48 and 34 bp, which represent the PAH^{ENU2} mouse (-/-). (**2**) 4 bands are visible, corresponding to 82, 50, 48 and 34 bp, typical of the condition of heterozygosity (+/-). (**3**) The presence of the 82 bp band and the 50 bp band is indicative of a healthy homozygous mouse (WT +/+ mouse).

3.4 WESTERN BLOTTING

WT and ENU2 brains of different PND (see **Table 2**) were collected and snap frozen immediately in liquid nitrogen after washing in PBS. 30 mg of brain lysates were then homogenized in RIPA buffer -

Mice post-natal days	N samples per genotype	
	WT	ENU2
14 PND	6	4
60 PND	5	9
180 PND	5	5
270 PND	5	5
360 PND	6	6
540 PND	4	6

Table 2: Mouse brains numerosity utilized in this work

Milli-Q Water, 0.05 M Tris Hydrochloride pH 7.4, 0.001 M Potassium Chloride, 0.0015 M Magnesium Chloride, 0.001 M EDTA, 0.001 M Dithiothreitol, 0.005 M Sodium Fluoride, 0.001 M Sodium Metavanadate, 0.1% SDS - with 10% Na-DOC, 1% Triton X-100 and 1X Protease Inhibitor for the subsequent Western Blotting (WB) procedure. Samples were kept on ice for 20 minutes

and then sonicated 30s at 50 W with pulse mode. After centrifugation (15 min at 4°C, 12200 x *g*), supernatants were collected, and proteins were quantified using Bradford assay. 10 µg of total proteins from each sample were loaded in 12% polyacrylamide gels for SDS-PAGE. After 1h running (40 mA), gels were placed in sandwich cassettes with nitrocellulose membranes and submitted to the blotting transfer procedure for 70 min at 100 V. Efficiency of electrophoretic transfer was assessed with Ponceau S staining (0.1% Ponceau S (w/v) in 5% (v/v) acetic acid) at the ChemiDoc Imaging System (Bio-Rad). Membranes were then blocked with TBS/non-fat dry milk 5% for 1h and incubated ON with the following primary antibodies: rat anti-Myelin Basic Protein (anti-MBP, MAB386; 1:1000 in TTBS/non-fat dry milk 5%; Merck Millipore), rabbit anti-Myelin Proteolipid Protein (anti-Myelin PLP1, ab28486; 1:1000 in TTBS/non-fat dry milk 5%; Abcam), rabbit anti-Myelin-Associate Glycoprotein (anti-MAG, 346200; 1:1000 in TTBS/non-fat dry milk 5%; Thermo Fisher Scientific), rabbit anti-Anillin (anti-ANLN, PA5114851; 1:500 in TTBS/non-fat dry milk 5%; Thermo Fisher Scientific), rabbit anti-Contactin Associated Protein 2 (anti-CNTNAP2, PA528969; 1:5000 in TTBS/non-fat dry milk 5%; Thermo Fisher Scientific), mouse anti-β-Actin (anti-ACTB, 8H10D10; 1:1000 in TTBS/non-fat dry milk 5%; Cell Signaling Technology). The next day, membranes were washed 3 times (10 min each) with TTBS and then incubated 1h at room temperature with the appropriate secondary antibodies (donkey anti-rat IgG ab, AP189P; 1:2000 in TTBS/non-fat dry milk 5%, Merck Millipore; goat anti-rabbit IgG-HRP, sc-2004; 1:2000 in TTBS/non-fat dry milk 5%, Santa Cruz Biotechnology; goat anti-mouse IgG (H+L)-HRP, 170-6516; 1:2000 in TTBS/non-fat dry milk 5%, Bio-Rad). After that, membranes were washed again 3 times with TTBS (10 min each) and then exposed to the ChemiDoc Imaging System using the enhanced chemiluminescence (ECL) procedure after 2 min incubation with a mixture of H_2O_2 and luminol substrate. Protein bands intensities were acquired through densitometric analysis and the immunoblots were quantified using Image Lab software (Bio-Rad). Mean ratios between MBP, Myelin PLP1, MAG, ANLN and CNTNAP2 bands intensity were reported as percentage of control values, with β-Actin as loading control.

3.5 IMMUNOFLUORESCENCE AND DENSITOMETRIC ANALYSIS OF FLUORESCENCE IMAGES

WT and ENU2 brain hemispheres of young and adult mice (60 PND WT n=3, ENU2 n=3; 360 PND ENU2 n=1; 480 PND WT n=2; 540 PND ENU2 n=2) were collected and soaked in PFA 4% PBS 1X with overnight incubation for tissue fixation. After 24h, brains were put in a sucrose 30% PBS 1X solution and left at 4°C until precipitation. Brain sections were then incubated overnight with a cocktail of primary antibodies, including rat anti-MBP (Abcam #ab7349), and rabbit anti-PLP1

(Abcam #28846) in a solution of PBS and 0.3% Triton X-100, followed by a cocktail of secondary antibodies (1:200, Invitrogen), including Alexa Fluor 555 conjugated donkey anti-rat and Alexa Fluor 488 conjugated donkey anti-rabbit and NeuroTrace™ 640/660 Deep-Red Fluorescent Nissl Stain. Sections were examined under a confocal laser scanning microscope (Leica SP5). Densitometric analysis of MBP and PLP1 was performed on 5 brain sections per mice (at the level of the striatum). Specifically, MBP- and PLP1-associated signals were quantified by manually outlining the area of interest. Mean signal intensity (F) of the marker of interest was performed on two squared frames (35 µm per side) on 5 sections sampled to cover the rostro-caudal extent of the areas of interest (striatum and corpus callosum) entirely (n = 10 samples per mouse). The F/A ratio defines mean fluorescence of individual samples (F) normalized to total cellular surface (A).

3.6 RT-qPCR

WT and ENU2 brains of different PND (see **Table 2**, *no 540 PND*) were collected and snap frozen immediately in liquid nitrogen after washing in PBS. After homogenization, whole brain lysates (30 mg) were treated for RNA extraction using the RNeasy Plus Mini Kit (QIAGEN) following the manufacturer's instructions. RNA samples were quantified using Nanodrop® ND-100 Spectrophotometer (Thermo Fisher Scientific), keeping A260/A280 and A260/A230 ratios between 1.8 and 2.2 as critical values for evaluating RNA purity and possible contaminants. Subsequently, retrotranscription procedure was performed taking 500 ng from each RNA sample using the PrimeScript™ RT Master Mix (Takara Bio Inc.), following the manufacturer's instructions. This procedure utilizes random primers to retrotranscribe the entire RNA pool into cDNA. cDNA samples were then diluted in DNAse-free H_2O to have 10 ng/µl to be used in the qPCR for the MBP mRNA quantification. For each cDNA sample from WT and ENU2 brains of different ages, the reaction mix was settled using TaqMan probes specific for MBP (Mm01266402_m1, Thermo Fisher Scientific) and HPRT (Mm03024075_m1, Thermo Fisher Scientific). 10 µl of mix with cDNA from each sample were loaded in a reaction plate (final volume: 20 µl) and then put in the 7500 Applied Biosystem machine for cDNA amplification. Results expressed in $2^{-\Delta\Delta Ct}$ were used for the subsequent relative quantification of MBP mRNA expression levels, using HPRT as housekeeping gene.

3.7 L-PHE AND L-TYR EVALUATION IN DRIED BLOOD SPOT (DBS)

Mouse whole blood was collected on Whatman TM 903, dried under ambient conditions, and stored at -80°C in plastic bags. A 3-mm diameter dot was punched from the DBS into a single well of 96-well micro plate. The analysis of L-Phe and L-Tyr in the DBS was performed using a previously published method (Chace *et al.*, 1993) with some modifications (Rossi *et al.*, 2014). 3 mm diameter dots were punched out and eluted in 100 µl of methanol/water (80:20) solution containing labeled amino acid internal standards (CIL, Andover, MA, USA). The samples were shaken for 30 min at 30 °C. Then 65 µl of supernatant was dried under nitrogen flow at 45 °C. The residues were treated with 50 µl of 3 M hydrochloric acid in n-butanol solution at 60 °C for 30 min. After derivatization, the samples were dried under nitrogen flow at 45 °C and recovered in 70 µl of acetonitrile/water (80:20) containing 0.1% formic acid. Twenty microliters were injected into a LC-MS/MS system (API 2000, Sciex, Toronto, Canada). A Series 200 micro pump (PerkinElmer, Norwalk, CT, USA) and a Series 200 autosampler (PerkinElmer) were used for solvent delivery and automated sample loading. The mobile phase was acetonitrile/water (80:20) at a flow rate of 50 µl/min. Neutral loss scan of 102 Da fragment was used for the detection of L-Phe. The total acquisition time was 2 min.

3.8 BRAIN LNAAs EVALUATION

For brain large neutral amino acid quantification, frozen brain samples (14-60 PND) were weighted and homogenized in 0.1 N $HClO_4$ (Carlo Erba) containing Na-metabisulphite (Carlo Erba) and 1mM EDTA (Carlo Erba), in order to have a ratio of 1:100 ml/mg. Homogenates were then centrifuged at 10000 x *g* for 20 min at 4°C. Supernatants were collected and subsequently transferred to the HPLC system (Alliance, Waters Corporation, Milford, MA) coupled with a coulometric detector (model 5200 Coulochem II; ESA, Chelmsford, MA). The potentials were set at +450 mV and +100 mV at the analytical and conditioning cell, respectively. The flow pack rate was 1 ml/min and the mobile Phase consisted of 3% methanol in 0.1M Na-phosphate buffer pH 3, 0.1mM, Na2 EDTA and 0.5 mM 1-octane sulphonic acid Na salt (Merck Millipore) (Pascucci *et al.*, 2013).

3.9 miRNA MICROARRAY OUTPUT AND miRNA DEVELOPMENTAL EVALUATION

Selected WT and ENU2 brain lysates of 60 PND (WT, n=4; ENU2, n=4 per condition) were prepared in QIAzol reagent and total RNA from each sample was extracted with miRNeasy Mini

Kit (QIAGEN) according to the manufacturer's instructions. RNA samples were quantified using Nanodrop® ND-100 Spectrophotometer (Thermo Fisher Scientific), keeping A260/A280 and A260/A230 ratios between 1.8 and 2.2 as critical values for evaluating RNA purity and possible contaminants. Total RNA was further analyzed by denaturing gradient gel electrophoresis (agarose 1.3%, formaldehyde 2.2 M, MOPS 1X), with the purpose of checking RNA integrity and the possible presence of genomic DNA. miRNA expression profile between WT and ENU2 was performed according to the manufacturer's protocols (Affymetrix, Santa Clara, CA, United States) by Cogentech Affymetrix microarray unit (Campus IFOM-IEO, Milan, Italy) using *Mus musculus* Affymetrix GeneChip miRNA 4.0 (Affymetrix). The different gene expression patterns were analyzed by using Partek Genomics Suite updated to version 7019 (Partek®). PCA (Principal Component Analysis) was carried out to highlight differentially expressed miRNAs and the normalized background-corrected data were transformed to the log2 scale. Unpaired t-test was performed to determine which miRNAs were modulated at a significance level ($P < 0.05$) and statistically significant miRNAs were selected for final consideration when their expression was at least 1.2-fold different between ENU2 and WT samples.

For microarray validation and developmental evaluation, total RNA from WT and ENU2 brain lysates of different ages (14-60-180-270-360 PND, n=4/condition) was extracted as displayed previously. miRNA RT-qPCR from total RNA were performed using the TaqMan® MicroRNA Reverse Transcription Kit together with the TaqMan® MicroRNA Assays (both from Thermo Fisher Scientific) specific for the miRNA of interest. Retrotranscription and qPCR were carried out following manufacturer's instructions. Briefly, 10 ng of total RNA were retrotranscribed and 1.34 µl of the RT reaction product were placed into each tube with the qPCR reaction mix. The reaction mix was then loaded in the 7500 Applied Biosystem machine for cDNA amplification. Results expressed in $2^{-\Delta\Delta Ct}$ were used for the subsequent relative quantification of the selected miRNAs (mmu-miR-217-5p, MIMAT0000679_st; mmu-miR-671-3p, MIMAT0004821_st; mmu-miR-448-5p, MIMAT0017176_st; mmu-miR-1231-3p, MIMAT0022358_st; mmu-miR-218-1-3p, MIMAT0004665_st; snoRNA202), using snoRNA202 as endogenous control.

3.10 PROTEOMIC ANALYSES ON WT AND ENU2 BRAINS

20 µg of each selected WT and ENU2 brain lysates of 60 and 360 PND (WT, n=4; ENU2, n=4 per age) were processed by EasyPep MS Sample Kit (Thermo Scientific Pierce) by the TMT labelling option (16plex TMTpro, Thermo Fisher Scientific) and finally mixed in equimolar ratio. The sample was fractionated by Pierce High pH Reversed-Phase Peptide Fractionation Kit.

Subsequently, drying fractions were dissolved in water 0.1% formic acid and 2 µg were injected in an UltiMate 3000 RSLC nano system coupled to the Exploris 240 mass spectrometer. Briefly, peptides were desalted online by Acclaim PepMap C18 Reversed Phase HPLC Column (5 µm, 0.3 mm x 5 mm Thermo Fisher Scientific), and then resolved by Easy-Spray Pepmap RSLC C18 (2 µm, 50 cm x 75 µm) at a flow rate of 300 nl/min with a gradient of phase B (80% acetonitrile/0.1% formic acid, solvent A was 0.1% formic acid in water) from 2% to 40% in 220 min. Then (B) was changed up 99% in 12 min, kept for 7 min, and then the column was re-equilibrated for 10 min. Data were acquired in a positive mode and data-dependent manner. For MS1 m/z range was set to 350-1500 at 120,000 resolution (at m/z 200), ACG target 3e6, and auto maximum injection time. MS2 was adopted when ions intensity was above 5e3, with m/z range in auto mode, normalized HCD energy 35%, ACG target 7.5e4, and maximum injection time 40 ms. The resolution was set to 15000 at m/z 200 and the internal calibrant for employed in run start mode. Fractions were analyzed in quadruplicates and raw data were employed in Proteome Discoverer software v2.5 adopting the TMT signal quantification strategy. Master proteins were considered differentially expressed with a fold change 1.5 and FDR<0.1 (False Discovery Rate).

3.11 *IN SILICO* ANALYSES

3.11.1 GENE ONTOLOGY AND KEGG PATHWAY ANALYSES FOR PREDICTED miRNAs' TARGETS

Predicted target genes of the mature upregulated (fc > 1.2) and downregulated (fc < -2.5) miRNAs in ENU2 were evaluated using three online databases: miRDB (Chen and Wang, 2020) (>70 target score cutoff), TargetScanMouse 8.0 (Agarwal *et al.*, 2015) (<-30 total context++ score cutoff) and DIANA TOOLS-microT-CDS (Paraskevopoulou *et al.*, 2013) (>0.7 miTG score cutoff). While miRDB works through the retrieval of computationally predicted miRNA targets and miRNA functional annotations with a wiki editing interface (Chen and Wang, 2020), TargetScan predicts biological targets of miRNAs by searching for the presence of conserved 8mer, 7mer, and 6mer sites that match the seed region of each miRNA (Agarwal *et al.*, 2015). On the other hand, DIANA TOOLS-microT-CDS is specifically trained on a positive and a negative set of miRNA Recognition Elements (MREs) located in both the 3'-UTR and CDS regions (Paraskevopoulou *et al.*, 2013). Only the target genes which were common in the prediction of all the above algorithms were screened out in ShinyGO v0.76 (Ge, Jung and Yao, 2020) (http://bioinformatics.sdstate.edu/go/) for gene set enrichment analysis through Gene Ontology (GO) and KEGG (Kyoto Encyclopedia of Genes and Genomes), with background default

parameters. The ontology covered three domains (biological process, cellular component, and molecular function), while KEGG was evaluated to look for potential interaction/relation networks that could be altered by up- or downregulated miRNAs. Gene enrichment analysis was carried out using the Benjamini-Hochberg FDR adjusted p-value ($p<0.05$). miRNAs-predicted targets networks were created through Cytoscape v3.9.1 software (Shannon *et al.*, 2003).

3.11.2 PROTEOMIC PROTEIN-PROTEIN INTERACTION

Protein-protein interaction (PPI) networks for the up- and downregulated proteins in ENU2 brains detected from proteomic analysis were constructed using the Cytoscape v3.9.1 built-in stringAPP, with minimum required interaction score set to medium confidence (>0.4) (Shannon *et al.*, 2003; Szklarczyk *et al.*, 2019). The resulting network was then analyzed through the Cytoscape plug-in MCODE in order to detect significant clusters and subnetworks among the principal one (Node Density Cutoff: 0.1; Node Score Cutoff: 0.2; K-Core: 2; Max Depth: 100) (Bader and Hogue, 2003). Gene set enrichment analyses over up- and downregulated proteins in ENU2 brains were performed using ShinyGO v0.76 (Ge, Jung and Yao, 2020) (http://bioinformatics.sdstate.edu/go/) with default background parameters ($p<0.05$).

3.12 BEHAVIORAL ANALYSES

Behavior analyses were performed testing the animals with the Open Field Test (OFT) and the Object Recognition Test (ORT). These tests take advantage of the spontaneous preference that rodents display for novel stimuli and environments, avoiding the use of explicit (positive or negative) reinforcement or the effects of lengthy training (Cabib *et al.*, 2003). All tests were performed in a sound and light attenuated room, putting mice in a round arena with walls to prevent their escape. Tests were videotaped by means of a camera placed above the apparatus and connected to a recorder placed outside the room. Three groups of adult male mice of different ages (180 PND, WT n=5 ENU2 n=6; 270 PND WT n=5 ENU2 n=6; 540 PND WT n=3 ENU2 n=3) were submitted to OFT and ORT and behaviors were analyzed by Video-based EthoVision System (Noldus, The Netherlands) to record, collect and analyze data.

3.12.1 OPEN FIELD TEST

The open field test (OFT) is an experiment used to evaluate general locomotory activity and, marginally, anxiety state in mice. The open field apparatus, 80 cm in diameter and 30 cm in height, is the same used for the ORT test and it comprises a round arena with a white plexiglas

floor and gray plexiglas walls. During the OFT, the mouse was introduced in a specific sector of the empty open arena and left to explore the apparatus for sessions of 5 min during which moved distance and velocity were videotaped (**Figure 25**).

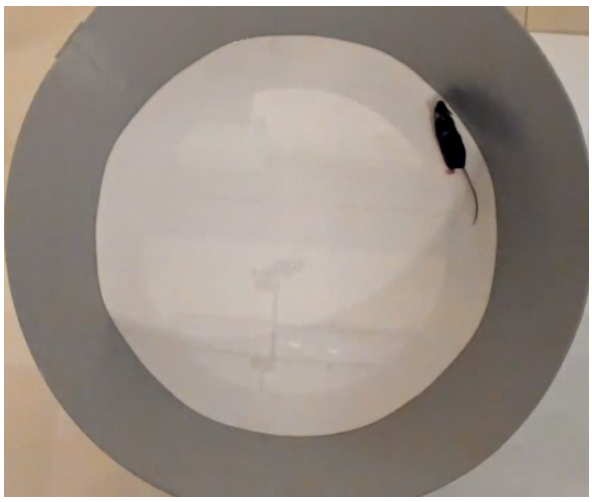

Figure 25: **Example of an Open Field Test (OFT) recording session**.

3.12.2 OBJECT RECOGNITION TEST

This is a non-associative test that does not use positive or negative reinforcement and allows the evaluation of mice spontaneous preference for novel stimuli. In detail, each mouse was individually submitted to two successive 5-min sessions, Pretest and Test sessions, using the same arena described for the OFT. At the end of each session, the subject was replaced in its home cage for 2 min and the apparatus was cleaned with a solution of water and ethanol. All sessions were videotaped. In the first session (Pretest) the mouse was introduced in the same sector of the open field containing two identical white objects and left to explore it for 5 min (**Figure 26A**). In the second session (Test session, **Figure 26B**) one white object was substituted with a new black object, while the other one was left unaltered. The mouse was left to explore

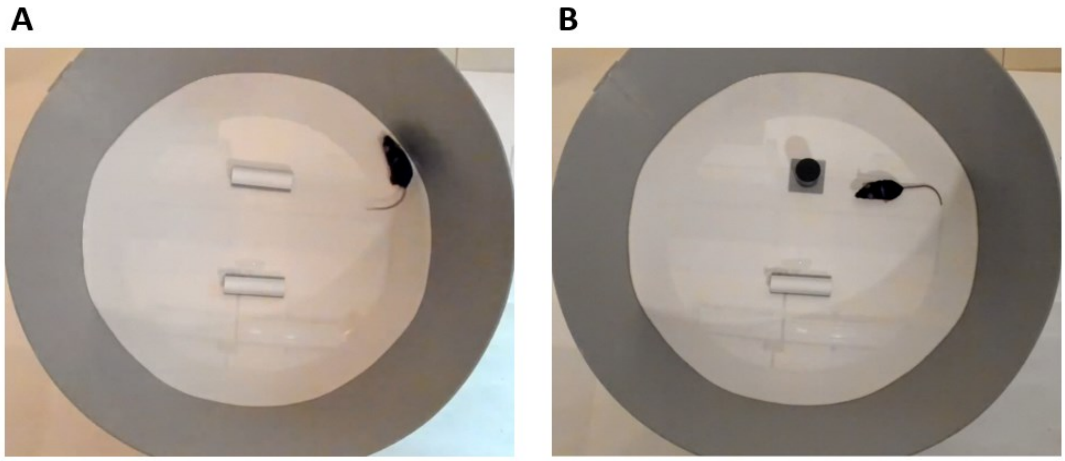

Figure 26: **Example of an Object Recognition Test (ORT) recording session**. (**A**) Pretest session, with two identical white objects in the middle of the arena. (**B**) Test session, with a black object in substitution to the upper white one.

for 5 min. The amount of time that the mouse took to explore the new object compared to the previous one, provides an index of its cognitive levels.

3.13 STATISTICAL ANALYSES

Statistical analyses were performed with GraphPad Prism 8.0.1 using two-way ANOVA in case of more than two groups to be measured or two-tailed t-test when each measure had only two groups. P-value threshold for significance was set to $p < 0.05$. The data are shown as Mean ± SEM.

4. RESULTS

4.1 MBP LEVELS INCREASE DURING AGING IN ENU2 MICE

In order to evaluate the possible MBP downregulation during development in PKU mice, WBs from WT and ENU2 mice brain lysates of various ages (14-60-180-270-360-540 PND) were performed. As reported in **Figure 27**, MBP levels are lower in ENU2 compared to WT mice at 14 and 60 PND (-57.8% and -64.9%, respectively), with significance found at 60 PND. This downregulation seems to be confirmed also for the ENU2 mice of 180 PND (-50.9%), although these differences are not statistically significant. However, at 270, 360 and 540 PND, a recovery of the MBP protein levels in ENU2 mice was observed (-20.4%, -14.7%, -9.11% respectively), almost returning to the protein levels observed in healthy WT mice. Taken together, the results depict that ENU2 mice brains show halved MBP protein levels compared to WT until 180 PND. After that interval, MBP seems to grow, reaching almost normal level in middle-aged ENU2 mice. The reported multiple bands confirm the four main MBP isoforms in the mouse and their intensity reflects their temporal and local regulation (Harauz and Boggs, 2013).

Myelin PLP1 immunoblots and densitometric analysis (blots *not shown*) revealed a significant although not marked protein reduction in ENU2 brain lysates of 14 and 60 PND (-17% and -15%, respectively), while at 180 PND no differences are detectable (**Figure 28**).

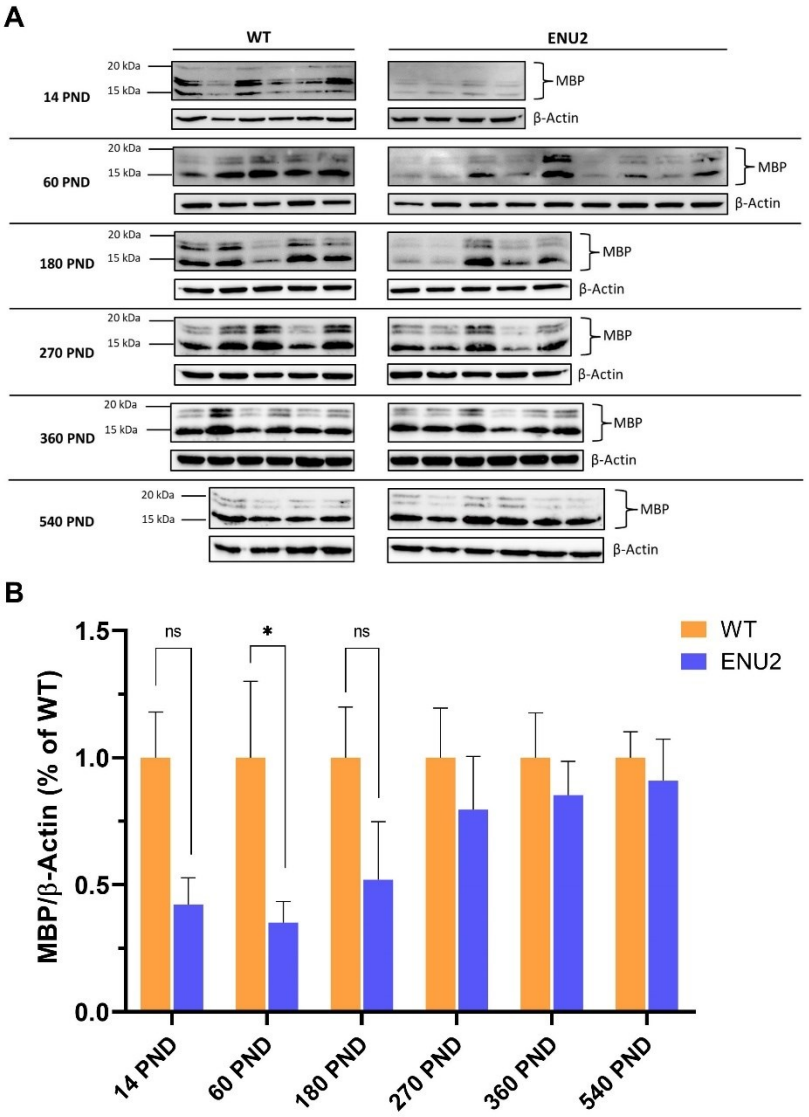

Figure 27: **Representative immunoblots (A) and densitometric analysis (B) of MBP protein showing the expression levels in WT and ENU2 brains**. Each lane corresponds to a different animal. Data are expressed as Mean ± SEM (14 PND, WT n=6, ENU2 n=4; 60 PND, WT n=5, ENU2 n=9; 180 PND, WT n=5, ENU2 n=5; 270 PND, WT n=5, ENU2 n=5; 360 PND, WT n=6, ENU2 n=6; 540 PND, WT n=4, ENU2 n=6). All the reported values in the graph are densitometric values obtained calculating the mean of the sum between the relative intensities of each band using Image Lab software. Bands are placed at known molecular weights (14.5-21 kDa). Two-way ANOVA followed by Bonferroni's multiple comparison test, *p<0.05.

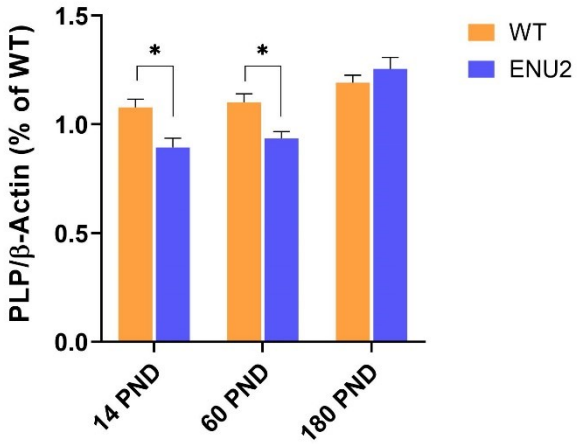

Figure 28: **Representative densitometric analysis of Myelin PLP1 showing the expression levels of the protein in WT and ENU2 brains**. Data are expressed as Mean ± SEM (n = see **Table 1**). All the reported values in the graph are densitometric values obtained using Image Lab software. Immunoblots are not shown. Two-way ANOVA followed by Bonferroni's multiple comparison test, *p<0.05.

4.2 IMMUNOFLUORESCENCE IMAGES FOR MBP AND PLP1 CONFIRM MBP RECOVERY

In order to confirm and further validate WBs densitometric results, we performed an immunofluorescence (IF) analysis on 5 brain sections per mice (at the level of the striatum). Provided results (**Figure 29**) confirmed data already obtained through WBs, with a MBP expression level which is significantly lower in ENU2 mice at 60 PND and an almost complete expression recovery of the protein during adulthood. Neurotrace imaging as well indicated an altered physiological state of the neurons at 60 PND, with no detectable differences between adult WT and ENU2 mice.

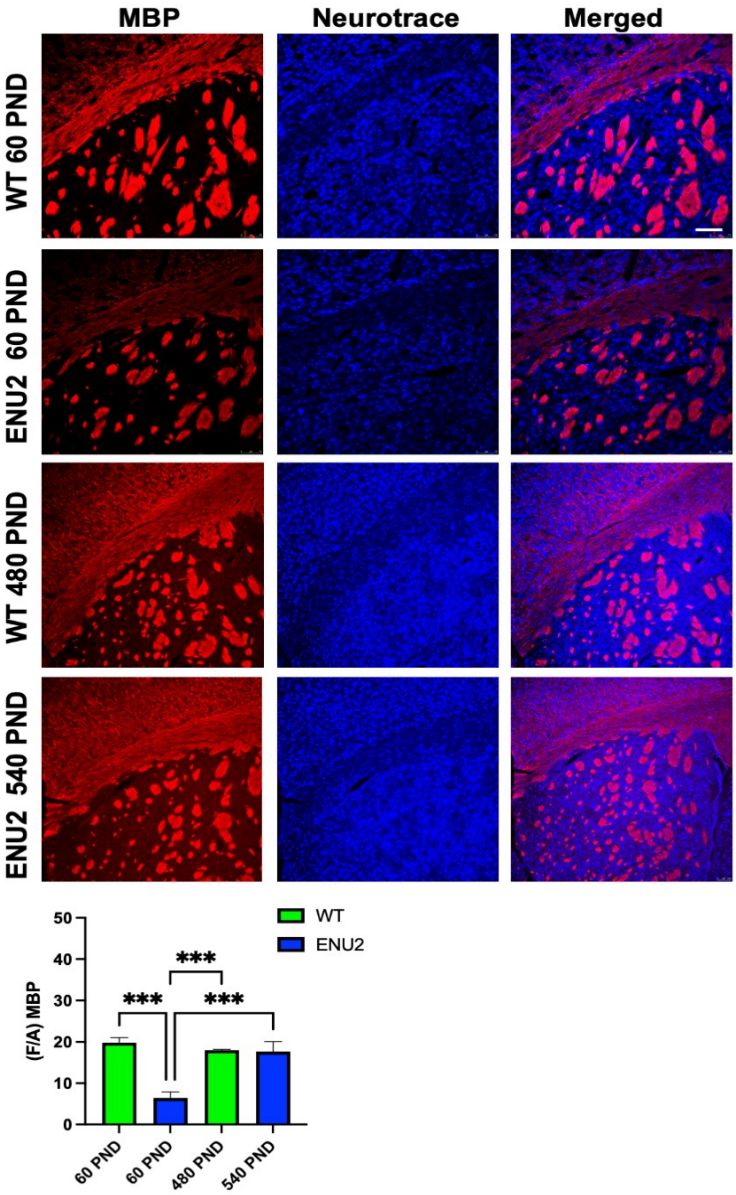

Figure 29: **Confocal images and relative densitometric results (in the lower part) of the expression levels of MBP (in red) and neurons physiological state evaluation in two groups of mice at different ages**. Expression levels of MBP at 60 PND in ENU2 brain are significantly lower compared to 60 PND WT mice and to aged ENU2 mice. MBP expression in adult mice shows no statistical differences. ENU2 neurons at 60 PND show an altered physiological state, with a detectable complete recovery during adulthood. The F/A ratio defines mean fluorescence of individual samples (F) normalized to total cellular surface (A). Two-way ANOVA followed by Bonferroni's multiple comparison test, *p<0.05; **p<0.01; ***p<0.0005; ***p<0.0001.

On the other hand, PLP1 resulted unaltered in both the evaluated time points (**Figure 30**). The latter do not completely match with the previous PLP1 WBs at 60 PND, probably due to a greater sensibility of the WB compared to the IF procedure. Taken together, these data could indicate a specific hindrance only over MBP expression, with no relevance over PLP1 expression.

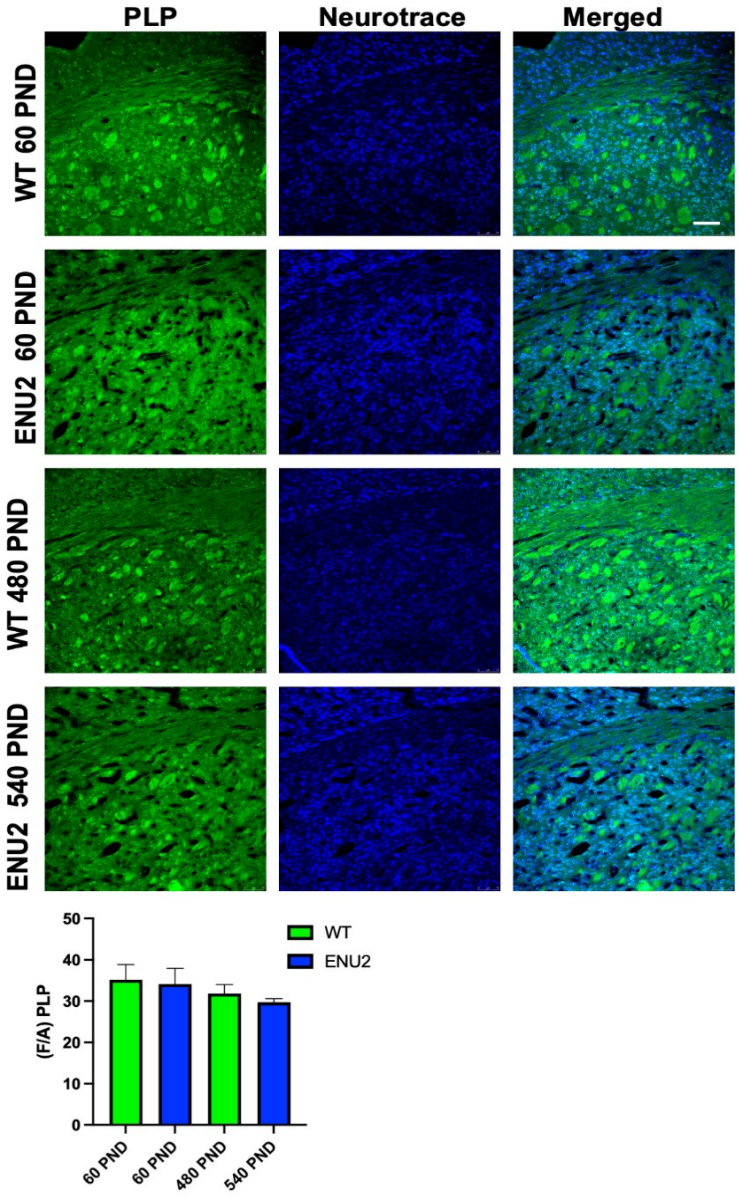

Figure 30: **Confocal images and relative densitometric results (in the lower part) of the expression levels of PLP1 (in green) and neurons physiological state evaluation in two groups of mice at different ages**. Expression levels of PLP1 at 60 PND in ENU2 brains is equal to that found in WT brains. No statistically significant differences are detectable for the other time point considered, and no detectable differences are noticeable from neurotrace analysis. The F/A ratio defines mean fluorescence of individual samples (F) normalized to total cellular surface (A). Two-way ANOVA followed by Bonferroni's multiple comparison test, *p<0.05.

4.3 MBP mRNA IN ENU2 MICE REMAINS UNALTERED DURING DEVELOPMENT

Our studies focused on the MBP transcription mechanism, hypothesizing that low protein levels could correspond to a reduced amount of the MBP mRNA expression levels. To do so, RT-qPCR on RNA extracted from the same ENU2 and WT brain samples (see **Table 2**, *no 540 PND*) were performed. In contrast to what was expected, mRNA MBP was equally expressed in the two conditions. Indeed, no significant differences were found, and in the early developmental stages (14-60-180 PND), MBP mRNA expression seems even to be higher in ENU2 compared to WT, although differences are not statistically significant (**Figure 31**). These data, together with those obtained from WBs, suggest a possible impairment at the translational level during the first phases of development, which may result in the low MBP protein expression observed in ENU2 mice. As reported previously, MBP translation is a finely regulated process, and disturbance on the transcription or translation of cis- or trans- acting factors which regulate its translation could provoke a destabilization of the MBP translational process.

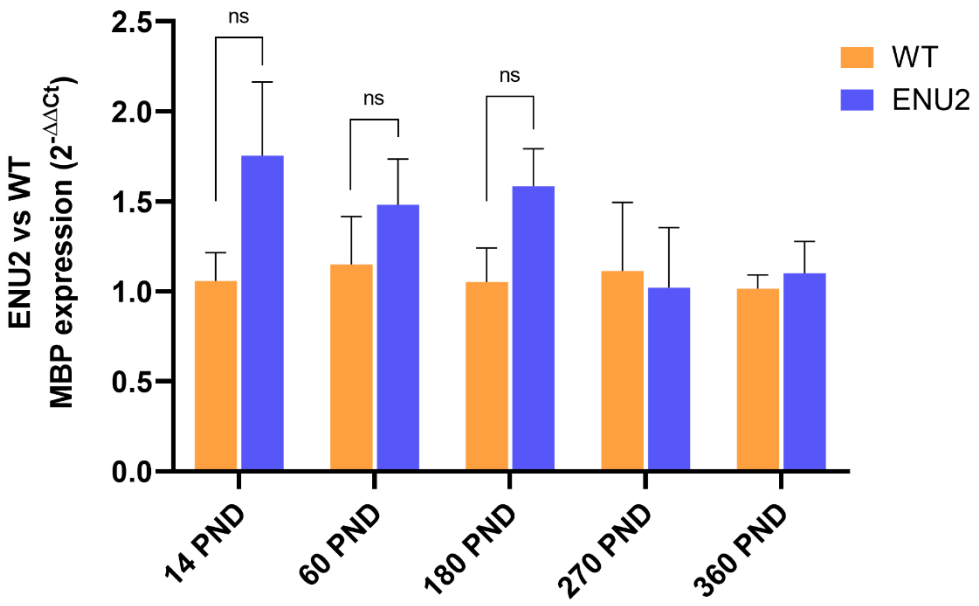

Figure 31: RT-qPCR of relative MBP mRNA expression in WT and ENU2 brains (14 PND, WT n=6, ENU2 n=4; 60 PND, WT n=5, ENU2 n=9; 180 PND, WT n=5, ENU2 n=5; 270 PND, WT n=5, ENU2 n=5; 360 PND, WT n=6, ENU2 n=6). HPRT has been used as endogenous control. Two-way ANOVA followed by Bonferroni's multiple comparison test, *p<0.05.

4.4 L-PHE LEVELS IN BLOODSTREAM DECREASE DURING DEVELOPMENT IN ENU2 MICE

As expected, L-Phe levels in ENU2 mice were higher compared to WT mice (ENU2 mean range: 1172-2894 µM; WT mean range: 106-247 µM), while L-Tyr levels were significantly lower in ENU2 mice compared to WT (ENU2 mean range: 26-58 µM; WT mean range: 65-112 µM). As shown in **Figure 32A**, L-Phe levels in the bloodstream of ENU2 mice of 14 PND were significantly higher than any other time points. Levels of L-Phe remained higher until 60 PND with respect to those detected in the adult ENU2 animals aged 180 to 360 PND. L-Tyr levels were persistently lower than in the control mice and declined with aging following the same trend observed in controls (**Figure 32B**).

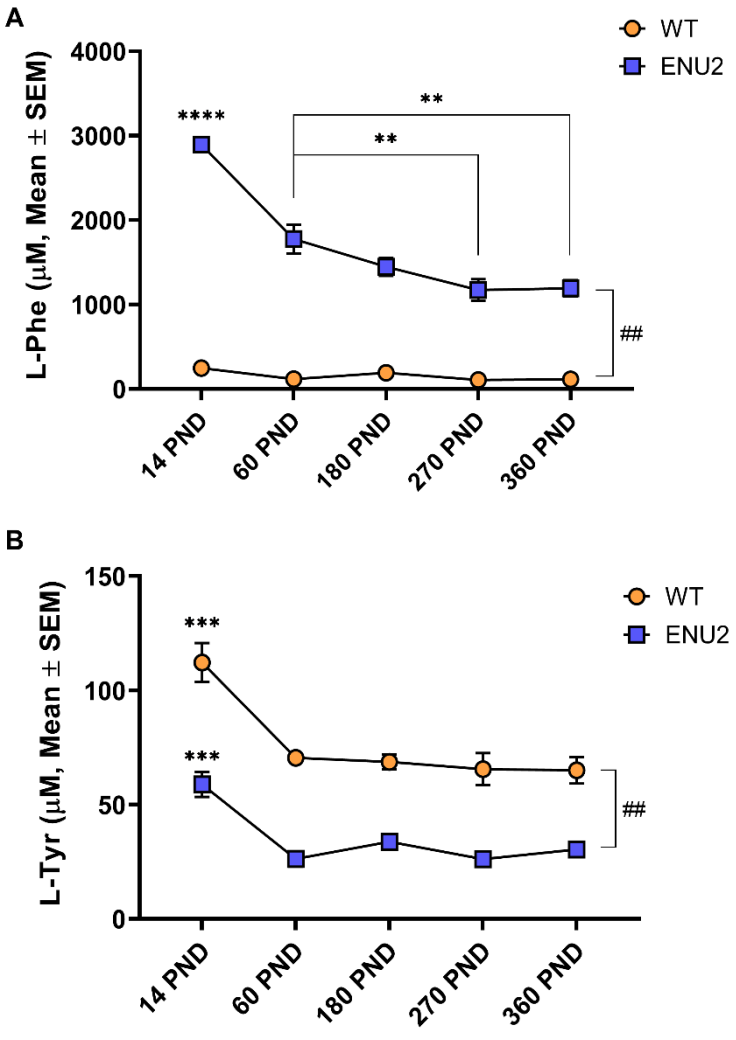

Figure 32: **L-Phe levels (A) and L-Tyr levels (B) in ENU2 and WT dried blood spots, indicating amino acids levels in the bloodstream**. Data are expressed as Mean ± SEM (14 PND, WT n=3, ENU2 n=11; 60 PND, WT n=5, ENU2 n=5; 180 PND, WT n=4, ENU2 n=4; 270 PND, WT n=5, ENU2 n=5; 360 PND, WT n=4, ENU2 n=6). Two-way ANOVA followed by Bonferroni's multiple comparison test, *p<0.05; **p<0.01; ***p<0.0005; ****p<0.0001; ## p<0.0001 WT vs ENU2.

4.5 AMINOACIDIC POOL EVALUATION IN YOUNG ENU2 MICE BRAINS

LNAAs deprivation at brain level is one of the hypotheses that try to explain the altered cerebral protein synthesis and the low levels of neurotransmitters observed in ENU2 mice. In fact, many authors indicate the LAT1 transporter inhibition mediated by high L-Phe levels as one of the factors that could subtract the availability of LNAAs to the translational machinery, with subsequent low levels of certain cerebral proteins and, consequently low levels of MBP (Hoeksma *et al.*, 2009; de Groot *et al.*, 2013). To confirm this hypothesis, we perform an aminoacidic pool evaluation in young ENU2 mice brains (14 PND, WT n=6, ENU2 n=4; 60 PND, WT n=5, ENU2 n=4), thus looking at the time points where MBP was lower compared to WT mice. As reported in **Table 3**, the cerebral concentration of many amino acids in ENU2 brain is significantly different compared to the WT. As expected, **L-Phe** levels in ENU2 mice brains were significantly higher compared to WT (**152.89 ± 12.15 vs 18.98 ± 1.55 nmol/g** wet weight at **14 PND**; **83.23 ± 14.98 vs 13.79 ± 2.04 nmol/g** wet weight at **60 PND**), while the opposite was observed for **L-Tyr** concentrations (**13.69 ± 0.75 vs 14.88 ± 0.50 nmol/g** wet weight at 14 PND; **7.93 ± 1.28 vs 9.74 ± 0.53 nmol/g** wet weight at 60 PND), although the latter was not significant. Interestingly, L-Phe cerebral levels seemed to decrease during development, thus following the same decreasing trend observed for L-Phe in the bloodstream. The total aminoacidic pool showed significant differences between ENU2 and WT mice brains; in fact, at 14 PND we found that **Ser**, **His**, **Gly**, **Cit**, **Ala**, **Tau**, **Abu**, **Met**, **Leu** and **Pro** resulted to be significantly higher compared to WT levels, with an increased concentration observed also for **Val**, despite not being significant. On the other hand, at 14 PND **Gln** and **Glu** resulted to be lower in ENU2, although the latter was not significant. At 60 PND we found that **Ser**, **His**, **Gly**, **Met** and **Orn** were higher in ENU2 brains, with a higher trend observed also for **Met** and **Pro**. At 60 PND, only **Leu** showed a reduced brain concentration compared to WT, even if the result was not significant. These data depict an aminoacidic brain imbalance occurring in ENU2 mice during the first months of life, outlining a new scenario over the LNAAs deprivation hypothesis.

	14 PND (nmol/g ± SEM)			60 PND (nmol/g ± SEM)		
	WT	**ENU2**	**p-value (ENU2 vs WT)**	**WT**	**ENU2**	**p-value (ENU2 vs WT)**
ASP	246,98 ± 5,48	247,22 ± 18,57	0,99	397,18 ± 32,55	442,74 ± 29,18	0,34
GLU	579,28 ± 8,59	543,77 ± 40,91	0,33	720,98 ± 49,44	676,91 ± 80,15	0,64
ASN	12,66 ± 0,45	12,29 ± 0,98	0,71	9,38 ± 0,85	8,61 ± 0,35	0,47
SER	**94,69 ± 2,24**	**112,12 ± 8,42[A]**	**0,04**	**67,59 ± 5,86**	**84,5 ± 3,29A**	**0,05**
GLN	**305,12 ± 11,25**	**234,99 ± 15,92[B]**	**0,01**	398,48 ± 25,72	326,2 ± 16,71	0,06
HIS	**18,19 ± 0,51**	**28,54 ± 2,21[C]**	**0,0005**	**12,75 ± 1,01**	**16,92 ± 1,5[A]**	**0,05**
GLY	**138,17 ± 8,12**	**236,89 ± 17,58[C]**	**0,0004**	**167,38 ± 17,46**	**261,55 ± 27,37[A]**	**0,02**
THR	45,54 ± 1,04	46,52 ± 2,96	0,72	29,04 ± 2,42	26,33 ± 1,55	0,41
CIT	**4,79 ± 0,28**	**6,61 ± 0,49[B]**	**0,01**	2,97 ± 0,24	3 ± 0,25	0,93
ALA	**125,01 ± 4,39**	**170,87 ± 13,99[B]**	**0,01**	101,89 ± 11,11	96,52 ± 4,06	0,69
TAU	**1280,45 ± 31,9**	**1722,83 ± 136,66[B]**	**0,005**	762,1 ± 54,42	901,94 ± 70,94	0,15
ARG	27,4 ± 0,78	30,04 ± 2,05	0,20	25,47 ± 2,05	25,41 ± 1,9	0,98
TYR	14,88 ± 0,5	13,69 ± 0,76	0,21	9,74 ± 0,54	7,93 ± 0,64	0,06
ABU	**77,93 ± 3,46**	**102,09 ± 6,32[B]**	**0,01**	40,33 ± 3,86	49,91 ± 2,31	0,09
VAL	20,78 ± 0,68	23,59 ± 1,23	0,06	14,45 ± 0,97	13,18 ± 0,91	0,38
MET	**48,72 ± 1,46**	**58,4 ± 4,51[A]**	**0,04**	37,11 ± 3,42	45,89 ± 3,06	0,10
PHE	**18,98 ± 1,56**	**152,89 ± 12,15[D]**	**$7,95*10^{-7}$**	**13,79 ± 2,05**	**83,23 ± 7,29[D]**	**$1,88*10^{-5}$**
ILE	11,62 ± 0,48	12,73 ± 1,05	0,31	7,1 ± 0,49	6,61 ± 0,51	0,51
ORN	5,4 ± 0,47	5,89 ± 1,02	0,64	**2,61 ± 0,12**	**4,59 ± 0,8[A]**	**0,03**
LEU	**21,06 ± 0,94**	**25,8 ± 1,45[A]**	**0,02**	14,88 ± 1,07	12,29 ± 0,61	0,09
LYS	37,54 ± 1,08	36,42 ± 2,24	0,63	23,42 ± 1,98	24,7 ± 0,75	0,60
PRO	**65,29 ± 2,56**	**80,18 ± 6,24[A]**	**0,04**	31,25 ± 3,57	37,45 ± 2,99	0,24

Table 3: **Aminoacidic pool for WT and ENU2 brains of 14-60 PND**. The significant differences between the concentrations found in both conditions are highlighted in bold and data are expressed as Mean ± SEM. 14 PND WT n=6, ENU2 n=4; 60 PND WT n=5, ENU2 n=4. Two-tailed t-test [A]*p<0.05; [B]**p<0.01; [C]***p<0.0005; [D]****p<0.0001.

4.6 miRNA MICROARRAY OUTPUT ANALYSIS

Dobrowolski *et al*. (Dobrowolski *et al.*, 2015, 2016) reported an important epigenetic remodeling in PKU patients and mice, which leads to the creation of hypo-/hypermethylated genomic loci and subsequent overexpression or downregulation of certain genomic elements such as miRNAs or lncRNAs. To verify if the MBP translation in ENU2 mice at developmental stage could be impaired by miRNAs, total RNA samples from 60 PND WT and ENU2 mice (n=4/condition) were analyzed through miRNA microarray technique. miRNA profiling for the differentially expressed miRNAs between the two conditions was depicted by hierarchical clustering (see **Figure 33A**). 156 miRNAs were found to be differentially expressed between WT and ENU2 mice after passing volcano plot filtering (fold change > 1.2-fold, p-value < 0.05; **Figure 33B**). Of these 156 miRNAs, 68 were downregulated and 88 were upregulated in ENU2 mice compared to WT mice.

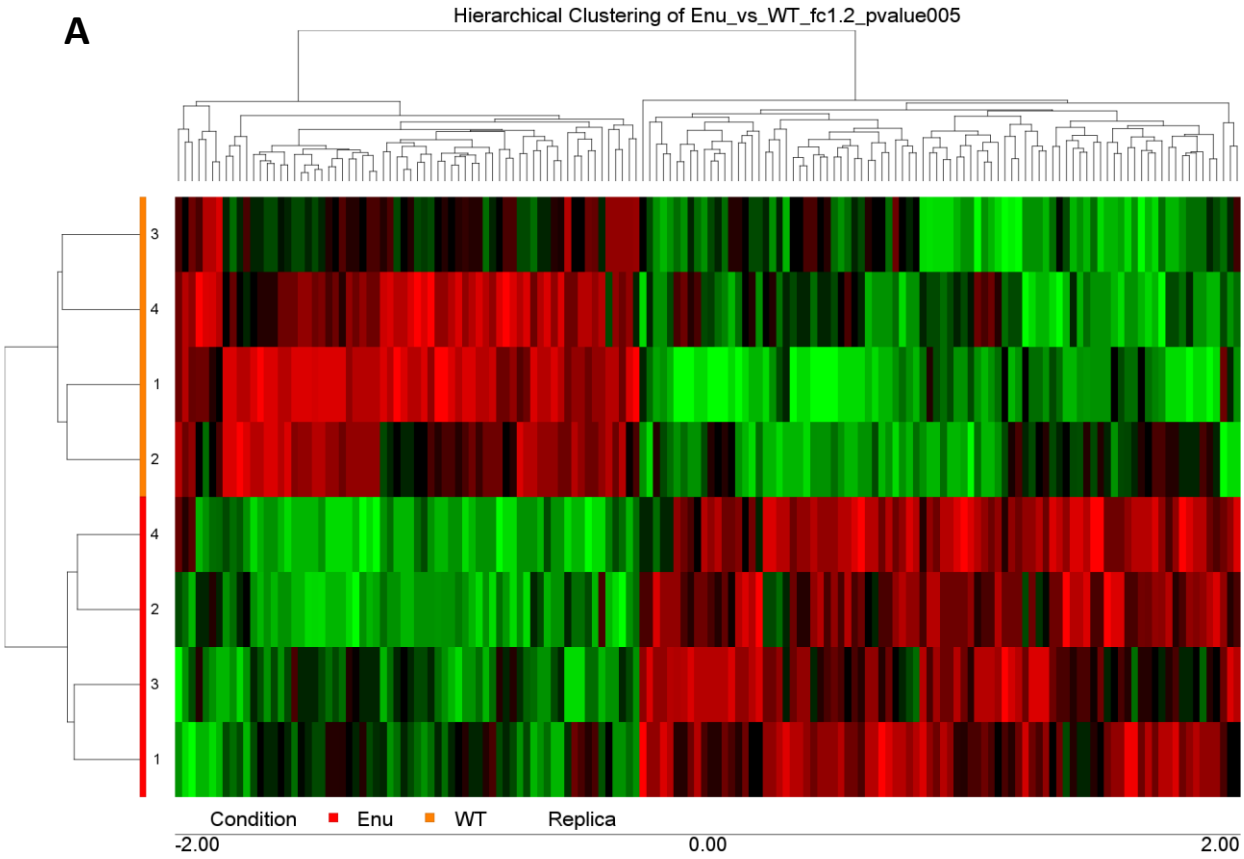

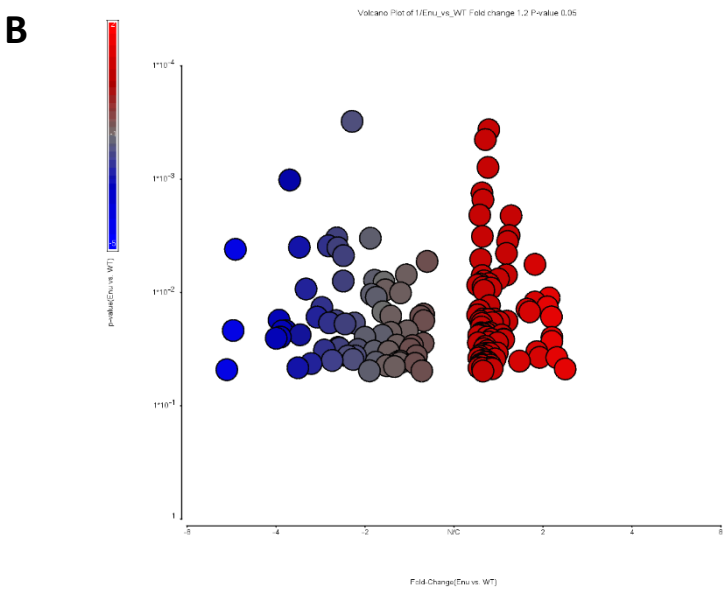

Figure 33: **Hierarchical clustering (A) analysis of differentially expressed microRNAs in WT (n=4) and ENU2 (n=4) mice brains with a fc > 1.2**. 156 microRNAs were differentially expressed in ENU2 compared to WT mice, with statistical significance set at p-value: 0.05. Color gradation shows the relative expression of microRNAs: green, downregulation; red, upregulation. Volcano plot (**B**) of differentially expressed microRNAs ENU2 and WT mice brains. Y-axis: p-value (0.05); X-axis: fold change (>1.2). Color gradation shows the relative expression of microRNAs: blue, downregulation; red, upregulation.

Target genes of the mature upregulated miRNAs with fc > 1.2 and mature downregulated miRNAs with fc < -2.5 were analyzed using target prediction bioinformatics tools (miRDB, TargetScanMouse 8.0 and DIANA TOOLS-microT-CDS), thus evaluating the possible molecular targets with the most promising scores in each of the mentioned tools. Only common target genes recognized by the three prediction tools were considered for further analyses. The expression of 5 upregulated miRNAs (miR-671-3p, miR-217-5p, miR-448-5p, miR-218-1-3p and miR-1231-3p) were examined through RT-qPCR to validate the fold change data obtained from the microarray analysis. As reported in **Figure 34**, RT-qPCR results were analogous to those of the microarray analysis, even if statistical significance only for miR-217-5p, miR-218-1-3p and miR-1231-3p was recorded.

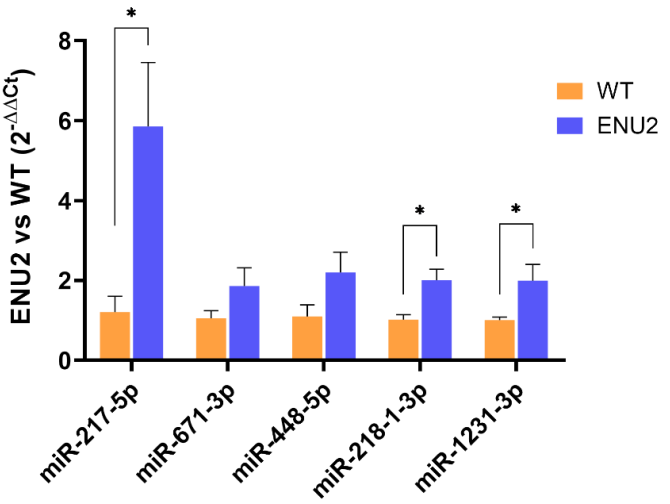

Figure 34: **Validation of upregulated miRNAs in ENU2 compared to WT in mice brains of 60 PND**. Data are expressed as Mean ± SEM (n=4/group) and presented as $2^{-\Delta\Delta CT}$ relative to the levels of WT miRNAs expression. snoRNA202 was used as endogenous control. Two-tailed t-test *p<0.05.

4.7 GENE SET ENRICHMENT ANALYSIS FOR miRNAs TARGETS

Gene Ontology (GO) was used to highlight and classify those biological process (BP), cellular component (CC) and molecular function (MF) that are over-represented between the upregulated (fc > 1.2) and downregulated (fc < -2.5) mature miRNAs' predicted targets. As shown in **Figure 35**, potentially differentially expressed genes targeted by upregulated miRNAs in ENU2 mice were enriched in numerous BP including neuron projection morphogenesis and development, cell projection morphogenesis, regulation of cellular catabolic process, neuron differentiation and development, generations of neurons, neurogenesis, positive regulation of developmental process, cell part morphogenesis and tissue development. Similarly, the following CC were potentially affected: neuron spine, dendritic spine, growth cone, synaptic vesicle, transport vesicle, Golgi apparatus subcompartment, early endosome, transport vesicle, neuron to neuron synapse, presynapse, axon, perinuclear region of cytoplasm, synapse and dendritic tree. Possible alteration of MF included the following: keratin filament binding, protein kinase B binding, semaphorin receptor binding, GDP binding, protein phosphatase regulator activity, histone deacetylase binding, DNA-binding transcription activator activity and mRNA binding. KEGG pathway analysis identified 9 pathways that could be potentially altered by upregulated miRNAs: mucin type O-glycan biosynthesis, amphetamine addiction, long-term potentiation, neurotrophin signaling pathway, oocyte meiosis, dopaminergic synapse, microRNAs in cancer, oxytocin signaling pathway and tuberculosis

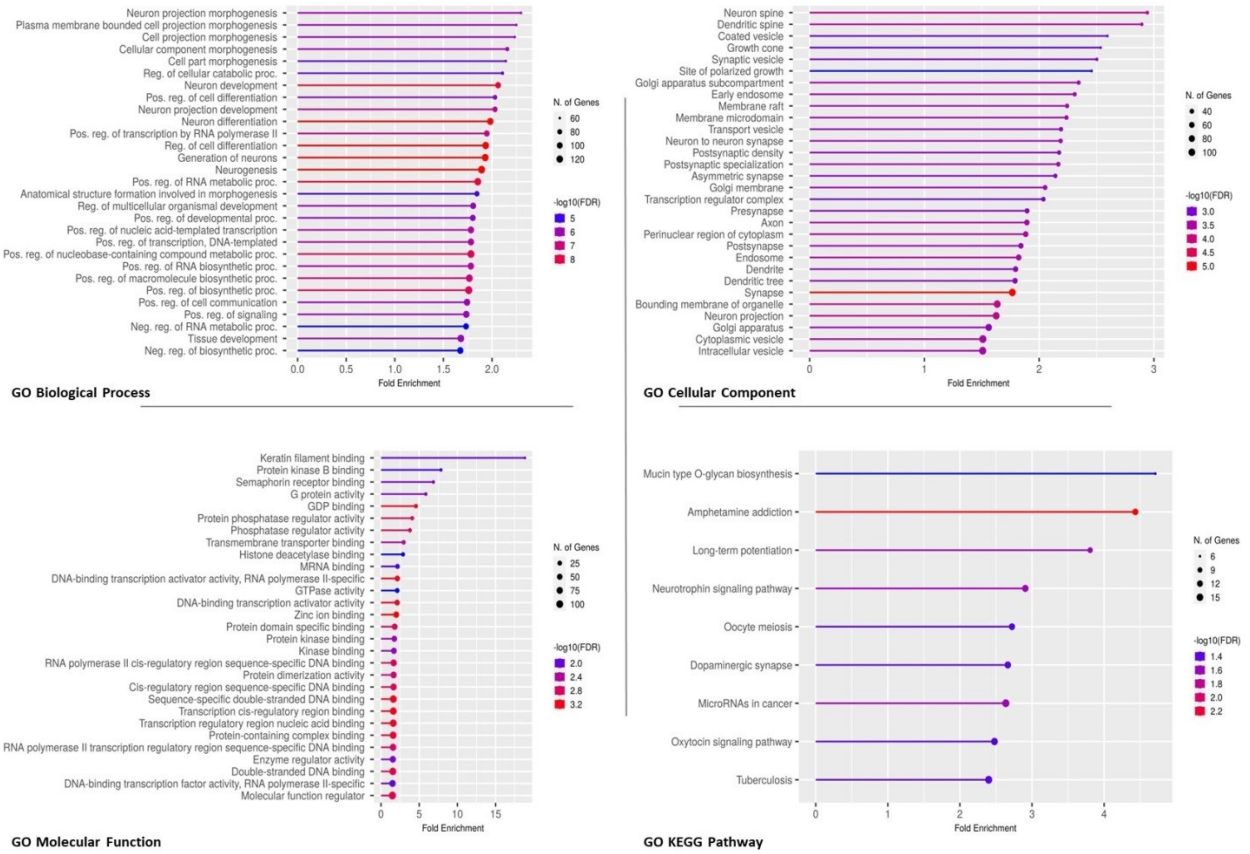

Figure 35: **Gene Ontology and KEGG pathway analysis of potential targets recognized by mature upregulated miRNAs (fc > 1.2)**. Enrichment analysis was performed for Biological Process (BP), Cellular Component (CC), Molecular Function (MF) and KEGG pathway analysis. Fold Enrichment and FDR are reported.

Gene set enrichment analysis was performed also for potential gene targets recognized by downregulated miRNAs in ENU2 with fc < -2.5; as shown in **Figure 36**, among the possibly altered BP we found synapse organization, cell junction organization, brain development, positive regulation of cell differentiation, head development, regulation of cell differentiation, positive regulation of RNA metabolic process, neuron differentiation, neurogenesis, generation of neurons and cell migration. Possibly altered CC included: F-actin capping protein complex, AMPA glutamate receptor complex, neurotransmitter receptor complex, presynaptic membrane, dendritic spine, neuron spine, glutamatergic synapse, axon, postsynaptic membrane, dendritic tree, somatodendritic compartment and neuron to neuron synapse. Concerning MF, the following process could be altered by downregulated miRNAs: vascular endothelial growth factor receptor 2 binding, structural constituent of postsynapse, glutamate receptor binding, DNA-binding transcription activator activity and GTPase activity. KEGG pathway analysis revealed 18 pathways that could potentially be affected by downregulated miRNAs, such as

Notch signaling pathway, adherent junction, glutamatergic synapse, endocytosis, Rap1 signaling pathway and PI3K-Akt signaling pathway.

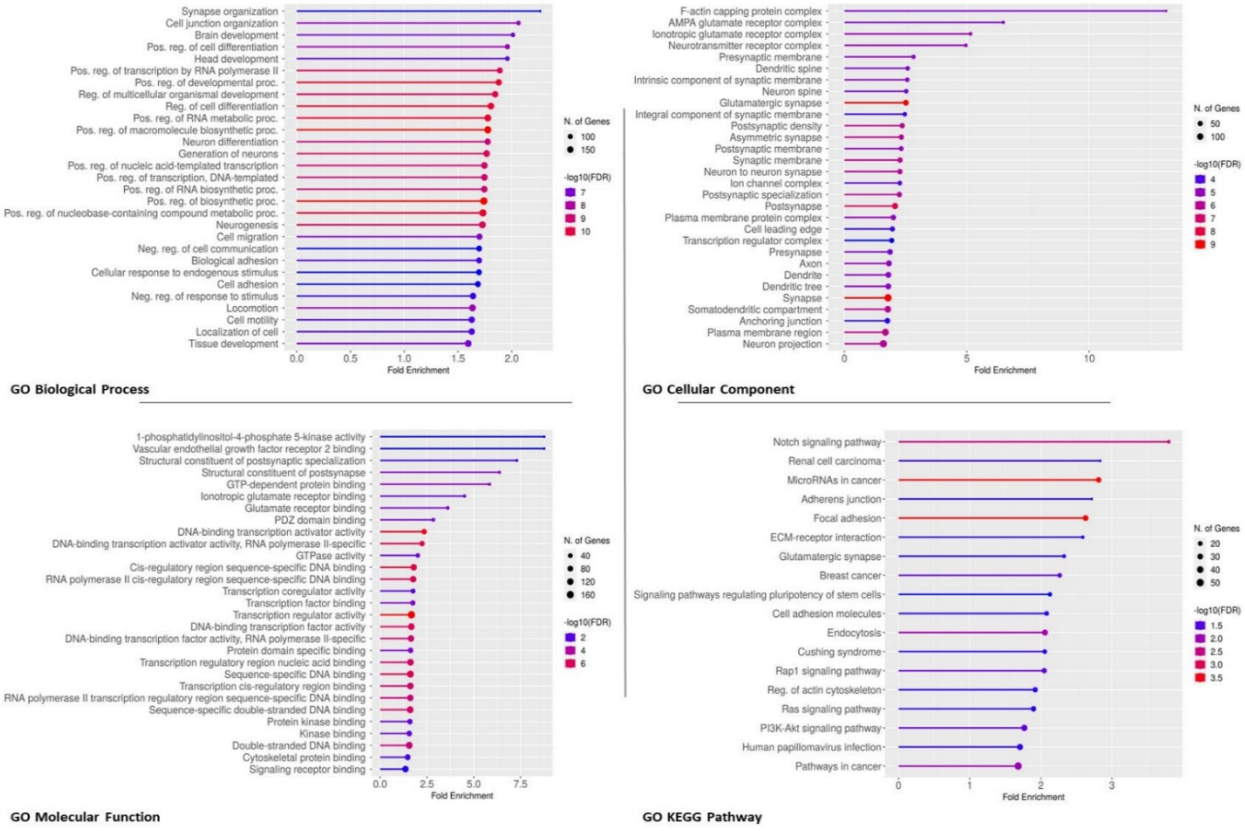

Figure 36: **Gene Ontology and KEGG pathway analysis of potential targets recognized by mature downregulated miRNAs (fc < -2.5)**. Enrichment analysis was performed for Biological Process (BP), Cellular Component (CC), Molecular Function (MF) and KEGG pathway analysis. Fold Enrichment and FDR are reported.

The miRNAs-targets networks were built via Cytoscape software, highlighting proteins which could be targeted by more than one miRNA (**Figure 37-38**). Interestingly, many miRNAs' targets are in common with two or more miRNAs, underlying their proximity and suggesting a possible mutual functionality.

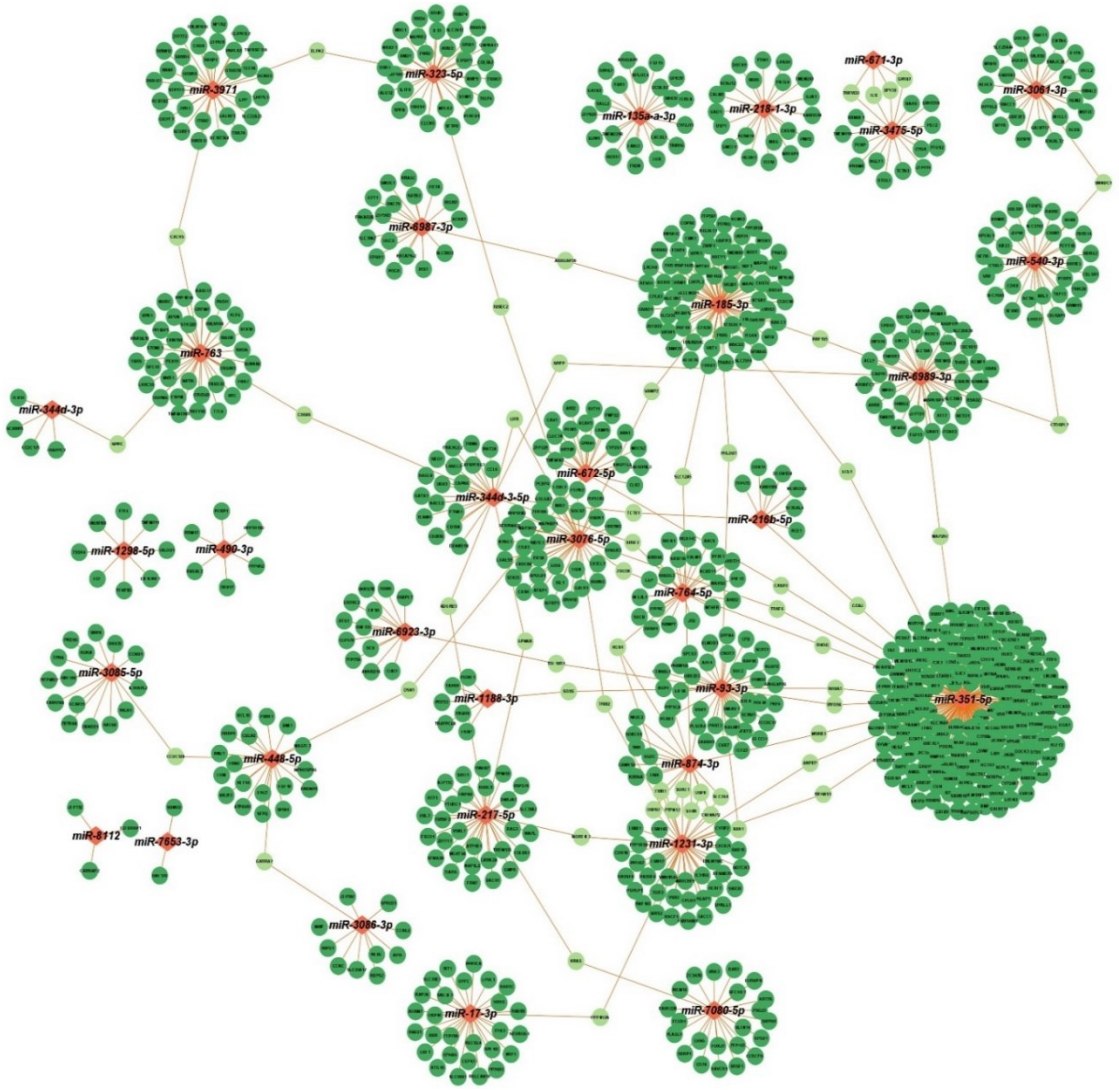

Figure 37: **Mature upregulated (fc > 1.2) miRNAs-targets network built in Cytoscape v3.9.1**. Possibly downregulated target genes are highlighted in green, and the common targets between two or more miRNAs are highlighted in light green.

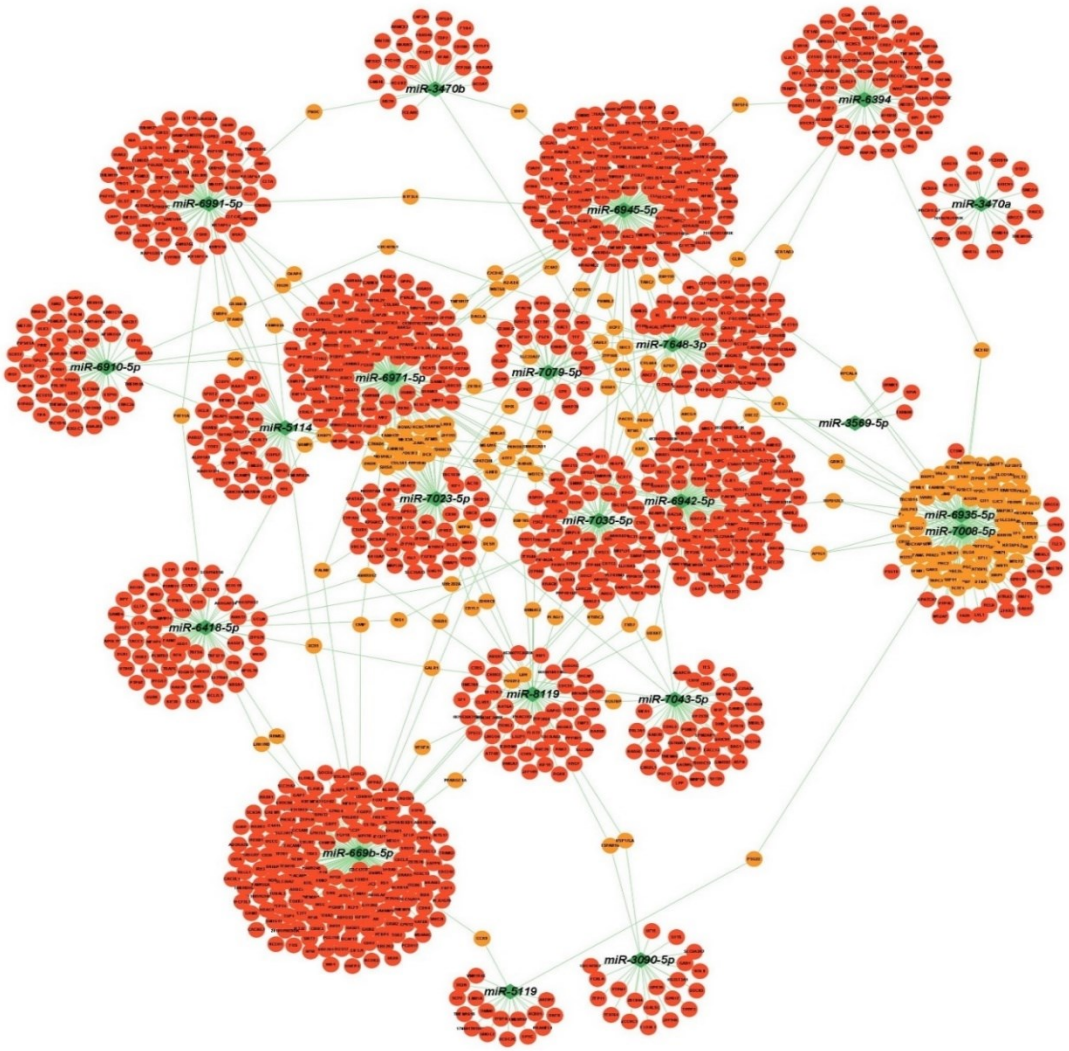

Figure 38: **Mature downregulated (fc < -2.5) miRNAs-targets network built in Cytoscape v3.9.1**. Possibly upregulated target genes are highlighted in red, and the common targets between two or more miRNAs are highlighted in orange.

4.8 PROTEOMIC ANALYSES OUTCOME

In order to identify and evaluate candidate proteins which could be potential targets of the mature upregulated miRNAs and could interfere with the correct MBP translation, we performed a proteomic analysis on WT and ENU2 brain lysates of 60 and 360 PND (n=4/condition) using TMT (Tandem Mass Tag) quantification and considering as significantly different expressed proteins with a fold change 1.5 and an FDR<0.1. As reported in **Figure 39A**, the peptide labelling efficiency was about 90%, with a 19.86% of labelled peptides which were filtered by isolation and thus not considered for the final evaluation. Moreover, the precursor contamination percentage was about 5%, with a good quality control after normalization of the ionic current signals (**Figure 39B-C**).

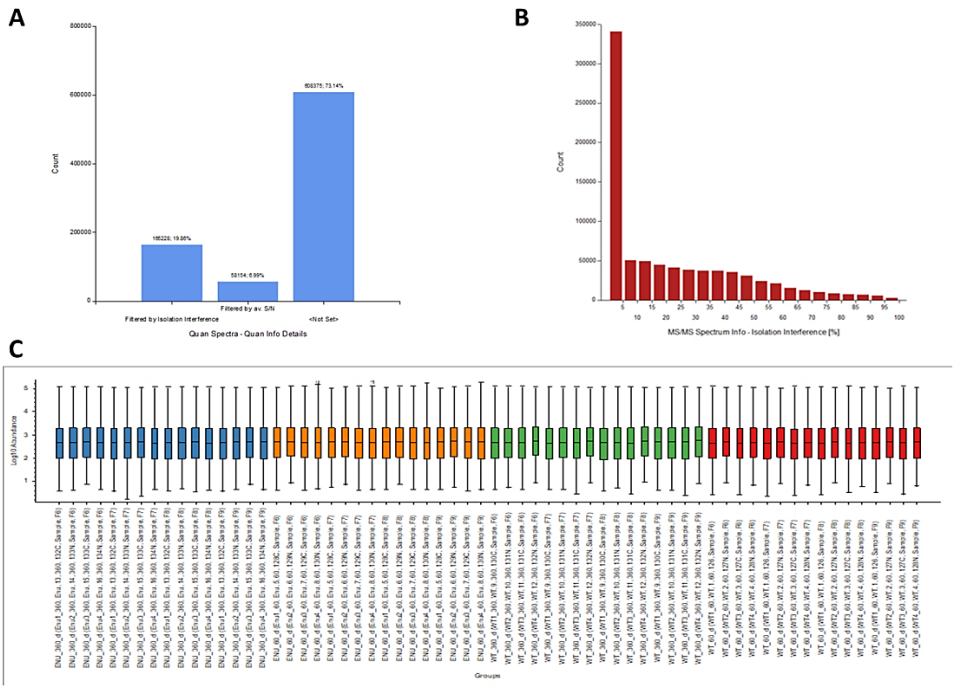

Figure 39: (**A**) Peptides labelling efficiency. Labelled peptides that were filtered by isolation interference and average signal-to-noise ratio (S/N) account for 26% of the total labelled peptides and were not considered in the final analysis. (**B**) Isolation Interference accounts only for 5% (contaminants). (**C**) Quality control after data signals normalization. The normalized samples are uniform and thus analyzable.

Differentially expressed proteins with fc > 1.5 were evaluated after passing volcano plot filtering (**Figure 40A-B**) and PCA analysis was performed in order to highlight both samples variability and the relationship between WT and ENU2 brain proteins over the time points considered (60-360 PND) (**Figure 40C**).

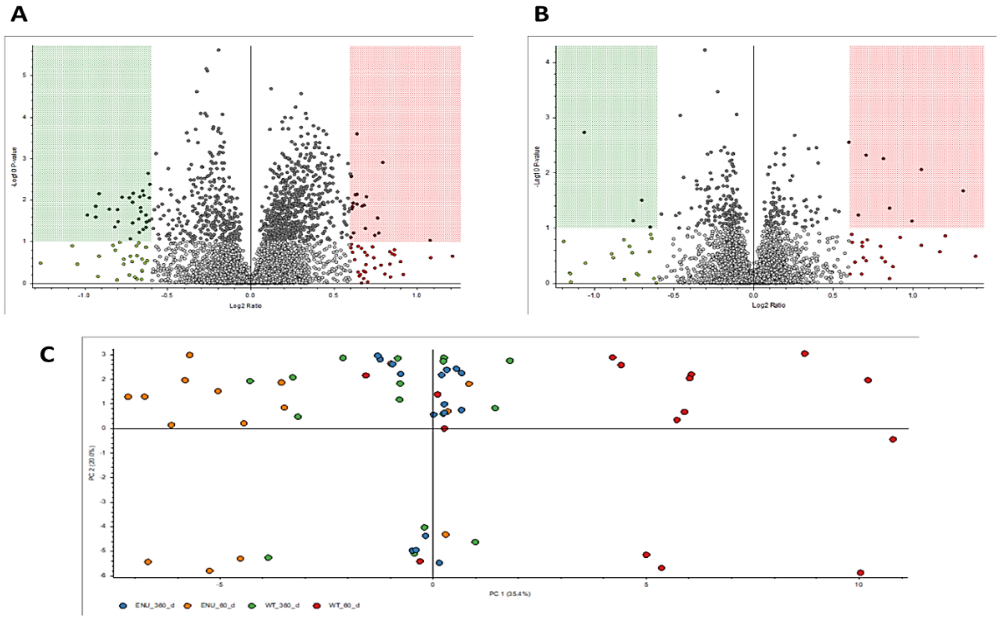

Figure 40: **Volcano plot representing differentially expressed proteins with fc > 1.5 in WT and ENU2 brains at 60 PND (A) and 360 PND (B)**. Color gradation shows the relative expression of proteins: green, downregulation; red, upregulation. (**C**) PCA on the evaluated proteins. This analysis highlights samples variability and the relationship between WT and ENU2 proteins at 360 PND, which is detectable in the middle of the diagram.

As reported in **Table 4**, proteomic analysis detected 47 differentially expressed proteins between WT and ENU2 at 60 PND, with fold change set at 1.5 and FDR<0.1. Of these proteins, 28 were significantly downregulated, while 19 were significantly upregulated at 60 PND. Interestingly, many downregulated proteins at 60 PND normalized their own expression at 360 PND, thus highlighting the great cerebral plasticity already observed during MBP analyses. Speaking of MBP, its expression normalization during development were confirmed also by the proteomic analysis; in fact, MBP raised from a ENU2/WT ratio of -1.639 at 60 PND to a ENU2/WT ratio of -1.052 at 360 PND, which is an indication of a complete normalization over protein expression during adulthood. Is also of note the protein expression recovery of many other myelin proteins, such as PLP1 (confirming what was seen on WBs), MOG, CNP, and, even not statistically significant, MAG (which went from a fold of -1.513 at 60 PND to a fold of 1.059 at 360 PND, not reported in **Table 4**). Moreover, protein expression normalization at 360 PND has been observed also for other important downregulated proteins at 60 PND that are involved in myelin constitution, such as ANLN, VAMP1, GJC3, SYT2 and ELP1 and for upregulated proteins at 60 PND which are involved as well in neuronal differentiation and migration (such as NRGN, STX7, GMP6A and SYNPO).

Accession	Description	Gene Symbol	Fold 60 PND	Fold 360 PND	Ratio Adj. P-Value: ENU2/WT 60 PND	Ratio Adj. P-Value: ENU2/WT 360 PND
P60202	Myelin proteolipid protein	Plp1	**-1,802**	**1,018**	0,19	1
Q8K298	Anillin	Anln	**-1,745**	**1,028**	0,19	1
P31650	Sodium- and chloride-dependent GABA transporter 3	Slc6a11	**-1,527**	**1,120**	0,25	1
Q9D1G3	Protein-cysteine N-palmitoyltransferase HHAT-like protein	Hhatl	**-1,565**	**1,741**	0,32	1
P48379	DNA-binding protein RFX2	Rfx2	**-1,976**	**-1,062**	0,21	1
P00920	Carbonic anhydrase 2	Car2	**-1,546**	**1,049**	0,26	1
Q8C4D5	Raftlin, Lipid Raft Linker 1	Rftn1	**-1,548**	**1,231**	0,21	1
Q61885	Myelin-oligodendrocyte glycoprotein	Mog	**-1,658**	**1,100**	0,14	1
G5E895	Aldo-keto reductase family 1, member B10 (aldose reductase)	Akr1b10	**-1,534**	**-1,076**	0,09	1
D3YTU0	Vesicle-associated membrane protein 1	Vamp1	**-1,572**	**1,031**	0,13	1
Q91W92	Cdc42 effector protein 1	Cdc42ep1	**-1,597**	**1,206**	0,23	1
Q9D154	Leukocyte elastase inhibitor A	Serpinb1a	**-1,634**	**1,158**	0,13	1
Q3TYV5	2',3'-cyclic-nucleotide 3'-phosphodiesterase	Cnp	**-1,527**	**1,075**	0,14	1
Q9QY42	Prosaposin receptor GPR37	Gpr37	**-1,563**	**1,080**	0,14	1

A0A654ICL5	Gap junction protein 3	Gjc3	**-1,637**	**-1,002**	0,16	1
Q542T4	Myelin basic protein	Mbp	**-1,639**	**-1,052**	0,27	1
B2RQX9	Transporter	Slc6a5	**-1,653**	**1,144**	0,44	1
Q91VC7	Protein phosphatase 1 regulatory subunit 14A	Ppp1r14a	**-1,883**	**1,170**	0,13	1
A0A1L1SRL4	Heme-binding protein 2	Hebp2	**-1,739**	**1,354**	0,26	1
P50114	Protein S100-B	S100b	**-1,908**	**-1,106**	0,18	1
E9Q804	Ankyrin repeat domain-containing protein 17	Ankrd17	**-1,585**	**1,053**	0,18	1
Q3U1V6	Ubiquitin-conjugating enzyme E2 variant 3	Uevld	**-1,764**	**1,438**	0,30	1
Q5DTI3	Synaptotagmin	Syt2	**-1,522**	**-1,050**	0,11	1
Q7TT37	Elongator complex protein 1	Elp1	**-1,590**	**1,635**	0,14	1
Q8R3P0	Aspartoacylase	Aspa	**-1,908**	**1,089**	0,22	1
Q9CWD9	Junctional adhesion molecule B	Jam2	**-1,546**	**-1,357**	0,30	1
Q6P9J5	KN motif and ankyrin repeat domain-containing protein 4	Kank4	**-1,580**	**1,043**	0,20	1
Q3U011	GLTP domain-containing protein	Gltp	**-1,709**	**1,034**	0,14	1
Q7TPG1	Phosphodiesterase	Pde10a	**1,557**	**1,003**	0,13	1
Q0VBU3	Muscarinic acetylcholine receptor	Chrm4	**1,537**	**1,262**	0,37	1
A0A0R4J1N6	Tyrosine-protein kinase	Matk	**1,707**	**-1,075**	0,37	1
E9PUC5	PH and SEC7 domain-containing protein 3	Psd3	**1,547**	**-1,074**	0,14	1
Q3U336	Synaptopodin	Synpo	**1,522**	**1,018**	0,09	1
O89020	Afamin	Afm	**1,696**	**-1,134**	0,23	1
P60761	Neurogranin	Nrgn	**1,603**	**1,177**	0,17	1
A0A8I4SYN6	H3.4 histone	H3f4	**1,679**	**1,076**	0,39	1
Q3UB06	Protein kinase domain-containing protein	Srpk1	**2,112**	**1,113**	0,46	1
P11031	Activated RNA polymerase II transcriptional coactivator p15	Sub1	**1,559**	**-1,131**	0,05	1
Q3TY78	G Protein subunit alpha L	Gnal	**1,533**	**1,038**	0,17	1
Q91W43	Glycine dehydrogenase (decarboxylating), mitochondrial	Gldc	**1,527**	**1,067**	0,18	1
Q5U4D8	Sodium-dependent multivitamin transporter	Slc5a6	**1,611**	**1,045**	0,31	1
Q8QZT2	Centriole, cilia and spindle-associated protein	Ccsap	**1,559**	**-1,042**	0,17	1
Q542P2	Glycoprotein M6A	Gpm6a	**1,527**	**-1,152**	0,18	1
Q3UTQ8	Cyclin-dependent kinase-like 5	Cdkl5	**1,621**	**1,096**	0,14	1
Q9D3P8	Plasminogen receptor (KT)	Plgrkt	**1,734**	**-1,105**	0,07	1
Q60829	Protein phosphatase 1 regulatory subunit 1B	Ppp1r1b	**1,59**	**1,041**	0,18	1
Q9CY18	Sorting nexin-7	Snx7	**1,519**	**1,051**	0,42	1

Table 4: **Differentially expressed proteins in the PKU mouse brain at 60 and 360 PND**. Downregulated proteins in ENU2 at 60 PND are highlighted in green, while upregulated ones are highlighted in red.

Proteomic results were then bioinformatically analyzed in order to understand which relationships and/or pathways resulted to be altered in the early stage of development for the ENU2 mice brain. Interactions between up- and downregulated proteins were analyzed after submission to the STRING database with a minimum required interaction score set to >0.40, while potential altered pathways were analyzed through gene set enrichment analysis. As reported in **Figure 41**, downregulated myelin proteins at 60 PND are strictly interconnected, forming a significant cluster with a score of 3.23 comprehensive of 14 nodes and 21 edges. From gene set enrichment analysis, we found that significant up- and downregulated proteins are involved in many biological processes such as response to amine, myelination, axon ensheathment and synaptic signaling, while we found dendritic spine head, dendritic spine, myelin sheath and presynaptic synapse among the possible altered cellular components. Lately, we found that alteration of the structural constituent of myelin sheath, amino acid sodium symporter activity and lipid binding can also occur in the young ENU2 mouse brain.

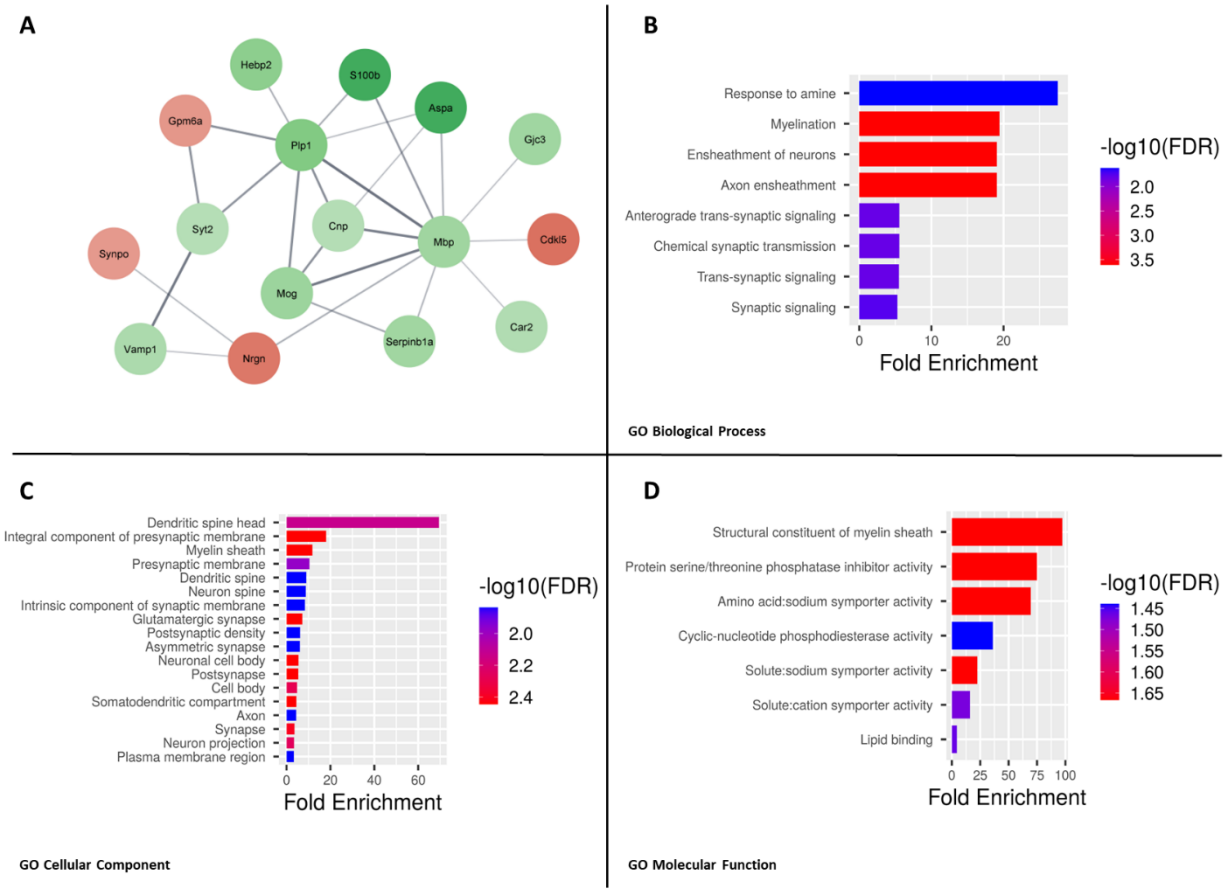

Figure 41: (**A**) Up- and downregulated proteins in ENU2 mouse brain forming a cluster of 14 nodes and 21 edges. The degree of up- or downregulation was reported as color gradient (green: downregulation; red: upregulation). (**B-C-D**) Gene Ontology for significant up- and downregulated protein at 60 PND (fold > 1.5). Enrichment analysis was performed for Biological Process (BP), Cellular Component (CC) and Molecular Function (MF). Fold Enrichment and FDR are reported.

4.9 miRNAs SELECTION AND RELATIVE VALIDATION OF DIFFERENTIALLY EXPRESSED PROTEINS

Proteomic analyses defined many downregulated proteins that could potentially be targets of the previously assessed upregulated miRNAs at 60 PND. In order to establish the most promising miRNA-protein relation that could explain the MBP trend observed during development, and with the purpose to validate proteomic analyses, we searched for the common proteins among the potential upregulated miRNAs' targets and the downregulated proteins at 60 PND.

In this case, to extend the research, we included in the analysis all the downregulated proteins with fold < -1.2, regardless of the significance; in fact, many potential proteins involved in MBP regulation might be resulted as not significant because of the great variability between samples.

As depicted from the Venn diagram in **Figure 42**, 27 proteins were in common between the two sets and thus were considered as potentially downregulated by the upregulated miRNAs (see **Table 5**).

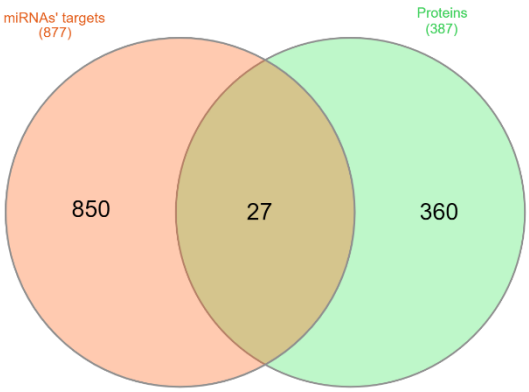

Figure 42: **Venn diagram between mature upregulated (fc > 1.2) miRNAs' targets and downregulated proteins (fold<-1.2) at 60 PND**. 27 downregulated proteins were in common between the two sets, suggesting the potential inhibitory action of upregulated miRNAs on their expression.

miRNA name	Fold change (ENU2 vs WT)	Downregulated targets at 60 PND in ENU2 (fold)	Targets description
miR-671-3p	2.10	GLRA1 (-1.7)	Glycine receptor, alpha 1 subunit [Source:MGI Symbol;Acc:MGI:95747]
miR-217-5p	**2.07**	**ANLN (-1.74)**	**Anillin, actin binding protein [Source:MGI Symbol;Acc:MGI:1920174]**
		BAG3 (-1.21)	BCL2-associated athanogene 3 [Source:MGI Symbol;Acc:MGI:1352493]
		SLC38A2 (-1.37)	Solute carrier family 38, member 2 [Source:MGI Symbol;Acc:MGI:1915010]
miR-218-1-3p	**2.14**	**MAG (-1.51)**	**Myelin-associated glycoprotein [Source:MGI Symbol;Acc:MGI:96912]**
		ANKRD29 (-1.25)	Ankyrin repeat domain 29 [Source:MGI Symbol;Acc:MGI:2687055]

miR-185-3p	1.9	ADD1 (-1.40)	Adducin 1 (alpha) [Source:MGI Symbol;Acc:MGI:87918]
		TLCD3B (-1.35)	TLC domain containing 3B [Source:MGI Symbol;Acc:MGI:1916202]
miR-764-5p	1.8	MARS2 (-1.41)	Methionine-tRNA synthetase 2 (mitochondrial) [Source:MGI Symbol;Acc:MGI:2444136]
miR-1231-3p	**1.77**	**CNTNAP2 (-1.26)**	**Contactin associated protein-like 2 [Source:MGI Symbol;Acc:MGI:1914047]**
		AAK1 (-1.30)	AP2 associated kinase 1 [Source:MGI Symbol;Acc:MGI:1098687]
miR-17-3p	1.51	RAP2C (-1.40)	RAP2C, member of RAS oncogene family [Source:MGI Symbol;Acc:MGI:1919315]
miR-7080-5p	1.47	SSRP1 (-1.31)	Structure specific recognition protein 1 [Source:MGI Symbol;Acc:MGI:107912]
miR-6989-3p	1.33	SLC16A1 (-1.30)	Solute carrier family 16, member 1 [Source:MGI Symbol;Acc:MGI:106013]
miR-93-3p	1.3	AAK1 (-1.30)	AP2 associated kinase 1 [Source:MGI Symbol;Acc:MGI:1098687]
		PHLDB1 (-1.20)	Pleckstrin homology like domain, family B, member 1 [Source:MGI Symbol;Acc:MGI:2143230]
		RAP1A (-1.23)	RAS-related protein 1a [Source:MGI Symbol;Acc:MGI:97852]
		PEAK1 (-1.44)	Pseudopodium-enriched atypical kinase 1 [Source:MGI Symbol;Acc:MGI:2442366]
miR-672-5p	1.29	LAMP5 (-1.41)	Lysosomal-associated membrane protein family, member 5 [Source:MGI Symbol;Acc:MGI:1923411]
		ANK1 (-1.21)	Ankyrin 1, erythroid [Source:MGI Symbol;Acc:MGI:88024]
		MOCS2 (-1.29)	Molybdenum cofactor synthesis 2 [Source:MGI Symbol;Acc:MGI:1336894]
		TNFAIP8L3 (-1.42)	Tumor necrosis factor, alpha-induced protein 8-like 3 [Source:MGI Symbol;Acc:MGI:2685363]
miR-540-3p	1.26	SLC25A5 (-1.25)	Solute carrier family 25, member 5 [Source:MGI Symbol;Acc:MGI:1353496]
miR-351-5p	1.26	VPS4B (-1.24)	Vacuolar protein sorting 4B [Source:MGI Symbol;Acc:MGI:1100499]
		ULK3 (-1.24)	Unc-51-like kinase 3 [Source:MGI Symbol;Acc:MGI:1918992]
miR-490-3p	1.25	RASAL2 (-1.26)	RAS protein activator like 2 [Source:MGI Symbol;Acc:MGI:2443881]
miR-763	1.25	PIKFYVE (-1.40)	Phosphoinositide kinase, FYVE type zinc finger containing [Source:MGI Symbol;Acc:MGI:1335106]
		NAT8L (-1.29)	N-acetyltransferase 8-like [Source:MGI Symbol;Acc:MGI:2447776]
miR-874-3p	1.25	CNTNAP2 (-1.26)	Contactin associated protein-like 2 [Source:MGI Symbol;Acc:MGI:1914047]

Table 5: **Potential relation between mature upregulated miRNAs' (fc > 1.2) targets and downregulated proteins at 60 PND (fold <-1.2) in ENU2 brains**.

Of the 27 candidate downregulated proteins, we decided to evaluate ANLN, MAG and CNTNAP2, which are potential targets for the significant upregulated miRNAs miR-217-5p, miR-218-1-3p and miR-1231-3p (**Figure 34**), respectively, through western blot analyses. These proteins are, in fact, actively involved in the myelination process and their downregulation can lead to detrimental effects over myelin formation and scaffolding, as well as lower levels of MBP (McKerracher and Rosen, 2015; Erwig *et al.*, 2019; Scott *et al.*, 2019). As reported in **Figure 43**, western blotting showed significant under-expression of ANLN and MAG proteins in PKU mouse

brain compared to the control – a finding that was confirmed by densitometric analysis. CNTNAP2 was downregulated as well compared to WT mice, even though the result was not significant with the two-way ANOVA test. At 360 PND all the three evaluated proteins normalized their own expression, confirming what was seen at the proteomic level.

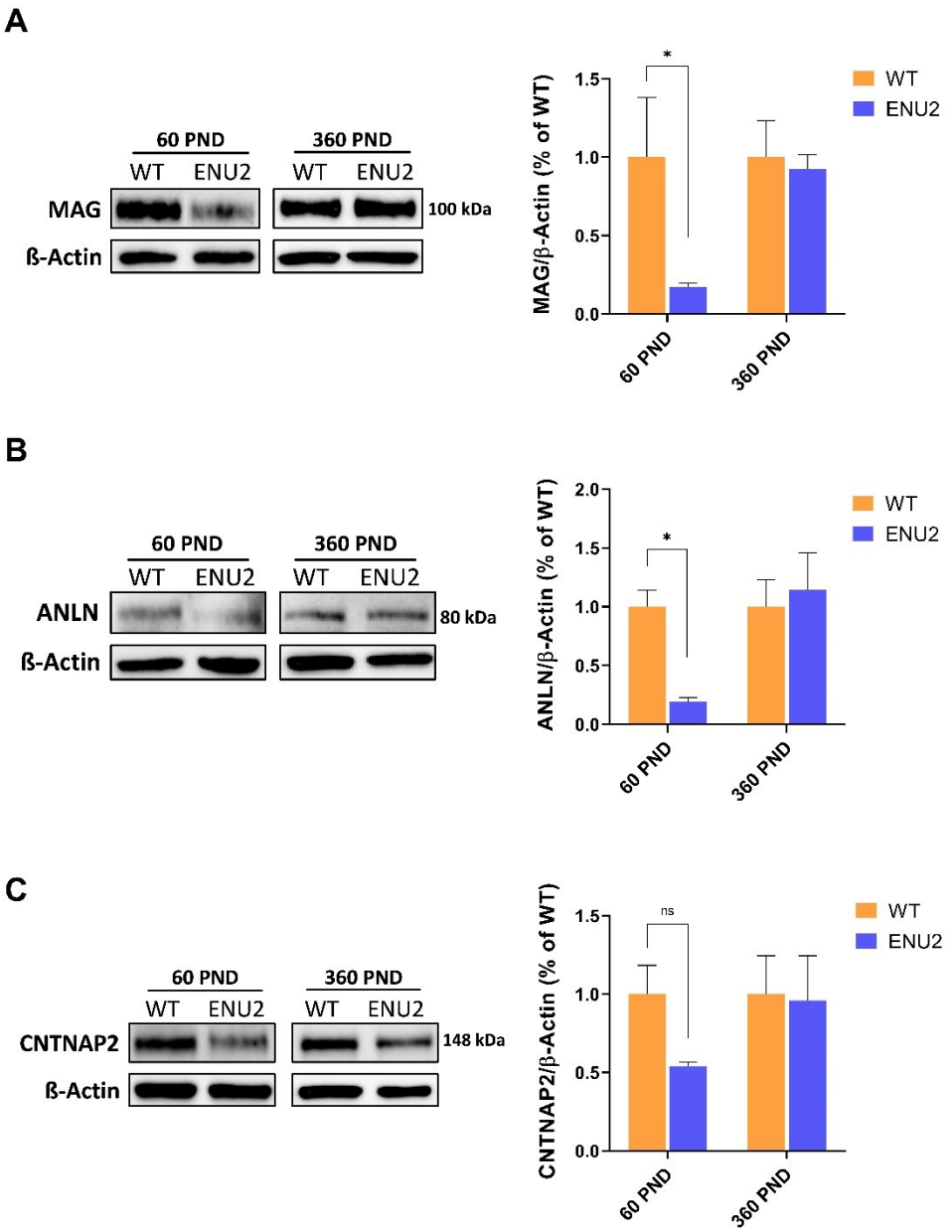

Figure 43: **Representative immunoblots and densitometric analysis of (A) MAG, (B) ANLN and (C) CNTNAP2 showing the expression levels of the proteins in WT and ENU2 brains at 60 and 360 PND**. Data are expressed as Mean ± SEM (n=4/condition). All the reported values in the graph are densitometric values obtained using Image Lab software. Two-way ANOVA followed by Bonferroni's multiple comparison test, *p<0.05.

4.10 miRNAs EVALUATION DURING DEVELOPMENT

The potential miRNAs that could be involved in the downregulation of the three proteins evaluated after proteomic and WBs (ANLN, MAG and CNTNAP2) were examined throughout development, to assess if their expression were correlated with the corresponding target proteins levels and, consequently, to MBP levels. Therefore, we decided to evaluate miR-218-1-3p, miR-217-5p, miR-1231-3p and miR-671-3p, because one of its potential targets is the glycine receptor, alpha 1 subunit (GLRA1); this protein is in fact downregulated at 60 PND in ENU2 brains (fold: -1.7) and is of relevance as it is fundamental in the generation of inhibitory postsynaptic currents and in the downregulation of neuronal excitability (Shiang *et al.*, 1993; Zhang *et al.*, 2015). As shown in **Figure 44**, miRNAs' levels between WT and ENU2 mice fluctuated greatly during development, with a peak in correspondence of 60 PND and a declining trend throughout adulthood. miRNAs expression was not as expected especially at 14 PND; however, at that age the L-Phe blood and brain concentrations were significantly higher compared to all the time points considered, thus leading us to hypothesize another epigenetic reprogramming that could lead to new hyper- or hypomethylated loci in the ENU2 mice brains. These considerations may not be applied for miR-218-1-3p, because the expression of this miRNA at 14 PND was higher in ENU2 compared to WT, even though not significant (**Figure 44B-C**). Concerning miR-218-1-3p, its trend is particularly interesting because its expression in ENU2 brains at 60 PND is significantly higher compared to the one found at 270 PND. The same consideration can be made for miR-1231-3p, since that its expression in young ENU2 brains is higher compared to the ones found at 270 and 360 PND. Moreover, although its low expression in ENU2 at 14 PND, miR-217-5p should be considered as a promising miRNA because its expression at 60 PND is significantly increased compared to all the other intervals of time (**Figure 44A**). On the other hand, miR-671-3p, despite an increasing trend at 60 PND (**Figure 44D**), should not be considered as the cause of GLRA1 downregulation because it resulted to be not significant, and its trend did not even follow the one observed for MBP. Surprisingly, 3 out of the 4 miRNAs evaluated during development (miR-217-5p, -671-3p and -218-1-3p) showed a mild increasing trend on their expression in ENU2 mice of 360 PND, which however may be due mostly to aging (Smith-Vikos and Slack, 2012; Noren Hooten *et al.*, 2013) rather than diverse L-Phe levels.

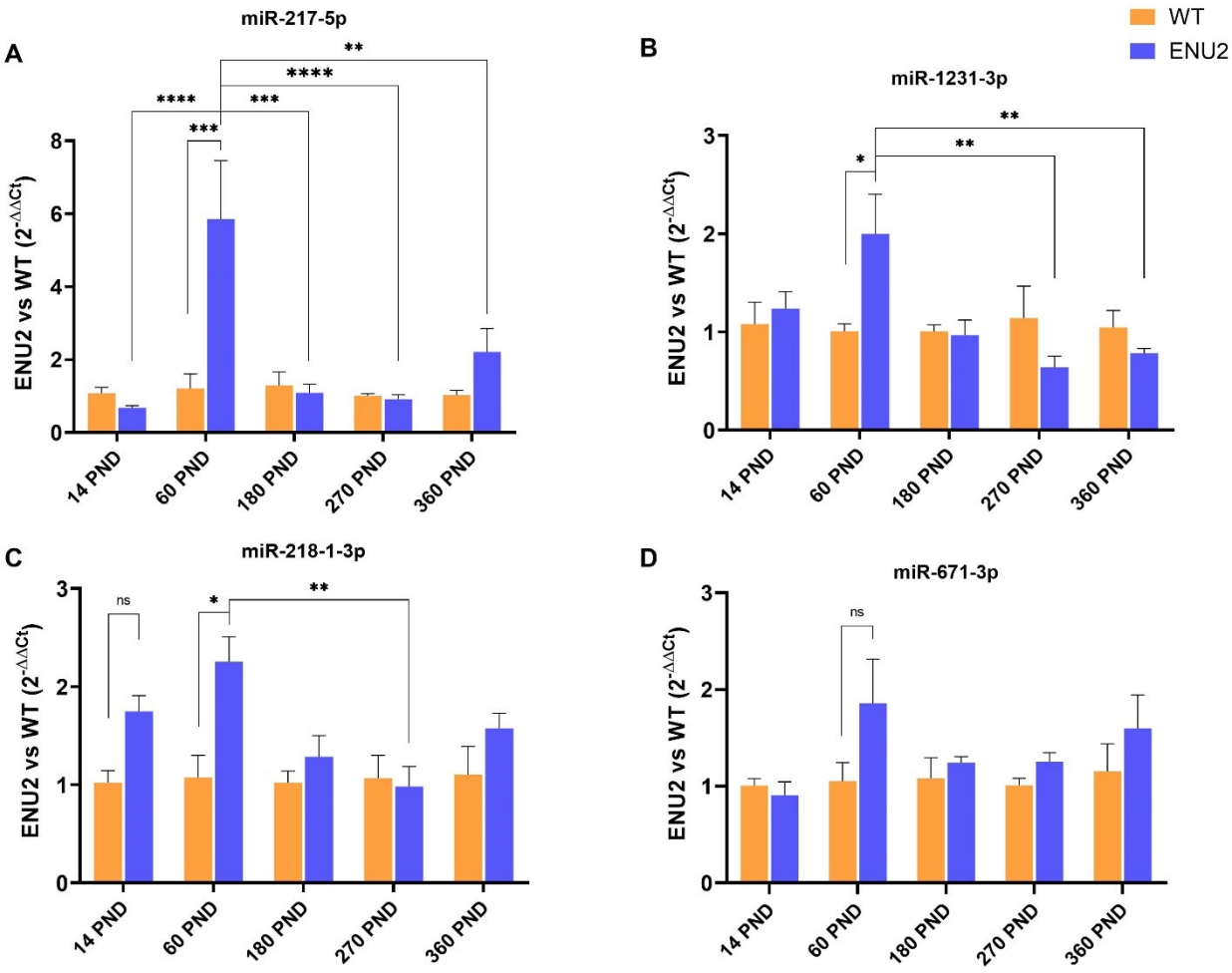

Figure 44: **(A) miR-217-5p, (B) miR-1231-3p, (C) miR-218-1-3p and (D) miR-671-3p expression profiling during development**. Data were analyzed through RT-qPCR and presented as $2^{-\Delta\Delta CT}$ relative to the levels of WT miRNAs expression. Data are expressed as Mean ± SEM (n=4/group). snoRNA202 was used as endogenous small non-coding RNA. Two-way ANOVA followed by Tukey's multiple comparison test, *p<0.05; **p<0.01; ***p<0.0005; ****p<0.0001.

4.11 BEHAVIORAL TESTS FOR ADULT ENU2 AND WT MICE

Adult ENU2 mice (180-270-540 PND) were subjected to OFT and ORT behavioral tests in order to check if the observed MBP and other myelin proteins (MAG, MOG, PLP1, CNP) recovery during adulthood could bring to a cognitive and locomotory activity retrieval. As reported in **Figure 45**, preliminary OFT test depicted a lower locomotory activity for the ENU2 mice, which was not observed in previous OFT tests made on ENU2 mice of 75 PND (Pascucci *et al.*, 2018). This test was also useful to confirm a greater anxiety for the diseased genotype, even if myelin proteins recover themselves during aging. Very old mice of 540 PND did not display the same locomotory deficit, even though they show the same trend observed for the other time points considered; however, the numerosity of the sample was too low (n=3 for each genotype) to develop clear conclusions.

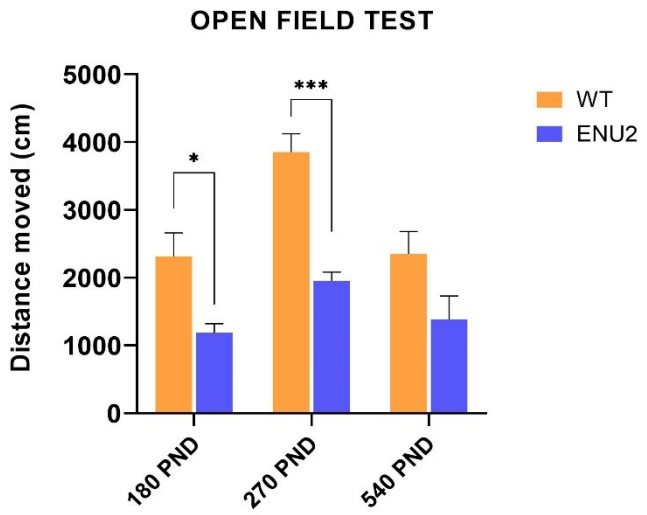

Figure 45: **OFT test for adult mice**. As depicted, ENU2 mice display a lower locomotory activity, together with a greater anxiety. In fact, ENU2 mice are less inclined to move along the arena, indicating a predilection to stay close to the border. The same trend is observed for very old mice of 540 PND, despite being not significant. Two-way ANOVA followed by Duncan's multiple comparison test, *p<0.05; ***p<0.001.

On the other hand, ORT tests did not provide any significant changes between adult WT and ENU2 mice. In fact, as reported in **Figure 46A-B**, Pretest and Test analyses revealed similar exploration time for both conditions regarding firstly the two new white objects and, secondly, the novel black one. At 270 and 540 PND, mice seemed to explore the novel object more than the familiar, indicating a greater curiosity which is unaltered between WT and ENU2. Again, even though these data could provide insights regarding a possible cognitive recovery during adulthood in ENU2 mice, more samples are necessary in order to strengthen this hypothesis.

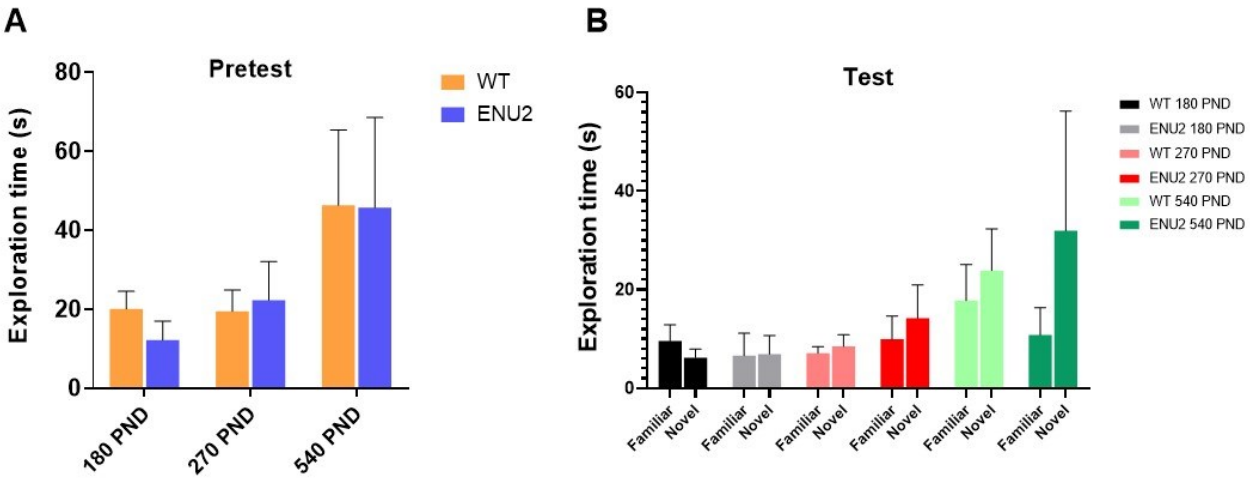

Figure 46: **ORT Pretest (A) and Test (B) analyses for adult WT and ENU2 mice**. The graphs display no statistical differences on the cognitive side for both genetic conditions. However, these analyses reveal no differences over curiosity and exploration time and more samples are needed to support this observation. Two-way ANOVA followed by Tukey's multiple comparison test, *p<0.05.

5. DISCUSSION

Hypomyelination and gliosis in the CNS are the possible neuropathological background of neurodevelopmental derangement and neurological impairment observed in untreated PKU patients and in preclinical models of the disease. In rodents, myelination completes its processes after ≈ 30 days of age (Norton and Poduslo, 1973) and, in the same period, the brain of PKU mouse is exposed to a relevant amount of blood L-Phe concentration that leads to an alteration of myelinated axons, as observed in hypomyelinated areas of mutant animals (Sarah Shefer *et al.*, 2000). MBP, the second most abundant protein of the CNS myelin, plays a crucial role in myelination and it is essential for the assembly of a mature and functioning myelin membrane (Boggs *et al.*, 1986; Campagnoni and Macklin, 1988; Nave and Werner, 2014). This protein is found to be reduced in frontal cortex and striatum of adult untreated PKU mice, with a recovery after a 4-week L-Phe restricted diet (Joseph and Dyer, 2003). To contribute to this topic, we explored MBP protein and MBP mRNA expression levels in ENU2 mice from youth to adulthood. Myelin PLP1 protein levels were also evaluated from 14 to 180 PND. WBs followed by densitometric analyses revealed that MBP protein is low in young ENU2 mice compared to WT, confirming previous data obtained by Pascucci *et al.* (Pascucci *et al.*, 2018). Interestingly, MBP seems to recover to nearly normal levels later in middle-aged ENU2 mice. Immunofluorescence imaging as well confirmed the MBP expression recovery during development, together with a restoration over neurons physiological condition, which was impaired at 60 PND. This observation would be consistent with the delayed myelination detected in biochemically generated hyperphenylalaninemic rats (Baba *et al.*, 1987; Burri *et al.*, 1990). Additionally, in the current work, a slight decrease was detected in Myelin PLP1 protein levels in ENU2 mice brains at 14-60 PND, data that was not confirmed by immunofluorescence analysis. Nonetheless, western blots data could be more precise in measuring protein expression quantities compared to the immunofluorescence technique, which is semi-quantitative and reliant over efficient fluorophore signaling. Together with MBP and PLP1 analyses, we evaluated MBP mRNA expression during development, which revealed no significant expression changes at the time points considered (14-60-180-270-360 PND) and a tendency to be more expressed in the first months of life in ENU2 mice. Together, MBP mRNA and Myelin PLP1 data obtained are consistent with the assessments made by Schoemans and colleagues (Schoemans *et al.*, 2010) and could pave the way to the hypothesis of an impaired MBP translation during the first months of life. One hypothesis that seeks to elucidate the lower MBP protein levels observed during early development lies on a diminished brain large neutral amino acids (LNAAs) availability due to high

L-Phe levels, which in turn may lead to an impaired protein synthesis (Hoeksma *et al.*, 2009; de Groot *et al.*, 2013, 2015). In fact, the low MBP protein expression and the unaltered mRNA could be compensatory in relation to a reduced synthesis of MBP from alteration of the tissutal aminoacidic profile during development. However, in this work we demonstrated that LNAAs concentrations during the early stages of mouse brain development are not lower in ENU2 mice compared to WT. On the contrary, many LNAAs cerebral concentrations resulted to be higher in ENU2 brains, overturning the first hypotheses over LNAAs deprivation in PKU mice and patients (Burlina *et al.*, 2019; van Vliet *et al.*, 2022). In our case, only His and Leu concentration seemed to follow the same trend observed previously on young ENU2 mice; in fact, His resulted to be higher in ENU2 mice of 14-60 PND, while Leu resulted to be lower (even not significant) in ENU2 mice of 60 PND (van Vliet *et al.*, 2016, 2018, 2022). Interestingly, LNAAs cerebral concentrations at 14 PND were significantly higher compared to the ones found at 60 PND, a condition that could be addressed by the increased amino acids uptake that occurs at that age (Pascucci *et al.*, 2008). Despite promising, these data will require more samples to be conclusive and L-Trp cerebral concentrations must be evaluated as well in order to establish the possible impairment on L-Trp derivatives (i.e. serotonin) and, overall, on other neurotransmitters (i.e. norepinephrine, dopamine) (Puglisi-Allegra *et al.*, 2000; Andolina *et al.*, 2011). Taken together, data on LNAAs aminoacidic pool pushed us to set aside the hypothesis of an impaired MBP protein synthesis due to lack of available amino acids in ENU2 brain. Moreover, in one of our previous work (Pascucci *et al.*, 2018), MBP reduction was accompanied by an unaltered neurofilament light polypeptide (NFL) expression in ENU2 mice at 60 PND, thus suggesting a selective hindrance only over MBP expression, leading us to focus on the possible alteration of the MBP translational process. In fact, several studies report that MBP mRNA translation does not occur immediately but is regulated locally and temporally by ribonucleoproteins (i.e. hnRNP-K and hnRNP-A2) (Müller *et al.*, 2013; Torvund-Jensen *et al.*, 2014), kinases (i.e. ERK2 and FYN) (Michel *et al.*, 2015), and a small non-coding RNA (sncRNA715, (Bauer *et al.*, 2012)) that allow MBP translation only once it has reached the plasma membrane through RNA granules. Previous studies by Dobrowolski *et al.* (Dobrowolski *et al.*, 2015, 2016) revealed altered DNA methylation patterns associated with high levels of blood L-Phe in mouse model of phenylketonuria as well as in the brain of two adult PKU patients. Following these preliminary data, we probed the hypothesis that these alterations may be implied in the pathogenesis of MBP deficiency by designing a longitudinal study in PKU ENU2 mice. Our results support the hypothesis that in the first months of life of the ENU2 mice some epigenetic alterations (i.e. differentially expressed miRNAs or ncRNAs), connected with the increase of the brain L-Phe, may disturb MBP

translational process, leading to low MBP expression. miRNA microarray analysis carried out on ENU2 and WT mice brains of 60 PND revealed that 156 miRNAs were differentially expressed in ENU2 mice compared to WT. This analysis was followed by gene set enrichment analysis on mature up- and downregulated miRNAs' targets (fc > 1.2 and fc < -2.5, respectively), which showed that many neuronal pathways could be altered in ENU2 mice brains. Unfortunately, none of the detected upregulated miRNAs has MBP among its potential targets, nor has the MBP regulatory elements mentioned before. Nonetheless, in order to confirm the *in silico* predictive hypotheses and to point out which miRNA could have an indirect impact over MBP correct translation, we analyzed the total protein pool of ENU2 mice brains of 60 and 360 PND through proteomic assay, with a fold > 1.5. Proteomic analyses reported a general normalization of brain proteins at 360 PND, confirming the recovery protein expression observed for MBP. Moreover, proteomic assay highlighted a general downregulation of myelin proteins expression at 60 PND, which was completely restored at 360 PND. In fact, apart from MBP, among the downregulated proteins we found PLP1, MOG, CNP, MAG and MOBP (the last two were not significant), all proteins involved in oligodendrocytes development, correct myelination and neuronal extracellular signaling (Solly *et al.*, 1996; Quarles, 2007; Cloake *et al.*, 2018). PLP1 downregulation (fold: -1.80) was particularly interesting because it could be an indicator of the altered lipid metabolism observed in PKU mice and patients (Sanayama *et al.*, 2011; Nagasaka *et al.*, 2014). In fact, PLP1 expression is mediated by its transport to the myelin membrane via a transcytotic mechanism mediated by sulfatide and the successful lipid-PLP1 interaction form a cholesterol- and galactosylceramide-rich membrane domain (myelin rafts) that may be critical for the sorting and assembly of PLP1 in oligodendrocytes myelin (Simons *et al.*, 2000; Baron *et al.*, 2015). Lipid impaired metabolism (Rondelli *et al.*, 2022) is not the only possible explanation for PLP1 downregulation; in fact, loss of axonal contact can cause under-expression of the PLP1 gene in oligodendrocytes (McPhilemy *et al.*, 1991) and myelin markers, including PLP1, MBP, MOG and MAG, were found to be significantly regulated in a cuprizone (a copper chelator known to cause demyelination in mice) treated rat model (Gregg *et al.*, 2009). The general lower level of myelin proteins observed in ENU2 brains could be explained by many assumptions, going from widespread demyelination to astrocyte cell death induced by high L-Phe levels (Gregg *et al.*, 2009; Preissler *et al.*, 2016; Thau-Zuchman *et al.*, 2022). Given the protein recovery and the lower levels of bloodstream L-Phe at 360 PND, we decided to move forward on the epigenetic remodeling hypothesis through development (Dobrowolski *et al.*, 2015, 2016), evaluating the potential miRNAs that could indirectly affect myelin formation and, consequently, MBP expression. To do so, we compared all the downregulated proteins at 60 PND (fold < -1.2) with

the upregulated miRNAs' targets (fc > 1.2), obtaining 27 candidate proteins which could be potential affected by miRNA upregulation. Among them, we selected and validated 3 protein that could be targeted by miRNAs: ANLN, MAG and CNTNAP2. ANLN (Anillin, Actin Binding Protein; Ensembl: ENSG00000011426) is fundamental in the correct myelin folding and its downregulation leads to the disruption of myelin septin assembly and consequently to pathological myelin outfoldings (Patzig *et al.*, 2016; Erwig *et al.*, 2019). This protein is potentially targeted by miR-217-5p (fc: 2.07), which is significantly upregulated at 60 PND and has BAG3 (Bcl2-associated athanogene 3, fold: -1.21) and SLC38A2 (Solute Carrier Family 38 Member 2, fold: -1.37) among other potential downregulated targets. Interestingly, BAG3 targeting and downregulation mediated by miR-217-5p has already been experimentally determined in colorectal cancer cells by Flum *et al.* (Flum *et al.*, 2018) and its impairment in brain may lead to an improper nervous system development and to an altered brain protein homeostasis (Santoro *et al.*, 2017). On the other hand, MAG (Myelin-Associated Glycoprotein; Ensembl: ENSG00000105695) is strictly associated with MBP (Mann *et al.*, 2008; Cheishvili *et al.*, 2014) and its downregulation or deletion can provoke demyelination and white matter damages similar to what observed during multiple sclerosis (Quarles, 2007; Rahmanzadeh *et al.*, 2018). The protein is potentially targeted by miR-218-1-3p (fc: 2.10) and this miRNA is particularly interesting because its expression follows an opposite trend compared to MBP expression. Finally, a deletion of CNTNAP2 (Contactin Associated Protein 2; Ensembl: ENSG00000174469) can cause defective neurotransmission, developmental delay in cortical neurons and a decreased MBP expression (Scott *et al.*, 2019; Lu *et al.*, 2021). In this case, the protein could be a potential target for miR-1231-3p (fc: 1.77), which, similarly to miR-218-1-3p, shows an opposite trend compared to MBP during development. Taken together, the upregulation of these miRNAs during early development may have a detrimental effect not only on the expression of their possible targets, but indirectly also on the MBP efficient translation (Bijlard *et al.*, 2015).

Among the stem-loop miRNAs, which were not analyzed through predictive bioinformatic tools, is of note the detected upregulation of mir-125a (fc: 1.35) in ENU2 mice brains, which is well-known to be one of the most important miRNAs in the nervous system development (Duffy and McCoy, 2020). In fact, mir-125a is involved in many remyelination processes such as oligodendrocyte progenitor cells (OPCs) differentiation, astrogliosis promotion (Rao *et al.*, 2019), blood-brain barrier maintenance (Reijerkerk *et al.*, 2013) and neurodegeneration (Long *et al.*, 2020).

The general protein expression recovery observed at 360 PND could suggest cognitive and neuromotor improvements in aged ENU2 mice. Even if there are no available data about aged

PKU rodents that could illustrate a possible cognitive recovery after MBP increasing, on clinical ground untreated adult mice with PKU are clinically impaired and no improvement may be detected without treatment (Winn *et al.*, 2022). However, this is not in contrast with the possible pathogenetic role of MBP defect since it happens during a critical stage of postnatal CNS maturation, thus potentially affecting the normal development of brain connectivity. To evaluate this assessment, we performed behavioral tests on aged ENU2 mice of 180, 270 and 540 PND; the OFT (Open Field Test) depicted a low locomotory activity in ENU2 compared to WT, a data which is in accordance with previous observation made by Pascucci *et al.* (2013) (Pascucci *et al.*, 2013) but potentially in contrast with other studies made at 75 and 120 PND (Pascucci *et al.*, 2018; Winn *et al.*, 2022). In fact, in both studies ENU2 mice showed no differences compared to WT mice, and actually at 120 PND they showed increased activity levels (Winn *et al.*, 2022). Conversely, in our case ORT (Object Recognition Test) did not provide any considerable changes between the two conditions, with WT and ENU2 which spent the same amount of time (s) on the novel and the familiar object. This data is in contrast with ORT performed at 60-75 PND (Cabib *et al.*, 2003; Pascucci *et al.*, 2013, 2018) but similar to the one observed at 120 PND (Winn *et al.*, 2022). It should be noted that the exploration time for both the genetic conditions is lower compared to the ones observed at 60-75 PND (Cabib *et al.*, 2003; Pascucci *et al.*, 2013, 2018), ranging from 20-50s in aged mice to 60-100s in younger mice. This data is in agreement with a study from Chao *et al.* (2018) (Chao, Yunger and Yang, 2018) and could indicate a lower predisposition to explore novel objects in aged mice. Taken together, despite our analyses revealed no differences over curiosity and exploration time in aged ENU2 mice compared to WT, more samples are needed to support this observation and to strengthen the cognitive retrieval during development.

Together with the previous assumptions made, L-Phe levels were measured during development, to evaluate if MBP upward trend and/or miRNAs different levels were linked to diverse L-Phe concentrations. The obtained results show a significant blood L-Phe levels decline during development in ENU2 mice, which is consistent with the decreasing tendency observed in our previous work from 15 to 70 PND (Pascucci *et al.*, 2018). Likewise, a remarkable reduction of L-Phe concentration was also found in ENU2 brains from 14 to 60 PND. This trend is possibly related to a residual activity of the PAH enzyme (Hamman *et al.*, 2005), which could be driven by developmental patterns. In fact, it has been observed that PAH activity is regulated during development in non-PKU mice and rats, with a marked increase on its expression and activity one week after birth (Yeoh *et al.*, 1988; Wang *et al.*, 1992). Noteworthy, L-Phe concentrations in ENU2 mice assessed in our work are higher compared to the ones found previously (Rossi *et al.*,

2014; Pascucci *et al.*, 2018), even though they are in line with other studies (Sarkissian *et al.*, 2008; Pascucci *et al.*, 2012).

6. CONCLUSION AND FUTURE PERSPECTIVES

We performed the first complete longitudinal study over ENU2 mouse brain development, opening new insights about PKU understanding and proposing new potential molecular targets to be focused on the path of PKU treatment. In summary, our studies report a progressive recovery of MBP in ENU2 mice brains, reaching almost normal levels during adulthood. At the same time, MBP mRNA expression levels were found to be unaltered between ENU2 and WT. In this scenario, miRNAs could have a key role, as we found miR-217-5p, miR-218-1-3p and miR-1231-3p to be potentially involved in the correct MBP translation. In fact, after proteomic analyses, we found a near complete normalization of the cerebral proteins in aged ENU2-mice, which can be partially guided by the miRNAs mentioned before. Moreover, in this work we highlighted the importance of miRNAs differential expression in ENU2 mice compared to WT. In fact, since that multiple possible miRNAs' targets belong to the neuronal network, an altered expression of target genes caused by miRNAs activity could have detrimental effects on CNS development. Further studies will be necessary in order to certainly assess if MBP increasing could lead to cognitive and/or myelination retrieval and if MBP could recover itself after antisense miRNAs administration. *In vitro* and subsequent *in vivo* studies will be required to understand if antisense miRNAs injection treatment, especially during the first stage of development, can revert the protein downregulation observed in young ENU2, thus countering the detrimental effects observed in PKU mice and patients. In addition, ANLN, MAG and CNTNAP2 knockout in an oligodendrocytes cellular model could give preliminary indications on their involvement over MBP correct expression. Brain and blood metabolites and/or markers between 60 and 360 PND ENU2 mice will be also needed in order to check if some proteins (i.e. hormones) or metabolites are involved in the L-Phe lower levels observed in aged ENU2 bloodstream and, consequently, in the PKU cerebral outcome.

Furthermore, since that we have evaluated only mature up- and downregulated miRNAs with fc > 1.2 and fc < -2.5, respectively, additional evaluation will be required on differentially expressed precursor stem-loop miRNAs and on the remaining downregulated miRNAs.

7. REFERENCES

Abrams, C. K. and Scherer, S. S. (2012) 'Gap junctions in inherited human disorders of the central nervous system.', *Biochimica et biophysica acta*, 1818(8), pp. 2030–2047. doi: 10.1016/j.bbamem.2011.08.015.

Agarwal, V. *et al.* (2015) 'Predicting effective microRNA target sites in mammalian mRNAs', *eLife*, 4, p. e05005. doi: 10.7554/eLife.05005.

Aggarwal, S. *et al.* (2011) 'A size barrier limits protein diffusion at the cell surface to generate lipid-rich myelin-membrane sheets.', *Developmental cell*. United States, 21(3), pp. 445–456. doi: 10.1016/j.devcel.2011.08.001.

Aggarwal, S. *et al.* (2013) 'Myelin membrane assembly is driven by a phase transition of myelin basic proteins into a cohesive protein meshwork.', *PLoS biology*, 11(6), p. e1001577. doi: 10.1371/journal.pbio.1001577.

Aggarwal, S., Yurlova, L. and Simons, M. (2011) 'Central nervous system myelin: structure, synthesis and assembly.', *Trends in cell biology*. England, 21(10), pp. 585–593. doi: 10.1016/j.tcb.2011.06.004.

Ainger, K. *et al.* (1997) 'Transport and localization elements in myelin basic protein mRNA.', *The Journal of cell biology*, 138(5), pp. 1077–1087. doi: 10.1083/jcb.138.5.1077.

Alcamí, P. and Pereda, A. E. (2019) 'Beyond plasticity: the dynamic impact of electrical synapses on neural circuits.', *Nature reviews. Neuroscience*. England, 20(5), pp. 253–271. doi: 10.1038/s41583-019-0133-5.

Allinquant, B. *et al.* (1991) 'The ectopic expression of myelin basic protein isoforms in Shiverer oligodendrocytes: implications for myelinogenesis.', *The Journal of Cell Biology*, 113(2), pp. 393–403. doi: 10.1083/jcb.113.2.393.

Andolina, D. *et al.* (2011) '5-Hydroxytryptophan during critical postnatal period improves cognitive performances and promotes dendritic spine maturation in genetic mouse model of phenylketonuria.', *The international journal of neuropsychopharmacology*, 14(4), pp. 479–489. doi: 10.1017/S1461145710001288.

Ashe, K. *et al.* (2019) 'Psychiatric and Cognitive Aspects of Phenylketonuria: The Limitations of Diet and Promise of New Treatments.', *Frontiers in psychiatry*, 10, p. 561. doi: 10.3389/fpsyt.2019.00561.

Baba, H. *et al.* (1987) 'Developmental changes of myelin-associated glycoprotein in rat brain: study on experimental hyperphenylalaninemia.', *Neurochemical Research*, 12(5), pp. 459–463. doi: 10.1007/BF00972298.

Bader, G. D. and Hogue, C. W. V (2003) 'An automated method for finding molecular complexes in large protein interaction networks', *BMC Bioinformatics*, 4(1), p. 2. doi: 10.1186/1471-2105-4-2.

Baron, W. *et al.* (2015) 'The major myelin-resident protein PLP is transported to myelin membranes via a transcytotic mechanism: involvement of sulfatide.', *Molecular and cellular biology*, 35(1), pp. 288–302. doi: 10.1128/MCB.00848-14.

Bartel, D. P. (2004) 'MicroRNAs: genomics, biogenesis, mechanism, and function.', *Cell*, 116(2), pp. 281–297. doi: 10.1016/s0092-8674(04)00045-5.

Bauer, N. M. *et al.* (2012) 'Myelin Basic Protein synthesis is regulated by small non-coding RNA 715', *EMBO Reports*. Nature Publishing Group, 13(9), pp. 827–834. doi: 10.1038/embor.2012.97.

de Baulny, H. O. *et al.* (2007) 'Management of phenylketonuria and hyperphenylalaninemia.', *The Journal of nutrition*. United States, 137(6 Suppl 1), pp. 1561S-1563S; discussion 1573S-1575S. doi: 10.1093/jn/137.6.1561S.

Bauman, M. L. and Kemper, T. L. (1982) 'Morphologic and histoanatomic observations of the brain in untreated human phenylketonuria.', *Acta neuropathologica*. Germany, 58(1), pp. 55–63. doi: 10.1007/BF00692698.

Baumann, N. and Pham-Dinh, D. (2001) 'Biology of oligodendrocyte and myelin in the mammalian central nervous system.', *Physiological reviews*. United States, 81(2), pp. 871–927. doi: 10.1152/physrev.2001.81.2.871.

Bedner, P., Steinhäuser, C. and Theis, M. (2012) 'Functional redundancy and compensation among members of gap junction protein families?', *Biochimica et biophysica acta*. Netherlands, 1818(8), pp. 1971–1984. doi: 10.1016/j.bbamem.2011.10.016.

Bernstein, E. *et al.* (2003) 'Dicer is essential for mouse development.', *Nature genetics*. United States, 35(3), pp. 215–217. doi: 10.1038/ng1253.

Beyer, E. C. and Berthoud, V. M. (2018) 'Gap junction gene and protein families: Connexins, innexins, and pannexins.', *Biochimica et biophysica acta. Biomembranes*, 1860(1), pp. 5–8. doi: 10.1016/j.bbamem.2017.05.016.

Bijlard, M. *et al.* (2015) 'Transcriptional expression of myelin basic protein in oligodendrocytes depends on functional syntaxin 4: a potential correlation with autocrine signaling.', *Molecular and cellular biology*, 35(4), pp. 675–687. doi: 10.1128/MCB.01389-14.

Bilder, D. A. *et al.* (2013) 'Psychiatric symptoms in adults with phenylketonuria.', *Molecular genetics and metabolism*. United States, 108(3), pp. 155–160. doi: 10.1016/j.ymgme.2012.12.006.

Birch, D. *et al.* (2014) 'MicroRNAs participate in the murine oligodendroglial response to perinatal hypoxia-ischemia.', *Pediatric research*, 76(4), pp. 334–340. doi: 10.1038/pr.2014.104.

Blau, N. *et al.* (2011) 'Diagnosis, classification, and genetics of phenylketonuria and tetrahydrobiopterin (BH4) deficiencies.', *Molecular genetics and metabolism*. United States, 104 Suppl, pp. S2-9. doi: 10.1016/j.ymgme.2011.08.017.

Blau, N., Shen, N. and Carducci, C. (2014) 'Molecular genetics and diagnosis of phenylketonuria: State of the art', *Expert Review of Molecular Diagnostics*. Informa UK, Ltd., 14(6), pp. 655–671. doi: 10.1586/14737159.2014.923760.

Blau, N., van Spronsen, F. J. and Levy, H. L. (2010) 'Phenylketonuria.', *Lancet (London, England)*. England, 376(9750), pp. 1417–1427. doi: 10.1016/S0140-6736(10)60961-0.

Boggs, J. M. *et al.* (1986) 'Interaction of myelin basic protein with different ionization states of phosphatidic acid and phosphatidylserine.', *Chemistry and physics of lipids*. Ireland, 39(1–2), pp. 165–184. doi: 10.1016/0009-3084(86)90110-6.

Boggs, J. M. (2006) 'Myelin basic protein: a multifunctional protein.', *Cellular and Molecular Life Sciences*, 63(17), pp. 1945–1961. doi: 10.1007/s00018-006-6094-7.

Bohnsack, M. T., Czaplinski, K. and Gorlich, D. (2004) 'Exportin 5 is a RanGTP-dependent dsRNA-binding protein that mediates nuclear export of pre-miRNAs.', *RNA (New York, N.Y.)*, 10(2), pp. 185–191. doi: 10.1261/rna.5167604.

Bolino, A. (2021) 'Myelin Biology.', *Neurotherapeutics : the journal of the American Society for Experimental NeuroTherapeutics*, 18(4), pp. 2169–2184. doi: 10.1007/s13311-021-01083-w.

Borrajo, G. J. C. (2007) 'Newborn screening in Latin America at the beginning of the 21st century.', *Journal of inherited metabolic disease*. United States, 30(4), pp. 466–481. doi: 10.1007/s10545-007-0669-9.

Bortoluzzi, V. T., Dutra Filho, C. S. and Wannmacher, C. M. D. (2021) 'Oxidative stress in phenylketonuria-evidence from human studies and animal models, and possible implications for redox signaling.', *Metabolic Brain Disease*, 36(4), pp. 523–543. doi: 10.1007/s11011-021-00676-w.

Bossa, F. *et al.* (2013) 'Erythrocytes-mediated delivery of dexamethasone 21-phosphate in steroid-dependent ulcerative colitis: a randomized, double-blind Sham-controlled study.', *Inflammatory bowel diseases*. England, 19(9), pp. 1872–1879. doi: 10.1097/MIB.0b013e3182874065.

Brenton, D. P. *et al.* (1996) 'Phenylketonuria: treatment in adolescence and adult life.', *European journal of pediatrics*. Germany, 155 Suppl, pp. S93-6. doi: 10.1007/pl00014261.

Burlina, A. P. *et al.* (2019) 'Large neutral amino acid therapy increases tyrosine levels in adult patients with phenylketonuria: A long-term study', *Nutrients*, 11(10), pp. 1–14. doi: 10.3390/nu11102541.

Burri, R. *et al.* (1990) 'Brain damage and recovery in hyperphenylalaninemic rats.', *Developmental Neuroscience*, 12(2), pp. 116–125. doi: 10.1159/000111840.

Cabib, S. *et al.* (2003) 'The behavioral profile of severe mental retardation in a genetic mouse model of phenylketonuria.', *Behavior genetics*. United States, 33(3), pp. 301–310. doi: 10.1023/a:1023498508987.

Calver, A. R. *et al.* (1998) 'Oligodendrocyte population dynamics and the role of PDGF in vivo.', *Neuron*. United States, 20(5), pp. 869–882. doi: 10.1016/s0896-6273(00)80469-9.

Camargo, N. *et al.* (2017) 'Oligodendroglial myelination requires astrocyte-derived lipids.', *PLoS biology*, 15(5), p. e1002605. doi: 10.1371/journal.pbio.1002605.

Camp, K. M. *et al.* (2014) 'Phenylketonuria Scientific Review Conference: state of the science and future research needs.', *Molecular genetics and metabolism*. United States, pp. 87–122. doi: 10.1016/j.ymgme.2014.02.013.

Campagnoni, A. T. *et al.* (1993) 'Structure and developmental regulation of Golli-mbp, a 105-kilobase gene that encompasses the myelin basic protein gene and is expressed in cells in the oligodendrocyte lineage in the brain.', *The Journal of biological chemistry*. United States, 268(7), pp. 4930–4938.

Campagnoni, A. T. and Macklin, W. B. (1988) 'Cellular and molecular aspects of myelin protein gene expression.', *Molecular Neurobiology*, 2(1), pp. 41–89. doi: 10.1007/BF02935632.

Cao, X. *et al.* (2006) 'Noncoding RNAs in the mammalian central nervous system.', *Annual review of neuroscience*. United States, 29, pp. 77–103. doi: 10.1146/annurev.neuro.29.051605.112839.

Castillo, M. *et al.* (1991) 'Effect of phenylalanine derivatives on the main regulatory enzymes of hepatic cholesterogenesis.', *Molecular and cellular biochemistry*. Netherlands, 105(1), pp. 21–25. doi: 10.1007/BF00230371.

Castro, M. *et al.* (2007) 'Long-term treatment with autologous red blood cells loaded with dexamethasone 21-phosphate in pediatric patients affected by steroid-dependent Crohn disease.', *Journal of pediatric gastroenterology and nutrition*. United States, 44(4), pp. 423–426. doi: 10.1097/MPG.0b013e3180320667.

Chace, D. H. *et al.* (1993) 'Rapid diagnosis of phenylketonuria by quantitative analysis for phenylalanine and tyrosine in neonatal blood spots by tandem mass spectrometry.', *Clinical Chemistry*, 39(1), pp. 66–71.

Chace, D. H. *et al.* (1998) 'Use of phenylalanine-to-tyrosine ratio determined by tandem mass spectrometry to improve newborn screening for phenylketonuria of early discharge specimens collected in the first 24 hours.', *Clinical chemistry*. England, 44(12), pp. 2405–2409.

Chao, O. Y., Yunger, R. and Yang, Y.-M. (2018) 'Behavioral assessments of BTBR T+Itpr3tf/J mice by tests of object attention and elevated open platform: Implications for an animal model of psychiatric comorbidity in autism.', *Behavioural brain research*. Netherlands, 347, pp. 140–147. doi: 10.1016/j.bbr.2018.03.014.

Cheishvili, D. *et al.* (2014) 'IKAP deficiency in an FD mouse model and in oligodendrocyte precursor cells results in downregulation of genes involved in oligodendrocyte differentiation and myelin formation.', *PloS one*, 9(4), p. e94612. doi: 10.1371/journal.pone.0094612.

Chen, Y. and Wang, X. (2020) 'miRDB: an online database for prediction of functional microRNA targets', *Nucleic Acids Research*, 48(D1), pp. D127–D131. doi: 10.1093/nar/gkz757.

Choi, T. B. and Pardridge, W. M. (1986) 'Phenylalanine transport at the human blood-brain barrier. Studies with isolated human brain capillaries.', *The Journal of biological chemistry*. United States, 261(14), pp. 6536–6541.

Cloake, N. C. *et al.* (2018) 'PLP1 Mutations in Patients with Multiple Sclerosis: Identification of a New Mutation and Potential Pathogenicity of the Mutations.', *Journal of clinical medicine*, 7(10). doi: 10.3390/jcm7100342.

Cockburn, F. *et al.* (1996) 'Fatty Acids in the Stability of Neuronal Membrane: Relavance to PKU', *International Pediatrics*. MIAMI CHILDRENS HOSPITAL MEDICAL JOURNAL INC, 11, pp. 56–60.

Costabeber, E. *et al.* (2003) 'Hyperphenylalaninemia reduces creatine kinase activity in the cerebral cortex of rats.', *International journal of developmental neuroscience : the official journal of the International Society for Developmental Neuroscience*. United States, 21(2), pp. 111–116. doi: 10.1016/s0736-5748(02)00108-9.

Dawson, M. R. L. *et al.* (2003) 'NG2-expressing glial progenitor cells: an abundant and widespread population of cycling cells in the adult rat CNS.', *Molecular and cellular neurosciences*. United States, 24(2), pp. 476–488. doi: 10.1016/s1044-7431(03)00210-0.

Denninger, A. R. *et al.* (2015) 'Claudin-11 Tight Junctions in Myelin Are a Barrier to Diffusion and Lack Strong Adhesive Properties.', *Biophysical journal*, 109(7), pp. 1387–1397. doi: 10.1016/j.bpj.2015.08.012.

Desviat, L. R. *et al.* (1999) 'Genetic and phenotypic aspects of phenylalanine hydroxylase deficiency in Spain: molecular survey by regions.', *European journal of human genetics : EJHG*. England, 7(3), pp. 386–392. doi: 10.1038/sj.ejhg.5200312.

Dhaunchak, A.-S. and Nave, K.-A. (2007) 'A common mechanism of PLP/DM20 misfolding causes cysteine-mediated endoplasmic reticulum retention in oligodendrocytes and Pelizaeus-Merzbacher disease.', *Proceedings of the National Academy of Sciences of the United States of America*, 104(45), pp. 17813–17818. doi: 10.1073/pnas.0704975104.

Dobrowolski *et al.* (2015) 'Altered DNA methylation in PAH deficient phenylketonuria', *Molecular Genetics and Metabolism*, 115(2), pp. 72–77. doi: https://doi.org/10.1016/j.ymgme.2015.04.002.

Dobrowolski, S. F. *et al.* (2014) 'Methylome repatterning in a mouse model of Maternal PKU Syndrome.', *Molecular genetics and metabolism*. United States, 113(3), pp. 194–199. doi: 10.1016/j.ymgme.2014.08.006.

Dobrowolski, S. F. *et al.* (2016) 'DNA methylation in the pathophysiology of hyperphenylalaninemia in the PAHenu2 mouse model of phenylketonuria', *Molecular Genetics and Metabolism*. Elsevier Inc., 119(1–2), pp. 1–7. doi: 10.1016/j.ymgme.2016.01.001.

Donlon, J. *et al.* (2019) 'Hyperphenylalaninemia: Phenylalanine Hydroxylase Deficiency', in Valle, D. L. et al. (eds) *The Online Metabolic and Molecular Bases of Inherited Disease*. New York, NY: McGraw-Hill Education. Available at: http://ommbid.mhmedical.com/content.aspx?aid=1181421626.

Dorland, L. *et al.* (1993) 'Phenylpyruvate, fetal damage, and maternal phenylketonuria syndrome.', *Lancet (London, England)*. England, pp. 1351–1352. doi: 10.1016/0140-6736(93)90866-f.

Duffy, C. P. and McCoy, C. E. (2020) 'The Role of MicroRNAs in Repair Processes in Multiple Sclerosis.', *Cells*, 9(7). doi: 10.3390/cells9071711.

Dugas, J. C. *et al.* (2010) 'Dicer1 and miR-219 Are required for normal oligodendrocyte differentiation and myelination.', *Neuron*, 65(5), pp. 597–611. doi: 10.1016/j.neuron.2010.01.027.

Dutta, D. J. and Fields, R. D. (2021) 'Deletion of the Thrombin Proteolytic Site in Neurofascin 155 Causes Disruption of Nodal and Paranodal Organization', *Frontiers in Cellular Neuroscience*, 15. doi: 10.3389/fncel.2021.576609.

Dutta, R. *et al.* (2013) 'Hippocampal demyelination and memory dysfunction are associated with increased levels of the neuronal microRNA miR-124 and reduced AMPA receptors.', *Annals of neurology*, 73(5), pp. 637–645. doi: 10.1002/ana.23860.

Dyer, C. A. *et al.* (1996) 'Evidence for central nervous system glial cell plasticity in phenylketonuria.', *Journal of Neuropathology and Experimental Neurology*, 55(7), pp. 795–814. doi: 10.1097/00005072-199607000-00005.

Elbaz, B. and Popko, B. (2019) 'Molecular Control of Oligodendrocyte Development.', *Trends in neurosciences*, 42(4), pp. 263–277. doi: 10.1016/j.tins.2019.01.002.

Erwig, M. S. *et al.* (2019) 'Anillin facilitates septin assembly to prevent pathological outfoldings of central nervous system myelin.', *eLife*, 8. doi: 10.7554/eLife.43888.

Fernandes, C. G. *et al.* (2010) 'Experimental evidence that phenylalanine provokes oxidative stress in hippocampus and cerebral cortex of developing rats.', *Cellular and molecular neurobiology*. United States, 30(2), pp. 317–326. doi: 10.1007/s10571-009-9455-6.

Ferris, H. A. *et al.* (2017) 'Loss of astrocyte cholesterol synthesis disrupts neuronal function and alters whole-body metabolism.', *Proceedings of the National Academy of Sciences of the United States of America*, 114(5), pp. 1189–1194. doi: 10.1073/pnas.1620506114.

Flum, M. *et al.* (2018) 'miR-217-5p induces apoptosis by directly targeting PRKCI, BAG3, ITGAV and MAPK1 in colorectal cancer cells.', *Journal of Cell Communication and Signaling*, 12(2), pp. 451–466. doi: 10.1007/s12079-017-0410-x.

Flydal, M. I. and Martinez, A. (2013) 'Phenylalanine hydroxylase: function, structure, and regulation.', *IUBMB Life*, 65(4), pp. 341–349. doi: 10.1002/iub.1150.

Fujiwara, T. and Yada, T. (2013) 'miRNA-target prediction based on transcriptional regulation.', *BMC genomics*, 14 Suppl 2(Suppl 2), p. S3. doi: 10.1186/1471-2164-14-S2-S3.

Fulton, D., Paez, P. M. and Campagnoni, A. T. (2010) 'The multiple roles of myelin protein genes during the development of the oligodendrocyte.', *ASN neuro*, 2(1), p. e00027. doi: 10.1042/AN20090051.

Furse, S. and de Kroon, A. I. P. M. (2015) 'Phosphatidylcholine's functions beyond that of a membrane brick.', *Molecular membrane biology*. England, 32(4), pp. 117–119. doi: 10.3109/09687688.2015.1066894.

Fyffe-Maricich, S. L. *et al.* (2011) 'The ERK2 mitogen-activated protein kinase regulates the timing of oligodendrocyte differentiation.', *The Journal of Neuroscience*, 31(3), pp. 843–850. doi: 10.1523/JNEUROSCI.3239-10.2011.

Galloway, D. A. and Moore, C. S. (2016) 'miRNAs As Emerging Regulators of Oligodendrocyte Development and Differentiation.', *Frontiers in Cell and Developmental Biology*, 4, p. 59. doi: 10.3389/fcell.2016.00059.

Ge, S. X., Jung, D. and Yao, R. (2020) 'ShinyGO: a graphical gene-set enrichment tool for animals and plants.', *Bioinformatics (Oxford, England)*, 36(8), pp. 2628–2629. doi: 10.1093/bioinformatics/btz931.

Gebert, L. F. R. and MacRae, I. J. (2019) 'Regulation of microRNA function in animals.', *Nature reviews. Molecular cell biology*, 20(1), pp. 21–37. doi: 10.1038/s41580-018-0045-7.

Georgiou, J. and Charlton, M. P. (1999) 'Non-myelin-forming perisynaptic schwann cells express protein zero and myelin-associated glycoprotein.', *Glia*. United States, 27(2), pp. 101–109. doi: 10.1002/(sici)1098-1136(199908)27:2<101::aid-glia1>3.0.co;2-h.

Gerasimova, N. S., Steklova, I. V and Tuuminen, T. (1989) 'Fluorometric method for phenylalanine microplate assay adapted for phenylketonuria screening.', *Clinical Chemistry*, 35(10), pp. 2112–2115. doi: 10.1093/clinchem/35.10.2112.

Givogri, M. I. *et al.* (2001) 'Expression and regulation of golli products of myelin basic protein gene during in vitro development of oligodendrocytes.', *Journal of neuroscience research*. United States, 66(4), pp. 679–690. doi: 10.1002/jnr.10031.

Gjetting, T. *et al.* (2001) 'In vitro expression of 34 naturally occurring mutant variants of phenylalanine hydroxylase: correlation with metabolic phenotypes and susceptibility toward protein aggregation.', *Molecular genetics and metabolism*. United States, 72(2), pp. 132–143. doi: 10.1006/mgme.2000.3118.

González, M. J. *et al.* (2018) 'White matter microstructural damage in early treated phenylketonuric patients', *Orphanet Journal of Rare Diseases*, 13(1), p. 188. doi: 10.1186/s13023-018-0912-5.

Greenfield, S. *et al.* (1973) 'Protein composition of myelin of the peripheral nervous system.', *Journal of neurochemistry*. England, 20(4), pp. 1207–1216. doi: 10.1111/j.1471-4159.1973.tb00089.x.

Gregg, J. R. *et al.* (2009) 'Downregulation of oligodendrocyte transcripts is associated with impaired prefrontal cortex function in rats.', *Schizophrenia research*, 113(2–3), pp. 277–287. doi: 10.1016/j.schres.2009.05.023.

de Groot, M. J. *et al.* (2013) 'Phenylketonuria: reduced tyrosine brain influx relates to reduced cerebral protein synthesis', *Orphanet Journal of Rare Diseases*, 8(1), p. 133. doi: 10.1186/1750-1172-8-133.

de Groot, M. J. *et al.* (2015) 'Phenylketonuria: brain phenylalanine concentrations relate inversely to cerebral protein synthesis.', *Journal of Cerebral Blood Flow and Metabolism*, 35(2), pp. 200–205. doi: 10.1038/jcbfm.2014.183.

Guldberg, P. *et al.* (1995) 'Phenylketonuria in a low incidence population: molecular characterisation of mutations in Finland.', *Journal of medical genetics*, 32(12), pp. 976–978. doi: 10.1136/jmg.32.12.976.

Guthrie, R. and Susi, A. (1963) 'A SIMPLE PHENYLALANINE METHOD FOR DETECTING PHENYLKETONURIA IN LARGE POPULATIONS OF NEWBORN INFANTS.', *Pediatrics*. United States, 32, pp. 338–343.

Hai, M. *et al.* (2002) 'Comparative analysis of Schwann cell lines as model systems for myelin gene transcription studies.', *Journal of neuroscience research*. United States, 69(4), pp. 497–508. doi: 10.1002/jnr.10327.

Hamilton, J. P. (2011) 'Epigenetics: principles and practice.', *Digestive diseases (Basel, Switzerland)*, 29(2), pp. 130–135. doi: 10.1159/000323874.

Hamman, K. *et al.* (2005) 'Low Therapeutic Threshold for Hepatocyte Replacement in Murine Phenylketonuria', *Molecular Therapy*, 12(2), pp. 337–344. doi: https://doi.org/10.1016/j.ymthe.2005.03.025.

Han, J. *et al.* (2004) 'The Drosha-DGCR8 complex in primary microRNA processing.', *Genes & development*, 18(24), pp. 3016–3027. doi: 10.1101/gad.1262504.

Hannun, Y. A. (1994) 'The sphingomyelin cycle and the second messenger function of ceramide.', *The Journal of biological chemistry*. United States, 269(5), pp. 3125–3128.

Harauz, G. and Boggs, J. M. (2013) 'Myelin management by the 18.5-kDa and 21.5-kDa classic myelin basic protein isoforms.', *Journal of neurochemistry*, 125(3), pp. 334–361. doi: 10.1111/jnc.12195.

Harding, C. O. *et al.* (2014) 'Pharmacologic inhibition of L-tyrosine degradation ameliorates cerebral dopamine deficiency in murine phenylketonuria (PKU).', *Journal of inherited metabolic disease*, 37(5), pp. 735–743. doi: 10.1007/s10545-013-9675-2.

Hargreaves, K. M. and Pardridge, W. M. (1988) 'Neutral amino acid transport at the human blood-brain barrier.', *The Journal of biological chemistry*. United States, 263(36), pp. 19392–19397.

Hayashi, C. and Suzuki, N. (2019) 'Heterogeneity of Oligodendrocytes and Their Precursor Cells.', *Advances in experimental medicine and biology*. United States, 1190, pp. 53–62. doi: 10.1007/978-981-32-9636-7_5.

Helle, S. C. J. *et al.* (2013) 'Organization and function of membrane contact sites.', *Biochimica et biophysica acta*. Netherlands, 1833(11), pp. 2526–2541. doi: 10.1016/j.bbamcr.2013.01.028.

Herbert, A. L. *et al.* (2017) 'Dynein/dynactin is necessary for anterograde transport of Mbp mRNA in oligodendrocytes and for myelination in vivo.', *Proceedings of the National Academy of Sciences of the United States of America*, 114(43), pp. E9153–E9162. doi: 10.1073/pnas.1711088114.

Hillert, A. *et al.* (2020) 'The Genetic Landscape and Epidemiology of Phenylketonuria.', *American journal of human genetics*, 107(2), pp. 234–250. doi: 10.1016/j.ajhg.2020.06.006.

ten Hoedt, A. E. *et al.* (2011) 'High phenylalanine levels directly affect mood and sustained attention in adults with phenylketonuria: a randomised, double-blind, placebo-controlled, crossover trial.', *Journal of inherited metabolic disease*, 34(1), pp. 165–171. doi: 10.1007/s10545-010-9253-9.

Hoeksma, M. *et al.* (2009) 'Phenylketonuria: High plasma phenylalanine decreases cerebral protein synthesis.', *Molecular Genetics and Metabolism*, 96(4), pp. 177–182. doi: 10.1016/j.ymgme.2008.12.019.

Hutchison, E. R. *et al.* (2013) 'Evidence for miR-181 involvement in neuroinflammatory responses of astrocytes.', *Glia*, 61(7), pp. 1018–1028. doi: 10.1002/glia.22483.

Huttenlocher, P. R. (2000) 'The neuropathology of phenylketonuria: human and animal studies.', *European journal of pediatrics*. Germany, 159 Suppl, pp. S102-6. doi: 10.1007/pl00014371.

Imperlini, E. *et al.* (2014) 'Altered brain protein expression profiles are associated with molecular neurological dysfunction in the PKU mouse model.', *Journal of neurochemistry*, 129(6), pp. 1002–1012. doi: 10.1111/jnc.12683.

Jäkel, S. and Dimou, L. (2017) 'Glial Cells and Their Function in the Adult Brain: A Journey through the History of Their Ablation.', *Frontiers in cellular neuroscience*, 11, p. 24. doi: 10.3389/fncel.2017.00024.

Jeffries, M. A. *et al.* (2016) 'ERK1/2 Activation in Preexisting Oligodendrocytes of Adult Mice Drives New Myelin Synthesis and Enhanced CNS Function.', *The Journal of Neuroscience*, 36(35), pp. 9186–9200. doi: 10.1523/JNEUROSCI.1444-16.2016.

Jenkins, D. *et al.* (1993) 'The New England Journal of Medicine Downloaded from nejm.org on March 29, 2011. For personal use only. No other uses without permission.', *New England Journal of Medicine*, 329(1), pp. 21–26.

Jin, S., Zhan, J. and Zhou, Y. (2021) 'Argonaute proteins: structures and their endonuclease activity.', *Molecular biology reports*. Netherlands, 48(5), pp. 4837–4849. doi: 10.1007/s11033-021-06476-w.

Joseph, B. and Dyer, C. A. (2003) 'Relationship between myelin production and dopamine synthesis in the PKU mouse brain.', *Journal of Neurochemistry*, 86(3), pp. 615–626. doi: 10.1046/j.1471-4159.2003.01887.x.

Justice, P. and Hsia, D. Y. (1965) 'STUDIES ON INHIBITION OF BRAIN 5-HYDROXYTRYPTOPHAN DECARBOXYLASE BY PHENYLALANINE METABOLITES.', *Proceedings of the Society for Experimental Biology and Medicine. Society for Experimental Biology and Medicine (New York, N.Y.)*. United States, 118, pp. 326–328. doi: 10.3181/00379727-118-29833.

Kajiwara, Y. *et al.* (2018) 'GJA1 (connexin43) is a key regulator of Alzheimer's disease pathogenesis.', *Acta Neuropathologica Communications*, 6(1), p. 144. doi: 10.1186/s40478-018-0642-x.

Kaufman, S. (1999) 'A model of human phenylalanine metabolism in normal subjects and in phenylketonuric patients.', *Proceedings of the National Academy of Sciences of the United States of America*, 96(6), pp. 3160–3164. doi: 10.1073/pnas.96.6.3160.

Kehl, T. *et al.* (2017) 'About miRNAs, miRNA seeds, target genes and target pathways.', *Oncotarget*, 8(63), pp. 107167–107175. doi: 10.18632/oncotarget.22363.

Kitamura, K., Suzuki, M. and Uyemura, K. (1976) 'Purification and partial characterization of two glycoproteins in bovine peripheral nerve myelin membrane.', *Biochimica et biophysica acta*. Netherlands, 455(3), pp. 806–816. doi: 10.1016/0005-2736(76)90050-x.

Klippel, B. *et al.* (2021) 'White matter disturbances in phenylketonuria : Possible underlying mechanisms', (February 2020), pp. 349–360. doi: 10.1002/jnr.24598.

Koppes, E. A. *et al.* (2020) 'A porcine model of phenylketonuria generated by CRISPR/Cas9 genome editing.', *JCI insight*, 5(20). doi: 10.1172/jci.insight.141523.

Kozak, L. *et al.* (2006) 'Identification and characterization of large deletions in the phenylalanine hydroxylase (PAH) gene by MLPA: evidence for both homologous and non-homologous mechanisms of rearrangement.', *Molecular genetics and metabolism*. United States, 89(4), pp. 300–309. doi: 10.1016/j.ymgme.2006.06.007.

Kozomara, A., Birgaoanu, M. and Griffiths-Jones, S. (2019) 'miRBase: from microRNA sequences to function.', *Nucleic acids research*, 47(D1), pp. D155–D162. doi: 10.1093/nar/gky1141.

Kuhn, S. *et al.* (2019) 'Oligodendrocytes in Development, Myelin Generation and Beyond.', *Cells*, 8(11). doi: 10.3390/cells8111424.

Laclair, C. E. *et al.* (2009) 'Purification and use of glycomacropeptide for nutritional management of phenylketonuria.', *Journal of food science*, 74(4), pp. E199-206. doi: 10.1111/j.1750-3841.2009.01134.x.

Lau, P. *et al.* (2008) 'Identification of dynamically regulated microRNA and mRNA networks in developing oligodendrocytes.', *The Journal of neuroscience : the official journal of the Society for Neuroscience*, 28(45), pp. 11720–11730. doi: 10.1523/JNEUROSCI.1932-08.2008.

Laursen, L. S., Chan, C. W. and Ffrench-Constant, C. (2011) 'Translation of myelin basic protein mRNA in oligodendrocytes is regulated by integrin activation and hnRNP-K.', *The Journal of Cell Biology*, 192(5), pp. 797–811. doi: 10.1083/jcb.201007014.

Lee, I. *et al.* (2009) 'New class of microRNA targets containing simultaneous 5'-UTR and 3'-UTR interaction sites.', *Genome research*, 19(7), pp. 1175–1183. doi: 10.1101/gr.089367.108.

LeVine, S. M., Wong, D. and Macklin, W. B. (1990) 'Developmental expression of proteolipid protein and DM20 mRNAs and proteins in the rat brain.', *Developmental neuroscience*. Switzerland, 12(4–5), pp. 235–250. doi: 10.1159/000111853.

Levy, H. L. and Waisbren, S. E. (1994) 'PKU in adolescents: rationale and psychosocial factors in diet continuation.', *Acta paediatrica (Oslo, Norway : 1992). Supplement*. Norway, 407, pp. 92–97. doi: 10.1111/j.1651-2227.1994.tb13463.x.

Lewandowski, K. E. *et al.* (2015) 'Myelin vs axon abnormalities in white matter in bipolar disorder.', *Neuropsychopharmacology : official publication of the American College of Neuropsychopharmacology*, 40(5), pp. 1243–1249. doi: 10.1038/npp.2014.310.

Lewis, B. P. *et al.* (2003) 'Prediction of mammalian microRNA targets.', *Cell*. United States, 115(7), pp. 787–798. doi: 10.1016/s0092-8674(03)01018-3.

Li, D. *et al.* (2010) 'Effects of phenylalanine on the survival and neurite outgrowth of rat cortical neurons in primary cultures: possible involvement of brain-derived neurotrophic factor.', *Molecular and Cellular Biochemistry*, 339(1–2), pp. 1–7. doi: 10.1007/s11010-009-0364-2.

Liang, L. *et al.* (2011) 'Phenylketonuria-related synaptic changes in a BTBR-Pah(enu2) mouse model.', *Neuroreport*, 22(12), pp. 617–622. doi: 10.1097/WNR.0b013e3283495acc.

Lin, S.-T. *et al.* (2013) 'MicroRNA-23a promotes myelination in the central nervous system.', *Proceedings of the National Academy of Sciences of the United States of America*, 110(43), pp. 17468–17473. doi: 10.1073/pnas.1317182110.

Lin, S.-T. and Fu, Y.-H. (2009) 'miR-23 regulation of lamin B1 is crucial for oligodendrocyte development and myelination.', *Disease models & mechanisms*, 2(3–4), pp. 178–188. doi: 10.1242/dmm.001065.

Liu, X. S. *et al.* (2017) 'MicroRNA-146a Promotes Oligodendrogenesis in Stroke.', *Molecular neurobiology*, 54(1), pp. 227–237. doi: 10.1007/s12035-015-9655-7.

Loeber, J. G. (2007) 'Neonatal screening in Europe; the situation in 2004.', *Journal of inherited metabolic disease*. United States, 30(4), pp. 430–438. doi: 10.1007/s10545-007-0644-5.

Long, D. *et al.* (2007) 'Potent effect of target structure on microRNA function.', *Nature structural & molecular biology*. United States, 14(4), pp. 287–294. doi: 10.1038/nsmb1226.

Long, H.-C. *et al.* (2020) 'MiR-125a-5p Regulates Vitamin D Receptor Expression in a Mouse Model of Experimental Autoimmune Encephalomyelitis.', *Neuroscience Bulletin*, 36(2), pp. 110–120. doi: 10.1007/s12264-019-00418-0.

Longo, N. *et al.* (2019) 'Evidence- and consensus-based recommendations for the use of pegvaliase in adults with phenylketonuria.', *Genetics in medicine : official journal of the American College of Medical Genetics*, 21(8), pp. 1851–1867. doi: 10.1038/s41436-018-0403-z.

Lu, P. *et al.* (2021) 'A Novel CNTNAP2 Mutation Results in Abnormal Neuronal E/I Balance', *Frontiers in neurology*. Frontiers Media S.A., 12, p. 712773. doi: 10.3389/fneur.2021.712773.

Lu, Z. *et al.* (2005) 'Developmental abnormalities of myelin basic protein expression in fyn knock-out brain reveal a role of fyn in posttranscriptional regulation', *Journal of Biological Chemistry*, 280(1), pp. 389–395. doi: 10.1074/jbc.M405973200.

Lyons, D. A. *et al.* (2009) 'Kif1b is essential for mRNA localization in oligodendrocytes and development of myelinated axons.', *Nature Genetics*, 41(7), pp. 854–858. doi: 10.1038/ng.376.

Macfarlane, L.-A. and Murphy, P. R. (2010) 'MicroRNA: Biogenesis, Function and Role in Cancer.', *Current genomics*, 11(7), pp. 537–561. doi: 10.2174/138920210793175895.

MacLeod, E. L. *et al.* (2009) 'Reassessment of phenylalanine tolerance in adults with phenylketonuria is needed as body mass changes.', *Molecular genetics and metabolism*, 98(4), pp. 331–337. doi: 10.1016/j.ymgme.2009.07.016.

Macleod, E. L. and Ney, D. M. (2010) 'Nutritional Management of Phenylketonuria.', *Annales Nestle [English ed.]*, 68(2), pp. 58–69. doi: 10.1159/000312813.

Magnani, M. *et al.* (1998) 'Erythrocyte engineering for drug delivery and targeting.', *Biotechnology and applied biochemistry*. United States, 28(1), pp. 1–6.

Mahen, E. M. *et al.* (2010) 'mRNA secondary structures fold sequentially but exchange rapidly in vivo.', *PLoS biology*, 8(2), p. e1000307. doi: 10.1371/journal.pbio.1000307.

Maier, O., Hoekstra, D. and Baron, W. (2008) 'Polarity development in oligodendrocytes: sorting and trafficking of myelin components.', *Journal of molecular neuroscience : MN*. United States, 35(1), pp. 35–53. doi: 10.1007/s12031-007-9024-8.

Malamud, N. (1966) 'Neuropathology of phenylketonuria.', *Journal of neuropathology and experimental neurology*. England, 25(2), pp. 254–268. doi: 10.1097/00005072-196604000-00006.

Mambrini, G. *et al.* (2017) 'Ex vivo encapsulation of dexamethasone sodium phosphate into human autologous erythrocytes using fully automated biomedical equipment.', *International journal of pharmaceutics*. Netherlands, 517(1–2), pp. 175–184. doi: 10.1016/j.ijpharm.2016.12.011.

Mann, S. A. *et al.* (2008) 'Corticosteroids reverse cytokine-induced block of survival and differentiation of oligodendrocyte progenitor cells from rats.', *Journal of neuroinflammation*, 5, p. 39. doi: 10.1186/1742-2094-5-39.

Manti, F. *et al.* (2016) 'Psychiatric disorders in adolescent and young adult patients with phenylketonuria.', *Molecular genetics and metabolism*. United States, 117(1), pp. 12–18. doi: 10.1016/j.ymgme.2015.11.006.

Martinez-Cruz, F. *et al.* (2002) 'Oxidative stress induced by phenylketonuria in the rat: Prevention by melatonin, vitamin E, and vitamin C.', *Journal of Neuroscience Research*, 69(4), pp. 550–558. doi: 10.1002/jnr.10307.

Martini, R. and Carenini, S. (1998) 'Formation and maintenance of the myelin sheath in the peripheral nerve: roles of cell adhesion molecules and the gap junction protein connexin 32.', *Microscopy research and technique*. United States, 41(5), pp. 403–415. doi: 10.1002/(SICI)1097-0029(19980601)41:5<403::AID-JEMT7>3.0.CO;2-Q.

Matthieu, J. M., Waehneldt, T. V and Eschmann, N. (1986) 'Myelin-associated glycoprotein and myelin basic protein are present in central and peripheral nerve myelin throughout phylogeny.', *Neurochemistry international*. England, 8(4), pp. 521–526. doi: 10.1016/0197-0186(86)90186-5.

Mazzio, E. A. and Soliman, K. F. A. (2012) 'Basic concepts of epigenetics: impact of environmental signals on gene expression.', *Epigenetics*, 7(2), pp. 119–130. doi: 10.4161/epi.7.2.18764.

McDonald, J. D. and Charlton, C. K. (1997) 'Characterization of mutations at the mouse phenylalanine hydroxylase locus.', *Genomics*, 39(3), pp. 402–405. doi: 10.1006/geno.1996.4508.

McHugh, D. M. S. *et al.* (2011) 'Clinical validation of cutoff target ranges in newborn screening of metabolic disorders by tandem mass spectrometry: a worldwide collaborative project.', *Genetics in medicine : official journal of the American College of Medical Genetics*. United States, 13(3), pp. 230–254. doi: 10.1097/GIM.0b013e31820d5e67.

McKerracher, L. and Rosen, K. M. (2015) 'MAG, myelin and overcoming growth inhibition in the CNS.', *Frontiers in molecular neuroscience*, 8, p. 51. doi: 10.3389/fnmol.2015.00051.

McPhilemy, K. *et al.* (1991) 'Loss of axonal contact causes down-regulation of the PLP gene in oligodendrocytes: evidence from partial lesions of the optic nerve.', *Neuropathology and applied neurobiology*. England, 17(4), pp. 275–287. doi: 10.1111/j.1365-2990.1991.tb00725.x.

Michel, K. *et al.* (2015) 'Translational control of myelin basic protein expression by ERK2 MAP kinase regulates timely remyelination in the adult brain.', *The Journal of Neuroscience*, 35(20), pp. 7850–7865. doi: 10.1523/JNEUROSCI.4380-14.2015.

Mighdoll, M. I. *et al.* (2015) 'Myelin, myelin-related disorders, and psychosis.', *Schizophrenia research*. Netherlands, 161(1), pp. 85–93. doi: 10.1016/j.schres.2014.09.040.

Miller, R. H. (2002) 'Regulation of oligodendrocyte development in the vertebrate CNS.', *Progress in neurobiology*. England, 67(6), pp. 451–467. doi: 10.1016/s0301-0082(02)00058-8.

Min, Y. *et al.* (2009) 'Interaction forces and adhesion of supported myelin lipid bilayers modulated by myelin basic protein.', *Proceedings of the National Academy of Sciences of the United States of America*, 106(9), pp. 3154–3159. doi: 10.1073/pnas.0813110106.

Mitchell, J. J., Trakadis, Y. J. and Scriver, C. R. (2011) 'Phenylalanine hydroxylase deficiency.', *Genetics in medicine : official journal of the American College of Medical Genetics*. United States, 13(8), pp. 697–707. doi: 10.1097/GIM.0b013e3182141b48.

Möbius, W. *et al.* (2010) 'Electron microscopy of the mouse central nervous system.', *Methods in cell biology*. United States, 96, pp. 475–512. doi: 10.1016/S0091-679X(10)96020-2.

Moffitt, M. C. *et al.* (2007) 'Discovery of two cyanobacterial phenylalanine ammonia lyases: kinetic and structural characterization.', *Biochemistry*, 46(4), pp. 1004–1012. doi: 10.1021/bi061774g.

Moon, J., Xu, L. and Giffard, R. G. (2013) 'Inhibition of microRNA-181 reduces forebrain ischemia-induced neuronal loss.', *Journal of cerebral blood flow and metabolism : official journal of the International Society of Cerebral Blood Flow and Metabolism*, 33(12), pp. 1976–1982. doi: 10.1038/jcbfm.2013.157.

Moraes, T. B. *et al.* (2013) 'Role of catalase and superoxide dismutase activities on oxidative stress in the brain of a phenylketonuria animal model and the effect of lipoic acid.', *Cellular and molecular neurobiology*. United States, 33(2), pp. 253–260. doi: 10.1007/s10571-012-9892-5.

Morita, K. *et al.* (1999) 'Claudin-11/OSP-based tight junctions of myelin sheaths in brain and Sertoli cells in testis.', *The Journal of cell biology*, 145(3), pp. 579–588. doi: 10.1083/jcb.145.3.579.

Moscarello, M. A. (1997) 'Myelin Basic Protein, the "Executive" Molecule of the Myelin Membrane BT - Cell Biology and Pathology of Myelin: Evolving Biological Concepts and Therapeutic Approaches', in Juurlink, B. H. J. et al. (eds). Boston, MA: Springer US, pp. 13–25. doi: 10.1007/978-1-4615-5949-8_2.

Müller, C. *et al.* (2013) 'Making myelin basic protein - From mRNA transport to localized translation', *Frontiers in Cellular Neuroscience*, 7(SEP), pp. 1–7. doi: 10.3389/fncel.2013.00169.

Müller, C. *et al.* (2015) 'SncRNA715 inhibits schwann cell myelin basic protein synthesis', *PLoS ONE*, 10(8), pp. 1–11. doi: 10.1371/journal.pone.0136900.

Nagasaka, H. *et al.* (2014) 'Changes of lipoproteins in phenylalanine hydroxylase-deficient children during the first year of life.', *Clinica chimica acta; international journal of clinical chemistry*. Netherlands, 433, pp. 1–4. doi: 10.1016/j.cca.2014.02.020.

Nave, K.-A. and Werner, H. B. (2014) 'Myelination of the nervous system: mechanisms and functions.', *Annual Review of Cell and Developmental Biology*, 30, pp. 503–533. doi: 10.1146/annurev-cellbio-100913-013101.

Newbern, J. M. *et al.* (2011) 'Specific functions for ERK/MAPK signaling during PNS development.', *Neuron*, 69(1), pp. 91–105. doi: 10.1016/j.neuron.2010.12.003.

Nickel, M. and Gu, C. (2018) 'Regulation of Central Nervous System Myelination in Higher Brain Functions.', *Neural plasticity*, 2018, p. 6436453. doi: 10.1155/2018/6436453.

Noren Hooten, N. *et al.* (2013) 'Age-related changes in microRNA levels in serum.', *Aging*, 5(10), pp. 725–740. doi: 10.18632/aging.100603.

Norton, W. T. and Poduslo, S. E. (1973) 'Myelination in rat brain: changes in myelin composition during brain maturation.', *Journal of Neurochemistry*. John Wiley & Sons, Ltd, 21(4), pp. 759–773. doi: https://doi.org/10.1111/j.1471-4159.1973.tb07520.x.

Nualart-Marti, A., Solsona, C. and Fields, R. D. (2013) 'Gap junction communication in myelinating glia.', *Biochimica et biophysica acta*, 1828(1), pp. 69–78. doi: 10.1016/j.bbamem.2012.01.024.

O'Brien (1965) 'STABILITY OF THE MYELIN MEMBRANE.', *Science (New York, N.Y.)*. United States, 147(3662), pp. 1099–1107. doi: 10.1126/science.147.3662.1099.

O'Brien, J. *et al.* (2018) 'Overview of MicroRNA Biogenesis, Mechanisms of Actions, and Circulation.', *Frontiers in endocrinology*, 9, p. 402. doi: 10.3389/fendo.2018.00402.

O'Mara, M., Oakley, A. and Bröer, S. (2006) 'Mechanism and putative structure of B(0)-like neutral amino acid transporters.', *The Journal of membrane biology*. United States, 213(2), pp. 111–118. doi: 10.1007/s00232-006-0879-3.

Okano, Y. *et al.* (1991) 'Molecular basis of phenotypic heterogeneity in phenylketonuria.', *The New England journal of medicine*. United States, 324(18), pp. 1232–1238. doi: 10.1056/NEJM199105023241802.

Ozgen, H. *et al.* (2016) 'Oligodendroglial membrane dynamics in relation to myelin biogenesis.', *Cellular and molecular life sciences : CMLS*, 73(17), pp. 3291–3310. doi: 10.1007/s00018-016-2228-8.

Paine, R. S. (1957) 'The variability in manifestations of untreated patients with phenylketonuria (phenylpyruvic aciduria).', *Pediatrics*. United States, 20(2), pp. 290–302.

Pangkanon, S. *et al.* (2009) 'Detection of phenylketonuria by the newborn screening program in Thailand.', *The Southeast Asian journal of tropical medicine and public health*. Thailand, 40(3), pp. 525–529.

Paraskevopoulou, M. D. *et al.* (2013) 'DIANA-microT web server v5.0: service integration into miRNA functional analysis workflows.', *Nucleic Acids Research*, 41(Web Server issue), pp. W169-73. doi: 10.1093/nar/gkt393.

Pardridge, W. M. (1998) 'Blood-brain barrier carrier-mediated transport and brain metabolism of amino acids.', *Neurochemical research*. United States, 23(5), pp. 635–644. doi: 10.1023/a:1022482604276.

Pascucci, T. *et al.* (2008) 'Reduced availability of brain amines during critical phases of postnatal development in a genetic mouse model of cognitive delay.', *Brain research*. Netherlands, 1217, pp. 232–238. doi: 10.1016/j.brainres.2008.04.006.

Pascucci, T. *et al.* (2012) 'In vivo catecholaminergic metabolism in the medial prefrontal cortex of ENU2 mice: an investigation of the cortical dopamine deficit in phenylketonuria.', *Journal of inherited metabolic disease*, 35(6), pp. 1001–1009. doi: 10.1007/s10545-012-9473-2.

Pascucci, T. *et al.* (2013) 'Behavioral and Neurochemical Characterization of New Mouse Model of Hyperphenylalaninemia', *PLOS ONE*. Public Library of Science, 8(12), p. e84697. Available at: https://doi.org/10.1371/journal.pone.0084697.

Pascucci, T. *et al.* (2018) 'A new therapy prevents intellectual disability in mouse with phenylketonuria.', *Molecular Genetics and Metabolism*, 124(1), pp. 39–49. doi: 10.1016/j.ymgme.2018.03.009.

Patzig, J. *et al.* (2016) 'Septin/anillin filaments scaffold central nervous system myelin to accelerate nerve conduction', *eLife*. Edited by B. Stevens. eLife Sciences Publications, Ltd, 5, p. e17119. doi: 10.7554/eLife.17119.

Pecce, R. *et al.* (2013) 'Optimization of an HPLC method for phenylalanine and tyrosine quantization in dried blood spot.', *Clinical biochemistry*. United States, 46(18), pp. 1892–1895. doi: 10.1016/j.clinbiochem.2013.08.022.

Peterson, S. M. *et al.* (2014) 'Common features of microRNA target prediction tools.', *Frontiers in genetics*, 5, p. 23. doi: 10.3389/fgene.2014.00023.

Pey, A. L. *et al.* (2007) 'Predicted effects of missense mutations on native-state stability account for phenotypic outcome in phenylketonuria, a paradigm of misfolding diseases.', *American journal of human genetics*, 81(5), pp. 1006–1024. doi: 10.1086/521879.

Pietz, J. *et al.* (1999) 'Large neutral amino acids block phenylalanine transport into brain tissue in patients with phenylketonuria.', *The Journal of clinical investigation*, 103(8), pp. 1169–1178. doi: 10.1172/JCI5017.

Preissler, T. *et al.* (2016) 'Phenylalanine induces oxidative stress and decreases the viability of rat astrocytes: possible relevance for the pathophysiology of neurodegeneration in phenylketonuria.', *Metabolic Brain Disease*, 31(3), pp. 529–537. doi: 10.1007/s11011-015-9763-0.

Puglisi-Allegra, S. *et al.* (2000) 'Dramatic brain aminergic deficit in a genetic mouse model of phenylketonuria.', *Neuroreport*. England, 11(6), pp. 1361–1364. doi: 10.1097/00001756-200004270-00042.

Quarles, R. H. (2007) 'Myelin-associated glycoprotein (MAG): past, present and beyond.', *Journal of neurochemistry*. England, 100(6), pp. 1431–1448. doi: 10.1111/j.1471-4159.2006.04319.x.

Raghu, V. K. *et al.* (2022) 'Domino liver transplant from a donor with maple syrup urine disease into a recipient with phenylketonuria', *Molecular Genetics and Metabolism Reports*. Elsevier Inc., 31(April), p. 100866. doi: 10.1016/j.ymgmr.2022.100866.

Rahmanzadeh, R. *et al.* (2018) 'Demyelination with preferential MAG loss: A complex message from MS paraffin blocks', *Journal of the Neurological Sciences*, 385, pp. 126–130. doi: https://doi.org/10.1016/j.jns.2017.12.029.

Rampini, S. *et al.* (1974) 'Aromatic acids in urine of healthy infants, persistent hyperphenylalaninemia, and phenylketonuria, before and after phenylalanine load.', *Pediatric research*. United States, 8(7), pp. 704–709. doi: 10.1203/00006450-197407000-00003.

Rao, V. T. S. *et al.* (2019) 'Astrocytes in the Pathogenesis of Multiple Sclerosis: An In Situ MicroRNA Study.', *Journal of Neuropathology and Experimental Neurology*, 78(12), pp. 1130–1146. doi: 10.1093/jnen/nlz098.

Rech, V. C. *et al.* (2002) 'Inhibition of the mitochondrial respiratory chain by phenylalanine in rat cerebral cortex.', *Neurochemical research*. United States, 27(5), pp. 353–357. doi: 10.1023/a:1015529511664.

Regier, D. S. and Greene, C. L. (1993) 'Phenylalanine Hydroxylase Deficiency.', in Adam, M. P. et al. (eds). Seattle (WA).

Reijerkerk, A. *et al.* (2013) 'MicroRNAs regulate human brain endothelial cell-barrier function in inflammation: implications for multiple sclerosis.', *The Journal of Neuroscience*, 33(16), pp. 6857–6863. doi: 10.1523/JNEUROSCI.3965-12.2013.

Ressler, K. J. and Nemeroff, C. B. (2000) 'Role of serotonergic and noradrenergic systems in the pathophysiology of depression and anxiety disorders.', *Depression and anxiety*. United States, 12 Suppl 1, pp. 2–19. doi: 10.1002/1520-6394(2000)12:1+<2::AID-DA2>3.0.CO;2-4.

Ribas, G. S. *et al.* (2011) 'Oxidative stress in phenylketonuria: what is the evidence?', *Cellular and Molecular Neurobiology*, 31(5), pp. 653–662. doi: 10.1007/s10571-011-9693-2.

Richards, D. Y. *et al.* (2020) 'AAV-Mediated CRISPR/Cas9 Gene Editing in Murine Phenylketonuria', *Molecular Therapy - Methods and Clinical Development*. Elsevier Ltd., 17(June), pp. 234–245. doi: 10.1016/j.omtm.2019.12.004.

Robert, M. *et al.* (2022) 'Multiparametric characterization of red blood cell physiology after hypotonic dialysis based drug encapsulation process.', *Acta pharmaceutica Sinica. B*, 12(4), pp. 2089–2102. doi: 10.1016/j.apsb.2021.10.018.

Rondelli, V. *et al.* (2022) 'Dysmyelination and glycolipid interference caused by phenylalanine in phenylketonuria', *International Journal of Biological Macromolecules*, 221, pp. 784–795. doi: https://doi.org/10.1016/j.ijbiomac.2022.09.062.

Rossi *et al.* (2001) 'Erythrocyte-mediated delivery of dexamethasone in patients with chronic obstructive pulmonary disease.', *Biotechnology and applied biochemistry*. United States, 33(2), pp. 85–89. doi: 10.1042/ba20000087.

Rossi *et al.* (2014) 'Erythrocyte-mediated delivery of phenylalanine ammonia lyase for the treatment of phenylketonuria in BTBR-Pah(enu2) mice.', *Journal of Controlled Release*, 194, pp. 37–44. doi: 10.1016/j.jconrel.2014.08.012.

Rossi *et al.* (2020) 'Efficient Cocaine Degradation by Cocaine Esterase-Loaded Red Blood Cells.', *Frontiers in physiology*, 11, p. 573492. doi: 10.3389/fphys.2020.573492.

Rossi *et al.* (2021) 'Preclinical developments of enzyme-loaded red blood cells.', *Expert opinion on drug delivery*. England, 18(1), pp. 43–54. doi: 10.1080/17425247.2020.1822320.

Rossi, L. *et al.* (2004) 'Low doses of dexamethasone constantly delivered by autologous erythrocytes slow the progression of lung disease in cystic fibrosis patients.', *Blood cells, molecules & diseases*. United States, 33(1), pp. 57–63. doi: 10.1016/j.bcmd.2004.04.004.

Saab, A. S. and Nave, K.-A. (2017) 'Myelin dynamics: protecting and shaping neuronal functions.', *Current opinion in neurobiology*. England, 47, pp. 104–112. doi: 10.1016/j.conb.2017.09.013.

Saadat, L. *et al.* (2010) 'Absence of oligodendroglial glucosylceramide synthesis does not result in CNS myelin abnormalities or alter the dysmyelinating phenotype of CGT-deficient mice.', *Glia*, 58(4), pp. 391–398. doi: 10.1002/glia.20930.

Saher, G. *et al.* (2005) 'High cholesterol level is essential for myelin membrane growth.', *Nature neuroscience*. United States, 8(4), pp. 468–475. doi: 10.1038/nn1426.

Saher, G. and Stumpf, S. K. (2015) 'Cholesterol in myelin biogenesis and hypomyelinating disorders.', *Biochimica et biophysica acta*. Netherlands, 1851(8), pp. 1083–1094. doi: 10.1016/j.bbalip.2015.02.010.

Salzer, J. L. and Zalc, B. (2016) 'Myelination.', *Current biology : CB*. England, 26(20), pp. R971–R975. doi: 10.1016/j.cub.2016.07.074.

Sanayama, Y. *et al.* (2011) 'Experimental evidence that phenylalanine is strongly associated to oxidative stress in adolescents and adults with phenylketonuria.', *Molecular genetics and metabolism*. United States, 103(3), pp. 220–225. doi: 10.1016/j.ymgme.2011.03.019.

Santoro, A. *et al.* (2017) 'BAG3 is involved in neuronal differentiation and migration.', *Cell and Tissue Research*, 368(2), pp. 249–258. doi: 10.1007/s00441-017-2570-7.

Sarkissian, C. N. *et al.* (1999) 'A different approach to treatment of phenylketonuria: Phenylalanine degradation with recombinant phenylalanine ammonia lyase', *Proceedings of the National Academy of Sciences of the United States of America*, 96(5), pp. 2339–2344. doi: 10.1073/pnas.96.5.2339.

Sarkissian, C. N. *et al.* (2008) 'Preclinical evaluation of multiple species of PEGylated recombinant phenylalanine ammonia lyase for the treatment of phenylketonuria.', *Proceedings of the National Academy of Sciences of the United States of America*, 105(52), pp. 20894–20899. doi: 10.1073/pnas.0808421105.

Sarkissian, C. N. and Gámez, A. (2005) 'Phenylalanine ammonia lyase, enzyme substitution therapy for phenylketonuria, where are we now?', *Molecular genetics and metabolism*. United States, 86 Suppl 1, pp. S22-6. doi: 10.1016/j.ymgme.2005.06.016.

Sawin, E. A., Murali, S. G. and Ney, D. M. (2014) 'Differential effects of low-phenylalanine protein sources on brain neurotransmitters and behavior in C57Bl/6-Pah(enu2) mice.', *Molecular genetics and metabolism*, 111(4), pp. 452–461. doi: 10.1016/j.ymgme.2014.01.015.

Schmitt, S., Castelvetri, L. C. and Simons, M. (2015) 'Metabolism and functions of lipids in myelin.', *Biochimica et biophysica acta*. Netherlands, 1851(8), pp. 999–1005. doi: 10.1016/j.bbalip.2014.12.016.

Schoemans, R. *et al.* (2010) 'Oligodendrocyte development and myelinogenesis are not impaired by high concentrations of phenylalanine or its metabolites.', *Journal of Inherited Metabolic Disease*, 33(2), pp. 113–120. doi: 10.1007/s10545-010-9052-3.

Schuck, P. F. *et al.* (2015) 'Phenylketonuria pathophysiology: On the Role of Metabolic Alterations', *Aging and Disease*, 6(5), pp. 390–399. doi: 10.14336/AD.2015.0827.

Schwer, B. *et al.* (2008) 'Mammalian 2',3' cyclic nucleotide phosphodiesterase (CNP) can function as a tRNA splicing enzyme in vivo.', *RNA (New York, N.Y.)*, pp. 204–210. doi: 10.1261/rna.858108.

Scott, R. *et al.* (2019) 'Loss of Cntnap2 Causes Axonal Excitability Deficits, Developmental Delay in Cortical Myelination, and Abnormal Stereotyped Motor Behavior', *Cerebral Cortex*, 29(2), pp. 586–597. doi: 10.1093/cercor/bhx341.

Scriver (2007) 'The PAH gene, phenylketonuria, and a paradigm shift.', *Human Mutation*, 28(9), pp. 831–845. doi: 10.1002/humu.20526.

Scriver, C. R. and Rosenberg, L. E. (1973) 'Amino acid metabolism and its disorders.', *Major problems in clinical pediatrics*. United States, 10, pp. 1–478.

Shannon, P. *et al.* (2003) 'Cytoscape: a software environment for integrated models of biomolecular interaction networks.', *Genome research*, 13(11), pp. 2498–2504. doi: 10.1101/gr.1239303.

Shefer, Sarah *et al.* (2000) 'Is There a Relationship Between 3-Hydroxy- 3-Methylglutaryl Coenzyme A Reductase Activity and Forebrain Pathology in the PKU Mouse ?', 563(May), pp. 549–563.

Shefer, S *et al.* (2000) 'Is there a relationship between 3-hydroxy-3-methylglutaryl coenzyme a reductase activity and forebrain pathology in the PKU mouse?', *Journal of Neuroscience Research*, 61(5), pp. 549–563. doi: 10.1002/1097-4547(20000901)61:5<549::AID-JNR10>3.0.CO;2-0.

Shiang, R. *et al.* (1993) 'Mutations in the alpha 1 subunit of the inhibitory glycine receptor cause the dominant neurologic disorder, hyperekplexia.', *Nature genetics*. United States, 5(4), pp. 351–358. doi: 10.1038/ng1293-351.

Simons, M. *et al.* (2000) 'Assembly of myelin by association of proteolipid protein with cholesterol- and galactosylceramide-rich membrane domains.', *The Journal of cell biology*, 151(1), pp. 143–154. doi: 10.1083/jcb.151.1.143.

Sirtori, L. R. *et al.* (2005) 'Oxidative stress in patients with phenylketonuria.', *Biochimica et biophysica acta*. Netherlands, 1740(1), pp. 68–73. doi: 10.1016/j.bbadis.2005.02.005.

Sitta, A., Manfredini, V., *et al.* (2009) 'Evidence that DNA damage is associated to phenylalanine blood levels in leukocytes from phenylketonuric patients.', *Mutation research*. Netherlands, 679(1–2), pp. 13–16. doi: 10.1016/j.mrgentox.2009.07.013.

Sitta, A., Barschak, A. G., *et al.* (2009) 'L-carnitine blood levels and oxidative stress in treated phenylketonuric patients.', *Cellular and molecular neurobiology*. United States, 29(2), pp. 211–218. doi: 10.1007/s10571-008-9313-y.

Smirnova, E. V *et al.* (2021) 'Comprehensive Atlas of the Myelin Basic Protein Interaction Landscape.', *Biomolecules*, 11(11). doi: 10.3390/biom11111628.

Smith-Vikos, T. and Slack, F. J. (2012) 'MicroRNAs and their roles in aging.', *Journal of Cell Science*, 125, pp. 7–17. doi: 10.1242/jcs.099200.

Smith, G. S. T. *et al.* (2013) 'Nucleus-localized 21.5-kDa myelin basic protein promotes oligodendrocyte proliferation and enhances neurite outgrowth in coculture, unlike the plasma membrane-associated 18.5-kDa isoform.', *Journal of Neuroscience Research*, 91(3), pp. 349–362. doi: 10.1002/jnr.23166.

Smith and Kang, J. (2000) 'Cerebral protein synthesis in a genetic mouse model of phenylketonuria.', *Proceedings of the National Academy of Sciences of the United States of America*, 97(20), pp. 11014–11019. doi: 10.1073/pnas.97.20.11014.

Snaidero, N. *et al.* (2014) 'Myelin membrane wrapping of CNS axons by PI(3,4,5)P3-dependent polarized growth at the inner tongue.', *Cell*, 156(1–2), pp. 277–290. doi: 10.1016/j.cell.2013.11.044.

Snaidero, N. *et al.* (2017) 'Antagonistic Functions of MBP and CNP Establish Cytosolic Channels in CNS Myelin.', *Cell reports*, 18(2), pp. 314–323. doi: 10.1016/j.celrep.2016.12.053.

Snipes, G. J. *et al.* (1992) 'Characterization of a novel peripheral nervous system myelin protein (PMP-22/SR13).', *The Journal of cell biology*, 117(1), pp. 225–238. doi: 10.1083/jcb.117.1.225.

Sock, E. and Wegner, M. (2019) 'Transcriptional control of myelination and remyelination.', *Glia*. United States, 67(11), pp. 2153–2165. doi: 10.1002/glia.23636.

Söhl, G., Maxeiner, S. and Willecke, K. (2005) 'Expression and functions of neuronal gap junctions.', *Nature reviews. Neuroscience*. England, 6(3), pp. 191–200. doi: 10.1038/nrn1627.

Solly, S. K. *et al.* (1996) 'Myelin/oligodendrocyte glycoprotein (MOG) expression is associated with myelin deposition.', *Glia*. United States, 18(1), pp. 39–48. doi: 10.1002/(SICI)1098-1136(199609)18:1<39::AID-GLIA4>3.0.CO;2-Z.

van Spronsen, F. J. *et al.* (2009) 'Phenylalanine tolerance can already reliably be assessed at the age of 2 years in patients with PKU.', *Journal of inherited metabolic disease*. United States, 32(1), pp. 27–31. doi: 10.1007/s10545-008-0937-3.

van Spronsen, F. J. *et al.* (2017) 'Key European guidelines for the diagnosis and management of patients with phenylketonuria.', *The lancet. Diabetes & endocrinology*. England, 5(9), pp. 743–756. doi: 10.1016/S2213-8587(16)30320-5.

Stepanov, A. I. *et al.* (2022) 'Studying Chromatin Epigenetics with Fluorescence Microscopy.', *International journal of molecular sciences*, 23(16). doi: 10.3390/ijms23168988.

Sundaramoorthy, R. and Owen-Hughes, T. (2020) 'Chromatin remodelling comes into focus.', *F1000Research*, 9. doi: 10.12688/f1000research.21933.1.

Surtees, R. and Blau, N. (2000) 'The neurochemistry of phenylketonuria.', *European journal of pediatrics*. Germany, 159 Suppl, pp. S109-13. doi: 10.1007/pl00014370.

Szklarczyk, D. *et al.* (2019) 'STRING v11: protein–protein association networks with increased coverage, supporting functional discovery in genome-wide experimental datasets', *Nucleic Acids Research*, 47(D1), pp. D607–D613. doi: 10.1093/nar/gky1131.

Tekki-Kessaris, N. *et al.* (2001) 'Hedgehog-dependent oligodendrocyte lineage specification in the telencephalon.', *Development (Cambridge, England)*. England, 128(13), pp. 2545–2554. doi: 10.1242/dev.128.13.2545.

Tessari, P. *et al.* (1999) 'Phenylalanine hydroxylation across the kidney in humans rapid communication.', *Kidney international*. United States, 56(6), pp. 2168–2172. doi: 10.1038/sj.ki.4491156.

Thau-Zuchman, O. *et al.* (2022) 'High phenylalanine concentrations induce demyelination and microglial activation in mouse cerebellar organotypic slices.', *Frontiers in neuroscience*, 16, p. 926023. doi: 10.3389/fnins.2022.926023.

Thöny, B. and Blau, N. (2006) 'Mutations in the BH4-metabolizing genes GTP cyclohydrolase I, 6-pyruvoyl-tetrahydropterin synthase, sepiapterin reductase, carbinolamine-4a-dehydratase, and dihydropteridine reductase.', *Human mutation*. United States, 27(9), pp. 870–878. doi: 10.1002/humu.20366.

Torvund-Jensen, J. *et al.* (2014) 'Transport and translation of MBP mRNA is regulated differently by distinct hnRNP proteins.', *Journal of Cell Science*, 127(Pt 7), pp. 1550–1564. doi: 10.1242/jcs.140855.

Trapp, B. D. *et al.* (1997) 'Differentiation and death of premyelinating oligodendrocytes in developing rodent brain.', *The Journal of cell biology*, 137(2), pp. 459–468. doi: 10.1083/jcb.137.2.459.

Uusitalo, M. *et al.* (2021) 'Human myelin protein P2: from crystallography to time-lapse membrane imaging and neuropathy-associated variants.', *The FEBS journal*. England, 288(23), pp. 6716–6735. doi: 10.1111/febs.16079.

Vassall, K. A., Bamm, V. V and Harauz, G. (2015) 'MyelStones: the executive roles of myelin basic protein in myelin assembly and destabilization in multiple sclerosis.', *The Biochemical journal*. England, 472(1), pp. 17–32. doi: 10.1042/BJ20150710.

Vasudevan, S. (2012) 'Posttranscriptional upregulation by microRNAs.', *Wiley interdisciplinary reviews. RNA*. United States, 3(3), pp. 311–330. doi: 10.1002/wrna.121.

Vaughn, M. J. and Haas, J. S. (2022) 'On the Diverse Functions of Electrical Synapses.', *Frontiers in cellular neuroscience*, 16, p. 910015. doi: 10.3389/fncel.2022.910015.

Velumian, A. A., Samoilova, M. and Fehlings, M. G. (2011) 'Visualization of cytoplasmic diffusion within living myelin sheaths of CNS white matter axons using microinjection of the fluorescent dye Lucifer Yellow.', *NeuroImage*. United States, 56(1), pp. 27–34. doi: 10.1016/j.neuroimage.2010.11.022.

Villiger, L. *et al.* (2018) 'Treatment of a metabolic liver disease by in vivo genome base editing in adult mice.', *Nature medicine*. United States, 24(10), pp. 1519–1525. doi: 10.1038/s41591-018-0209-1.

van Vliet, D. *et al.* (2016) 'Therapeutic brain modulation with targeted large neutral amino acid supplements in the Pah-enu2 phenylketonuria mouse model.', *The American journal of clinical nutrition*. United States, 104(5), pp. 1292–1300. doi: 10.3945/ajcn.116.135996.

van Vliet, D. *et al.* (2018) 'Large neutral amino acid supplementation as an alternative to the phenylalanine-restricted diet in adults with phenylketonuria: evidence from adult Pah-enu2 mice.', *The Journal of nutritional biochemistry*. United States, 53, pp. 20–27. doi: 10.1016/j.jnutbio.2017.09.020.

van Vliet, D. *et al.* (2022) 'The increasing importance of LNAA supplementation in phenylketonuria at higher plasma phenylalanine concentrations', *Molecular Genetics and Metabolism*, 135(1), pp. 27–34. doi: https://doi.org/10.1016/j.ymgme.2021.11.003.

Vockley, J. *et al.* (2014) 'Phenylalanine hydroxylase deficiency: diagnosis and management guideline.', *Genetics in medicine : official journal of the American College of Medical Genetics*. United States, 16(2), pp. 188–200. doi: 10.1038/gim.2013.157.

Wallimann, T., Tokarska-Schlattner, M. and Schlattner, U. (2011) 'The creatine kinase system and pleiotropic effects of creatine.', *Amino acids*, 40(5), pp. 1271–1296. doi: 10.1007/s00726-011-0877-3.

El Waly, B. *et al.* (2014) 'Oligodendrogenesis in the normal and pathological central nervous system.', *Frontiers in neuroscience*, 8, p. 145. doi: 10.3389/fnins.2014.00145.

Wang *et al.* (1992) 'Tissue- and development-specific expression of the human phenylalanine hydroxylase/chloramphenicol acetyltransferase fusion gene in transgenic mice', *Journal of Biological Chemistry*, 267(21), pp. 15105–15110. doi: 10.1016/s0021-9258(18)42152-7.

Wang, L. *et al.* (2005) 'Structure-based chemical modification strategy for enzyme replacement treatment of phenylketonuria.', *Molecular genetics and metabolism*. United States, 86(1–2), pp. 134–140. doi: 10.1016/j.ymgme.2005.05.012.

Wang, L. *et al.* (2008) 'Structural and biochemical characterization of the therapeutic Anabaena variabilis phenylalanine ammonia lyase.', *Journal of molecular biology*, 380(4), pp. 623–635. doi: 10.1016/j.jmb.2008.05.025.

van Wegberg, A. M. J. *et al.* (2017) 'The complete European guidelines on phenylketonuria: diagnosis and treatment.', *Orphanet journal of rare diseases*, 12(1), p. 162. doi: 10.1186/s13023-017-0685-2.

Weglage, J. *et al.* (1996) 'No fine motor deficits in patients with untreated non-phenylketonuria hyperphenylalaninaemia.', *Acta paediatrica (Oslo, Norway : 1992)*. Norway, 85(3), pp. 320–323. doi: 10.1111/j.1651-2227.1996.tb14024.x.

West, A. *et al.* (2020) 'How Do Ethanolamine Plasmalogens Contribute to Order and Structure of Neurological Membranes?', *The journal of physical chemistry. B*, 124(5), pp. 828–839. doi: 10.1021/acs.jpcb.9b08850.

Wettstein, S. *et al.* (2015) 'Linking genotypes database with locus-specific database and genotype-phenotype correlation in phenylketonuria.', *European journal of human genetics : EJHG*, 23(3), pp. 302–309. doi: 10.1038/ejhg.2014.114.

White, R. *et al.* (2008) 'Activation of oligodendroglial Fyn kinase enhances translation of mRNAs transported in hnRNP A2-dependent RNA granules.', *The Journal of cell biology*, 181(4), pp. 579–586. doi: 10.1083/jcb.200706164.

Winkler, C. C. and Franco, S. J. (2019) 'Loss of Shh signaling in the neocortex reveals heterogeneous cell recovery responses from distinct oligodendrocyte populations.', *Developmental biology*, 452(1), pp. 55–65. doi: 10.1016/j.ydbio.2019.04.016.

Winn, S. R. *et al.* (2022) 'Modeling the cognitive effects of diet discontinuation in adults with phenylketonuria (PKU) using pegvaliase therapy in PAH-deficient mice.', *Molecular Genetics and Metabolism*. doi: 10.1016/j.ymgme.2022.03.008.

Wyse, A. T. S. *et al.* (2021) 'Insights from Animal Models on the Pathophysiology of Hyperphenylalaninemia: Role of Mitochondrial Dysfunction, Oxidative Stress and Inflammation.', *Molecular neurobiology*. United States, 58(6), pp. 2897–2909. doi: 10.1007/s12035-021-02304-1.

Yan, Z. *et al.* (2021) 'Myelin basic protein enhances axonal regeneration from neural progenitor cells.', *Cell & bioscience*, 11(1), p. 80. doi: 10.1186/s13578-021-00584-7.

Yeoh, G. C. *et al.* (1988) 'The development of phenylalanine hydroxylase in rat liver; in vivo, and in vitro studies utilizing fetal hepatocyte cultures.', *Differentiation*, 38(1), pp. 42–48. doi: 10.1111/j.1432-0436.1988.tb00590.x.

Yu, Y. G. *et al.* (2007) 'Effects of phenylalanine and its metabolites on cytoplasmic free calcium in cortical neurons.', *Neurochemical Research*, 32(8), pp. 1292–1301. doi: 10.1007/s11064-007-9303-3.

Yue, D., Liu, H. and Huang, Y. (2009) 'Survey of Computational Algorithms for MicroRNA Target Prediction.', *Current genomics*, 10(7), pp. 478–492. doi: 10.2174/138920209789208219.

Zhan, J.-Y., Qin, Y.-F. and Zhao, Z.-Y. (2009) 'Neonatal screening for congenital hypothyroidism and phenylketonuria in China.', *World journal of pediatrics : WJP*. Switzerland, 5(2), pp. 136–139. doi: 10.1007/s12519-009-0027-0.

Zhang, Lu, Q. and Chang, C. (2020) 'Epigenetics in Health and Disease.', *Advances in experimental medicine and biology*. United States, 1253, pp. 3–55. doi: 10.1007/978-981-15-3449-2_1.

Zhang, Y. *et al.* (2015) 'Functional reconstitution of glycinergic synapses incorporating defined glycine receptor subunit combinations.', *Neuropharmacology*. England, 89, pp. 391–397. doi: 10.1016/j.neuropharm.2014.10.026.

Zhao, X. *et al.* (2010) 'MicroRNA-mediated control of oligodendrocyte differentiation.', *Neuron*, 65(5), pp. 612–626. doi: 10.1016/j.neuron.2010.02.018.

Zhou, Y.-A. *et al.* (2012) 'Mutations of the phenylalanine hydroxylase gene in patients with phenylketonuria in Shanxi, China.', *Genetics and molecular biology*, 35(4), pp. 709–713. doi: 10.1590/S1415-47572012005000069.

Zschocke, J. *et al.* (1997) 'Phenylketonuria and the peoples of Northern Ireland.', *Human genetics*. Germany, 100(2), pp. 189–194. doi: 10.1007/s004390050488.